CIGARETTE SMOKING AND BACTERIAL-HOST INTERACTIONS

THE IMPACT OF CIGARETTE SMOKE EXPOSURE ON BACTERIAL COLONIZATION AND INFECTION IN THE MOUSE RESPIRATORY TRACT

By
PEIHENG (PAMELA) SHEN, BHSc.

A Thesis
Submitted to the School of Graduate Studies
in Partial Fulfillment of the Requirements
for the Degree
Doctor of Philosophy
McMaster University

Descriptive Note

McMaster University DOCTOR OF PHILOSOPHY (2016) Hamilton, Ontario (Medical Sciences)

TITLE: The Impact of Cigarette Smoke Exposure on Bacterial Colonization and Infection in the Mouse Respiratory Tract

AUTHOR: Peiheng (Pamela) Shen, BHSc. (McMaster University)
SUPERVISOR: Dr. Martin R Stampfli
NUMBER OF PAGES: xvii, 143

Lay Abstract

Over 1.1 billion people smoke worldwide and can develop chronic obstructive pulmonary disease (COPD), a serious inflammatory disease compromising lung function. Additionally, smokers and COPD patients have higher rates of bacterial infection. The goal of this thesis is to understand how smoking impacts our ability to combat infection. Lung infection in COPD patients causes exacerbation, with worsened disease symptoms. Using mouse models, we learned how smoking causes increased lung inflammation following bacterial infection, contributing to damage reflective of COPD exacerbations, and identified a potential intervention. We elucidated smokers may have increased infections due to impaired immune responses in the nose, a major pathogen entry point. It is thought smoking reduced beneficial bacteria that counter pathogen acquisition in the nose. We confirmed smoking did not impact these bacteria, directing research focus towards other ways smokers acquire pathogens. Overall, this thesis advanced knowledge and will help efforts to control disease in smokers.

Abstract

Over 1.1 billion people smoke worldwide despite the association of smoking with numerous diseases including chronic obstructive pulmonary disease (COPD). The decline in lung function observed in COPD patients is thought to be related to smoke-induced inflammation. COPD patients are also at increased risk of acquiring lung bacterial infections that are associated with exacerbations, characterized by worsened disease symptoms and inflammation. The focus of this thesis is on how cigarette smoke impacts bacterial-host interactions and bacterial community interactions to promote infection and disease. In chapter 3.1, we sought to understand how cigarette smoke primed the lungs towards an amplified inflammatory response to bacterial infection reflective of COPD exacerbations that accelerate disease progression. We present a novel finding that exacerbated neutrophilia elicited by nontypeable *Haemophilus influenzae* (NTHi) lung challenge in smoke-exposed mice occurred dependent on IL-1α. Smokers and patients with COPD are additionally at increased risk of acquiring bacterial infection that may be related to impaired containment of nasally colonizing pathogens. In chapter 3.2, we found that cigarette smoke predisposed mice to invasive pneumococcal disease (IPD) following nasal pneumococcal colonization associated with attenuated nasal inflammatory responses. To our knowledge, this is the first study to describe the progression from asymptomatic nasal pneumococcal colonization to the development of IPD in the context of cigarette smoking. It has been suggested that smokers have higher rates of pathogen colonization as a consequence of cigarette smoke-induced nasal microbiome dysbiosis. The last study in chapter 3.3 advanced knowledge in the field by testing this hypothesis. We observed that cigarette smoke

alone did not alter the mouse nasal microbiome and concluded that microbiome dysbiosis observed in smokers likely occur as a consequence of nasal pathogen colonization. Overall, work presented in this thesis advanced our understanding of how cigarette smoking alters bacterial-host interactions to promote infection and disease.

Acknowledgements

Graduate school has been a long and exciting journey. I am extremely lucky to have worked with my supervisor Dr. Martin Stampfli, who provided support and advice not only regarding science but my personal development as well. I have learned things here that will help me for the rest of my career. His guidance has given me a strong foundation in scientific research. Training in his laboratory has allowed me to find my own style, gain confidence, and above all brought out the enjoyment in science. I am extremely grateful to my supervisor for an amazing graduate experience and I have truly enjoyed working with him.

I must also thank my committee members for their support and guidance over the years. Dr. Dawn Bowdish has been instrumental in helping us establish the *S. pneumoniae* projects and always offers insightful advice. Dr. Karen Mossman's attention to detail and critical questions during our committee meetings has added much to my learning throughout graduate school. Lastly, I always appreciate Dr. Chris Wynder's "big picture" perspective and pragmatic advice.

Much of the work presented in this thesis would not have been possible without our collaborators. I would like to thank our industrial collaborators Medimmune LLC, especially Drs. Alison Humbles and Roland Kolbeck, and Hoffmann-La Roche, especially Drs. Christopher Stevenson and Carla Bauer, for their valuable resources and advice. Dr. Dawn Bowdish's lab, especially Drs. Alicja Puchta and Michael Dorrington, was critical for the establishment of the nasal pneumococcal colonization model in our lab. Dr. Michael Surette's lab, especially Fiona Whelan and Patrick Schenck, was critical to the microbiome studies in chapter 3.3. Numerous others have

contributed to data presented in this thesis including Drs. Derek Chu, Nicole Barra, Jacek Kwiecien and Renee Labiris.

Perhaps the most important element in research is team work. I am extremely grateful to all Stampfli lab members, past and present. I would like to start with Dr. Gordon Gaschler, who taught me many basic laboratory techniques my first month of graduate school. I also appreciate support from our senior graduate students at the time, Drs. Cale Zavitz and Carla Bauer, as well as post-doc Dr. Fernando Botelho when I first began in the lab. I owe a lot to Dr. Jake Nikota, who trained me, mentored me and braved through much of grad school together with me, cumulating in our shared first authorship for the study in chapter 3.1. Another important team member to me is Dr. Mathieu Morissette, who also played a mentoring role for me and staunchly helped me with my mouse work even as my project got more and more demanding, requiring ever more sample collection. Other lab members who contributed greatly to my work include Drs. Gilles Vanderstocken, Yang Gao, and Abraham Roos. I have also received much help from newer members of the lab including Danya Thayaparan, Joshua McGrath, Ashley Beaulieu, and Steven Cass. I have had the pleasure of supervising two undergraduate thesis students Muhammad Hassan and Maria Merlano, who not only contributed to my work but also taught me about playing a supervising and teaching role. Other undergraduate students I am grateful to include Kimberly Fernandes and Kristen Lambert, who were wonderful to work with. Last but not least, I must give special thanks to Joanna Kasinsj, our wonderful lab technician. I could not have accomplished any of the studies in this thesis without Joanna's work that cigarette smoke-exposes all our mice. My project in chapter 3.2 also presented special

challenges with the development of survival studies requiring constant monitoring of the health status of mice. Joanna's thoughtful and constant support was crucial to the successful completion of these experiments.

The great open concept of the McMaster Immunology Research Centre (MIRC) means that everyone from the centre has helped me at some point over the years, including technicians, graduate students, and post-docs. I would like to thank all members of MIRC, notably our friendly neighbours the Jordana lab, who shares common lab space and resources with us, the Bowdish lab, who I turn to for anything *S. pneumoniae* related, the Xing lab, and the Mossman lab. I am extremely grateful to the administrative staff for all their support, especially Marie Bailey. Without them I would have surely been lost with the paperwork. I would also like to acknowledge the McMaster central animal facility (CAF), whose services contributed greatly to all my graduate work.

Finally, the support from friends and family are crucial to all my endeavours. I owe everything I have today to my wonderful mother, who immigrated to Canada from China and worked through much hardship to give me the life I enjoy now. She has also encouraged me to try my best and pursue whatever I am interested in. The constant support from my parents and my aunt has made it possible for me to pursue a career that I enjoy. I grew up with my grandparents and have a close relationship with them. Sadly, they are no longer with us. The precious time I spent with them has shaped who I am and will continue to influence my work and my life. I am lucky to meet my boyfriend Jeff early during my graduate studies and he has been strongly supporting me through

thick and thin. I must also thank Jeff's family, including his parents, brothers, aunt and cousin, all of whom have greatly encouraged me in my academic pursuits.

Contents

List of Figures and Tables

List of Abbreviations

AM	Alveolar macrophage
ASC	Apoptosis-associated speck-like protein containing a caspase-recruitment domain
BAL	Brochoalveolar lavage
CAP	Community acquired pneumonia
CCL	CC chemokine ligand
ChoP	Phosphorylcholine
CNT	Complete nasal turbinates
COPD	Chronic obstructive pulmonary disease
CXCL	CXC chemokine ligand
CXCR	CXC chemokine receptor
DAMP	Damage-associated molecular pattern
DNA	Deoxyribonucleic acid
ECM	Extracellular matrix
FEV1	Forced expiratory volume in 1 second
GM-CSF	Granulocyte-macrophage colony-stimulating factor
IL	Interleukin
IL-1R1	Interleukin 1 receptor 1
IPD	Invasive pneumococcal disease
KO	Knockout
LPS	Lipopolysaccharide
LTB4	Leukotriene B4
MAPK	Mitogen-activated protein kinase
MCP	Monocyte chemotactic protein
MMP	Matrix metalloproteinase
MNC	Mononuclear cells
MyD88	Myeloid differentiation primary response gene 88

NE	Neutrophil elastase
NEU	Neutrophils
NFκB	Nuclear factor kappa-light-chain-enhancer of activated B cells
NLR	Nod-like receptor
NTHi	nontypeable *Haemophilus influenzae*
OTU	Operational taxonomic unit
PAFR	Platelet activating factor receptor
Pam3CSK4	Synthetic triacylated lipoprotein
PBS	Phosphate-buffered saline
PCLS	Precision cut lung slices
PCoA	Principal Coordinates Analysis
PRR	Pattern recognition receptor
RNA	Ribonucleic acid
ROS	Reactive oxygen species
^{99m}Tc-DTPA	^{99m}Technetium-diethylene triaminepentaacetic acid
TCN	Total cell number
TLR	Toll-like receptor
TNF	Tumor necrosis factor
TPM	Total particulate matter
URT	Upper respiratory tract

Declaration of Academic Achievement

This thesis contains the data from three studies prepared for publication in peer reviewed journals for which I am listed first author. The studies outlined in chapters 3.1 and 3.2 are already published. The last study presented in chapter 3.3 is currently in preparation for submission to the journal *Infection and Immunity*. No one can work in isolation, and others have contributed to this work. However, I was overall largely responsible for experimental design, the majority of the experimental work, data analysis and data interpretation.

The published manuscript in chapter 3.1 (*Journal of Immunology* 193: 3134-45 Sept, 2014. Copyright 2014. The American Association of Immunologists, Inc.) is a shared first authorship with a former PhD student, Dr. Jake Nikota, from the same lab. Dr. Jake Nikota and I contributed equally to the data generated. Dr. Stampfli, Dr. Jake Nikota, and I were responsible for the experimental design and the interpretation of results. Dr. Mathieu Morissette and Kimberly Fernandes provided technical assistance during experiments, and Dr. Abraham Roos contributed additional experimental data. Drs. Derek Chu and Nicole Barra assisted with specific experimental procedures. Drs. Yoichiro Iwakura, Roland Kolbeck, and Alison Humbles provided critical reagents and advice.

For the published manuscript in chapter 3.2 (*Infection and Immunity* 84: 1536-47 April, 2016), Dr. Stampfli and I were responsible for the experimental design and the interpretation of results. Dr. Mathieu Morissette, Dr. Gilles Vanderstocken, Dr. Yang Gao, Dr. Abraham Roos, Muhammad Hassan, Danya Thayaparan, Maria Merlano, and Dr. Jake Nikota provided technical assistance during experiments. Dr. Michael

Dorrington, Dr. Jacek Kwiecien, and Dr. Renee Labiris assisted with specific experimental procedures and contributed to data analysis. Dr. Dawn Bowdish provided critical reagents and advice. Drs. Carla Bauer and Christopher Stevenson provided funding and advice.

For the manuscript in preparation in chapter 3.3, Dr. Stampfli and I were responsible for the experimental design and the interpretation of results. Pat Schenck provided critical technical assistance during experiments and Fiona Whelan carried out the processing and analysis of microbiome data. Dr. Gilles Vanderstocken, Danya Thayaparan, Josh McGrath, and Maria Merlano provided technical assistance during experiments. Drs. Dawn Bowdish and Michael Surette provided critical reagents and advice.

CHAPTER 1. INTRODUCTION

1.1. Cigarette smoking and human health

Cigarette smoking is well known to adversely impact human health[1–3]. Indeed, smoking is associated with a multitude of diseases including chronic obstructive pulmonary disease (COPD), cancer, cardiovascular disease, and microbial infection[4–6]. Thus, all-cause mortality is higher in current cigarette smokers compared to never smokers, with an average loss of up to 12 years of life[7,8]. Moreover, smokers have higher rates of hospitalization and place a greater burden on health care spending as compared to never smokers[4,9]. General morbidity associated with cigarette smoking also extends beyond specific diseases. For example, smokers are more likely to self-report poorer health than never smokers[10,11], and to have higher absenteeism from work[4,12].

Despite the continuous increase in our understanding of the harmful effects associated with smoking, the prevalence of cigarette smoking remains alarmingly high worldwide. The World Health Organization estimates that over 1 billion of the world's population continue to smoke. While emphasis needs to be placed on efforts to reduce smoking prevalence, a greater understanding of the mechanisms that contribute to disease is equally relevant, given the highly addictive nature and chronic persistence of cigarette smoking. The focus of this thesis is on how cigarette smoking impacts bacterial-host interactions to promote infection and disease.

1.2. Chronic obstructive pulmonary disease (COPD)

1.2.1. Clinical definition

COPD is a complex disease defined as "a progressive and largely irreversible airflow limitation associated with an enhanced chronic pulmonary inflammatory response to noxious particles or gases"[13]. COPD is a leading cause of morbidity and mortality globally[14]. According to the Global Burden of Disease (GBD) study, there was an estimated 328 million people worldwide with COPD in 2010, and COPD was projected to be the third leading cause of death by 2020[15,16]. Therefore much effort has been spent on understanding COPD disease pathogenesis.

The symptoms associated with airflow obstruction in COPD, as measured by forced expiratory volume in one second (FEV1) using spirometry, include chronic and progressive dyspnea, cough, and sputum production[17,18]. The decline in lung function is associated with obstructive bronchiolitis and emphysema, the relative contributions of which may differ between individuals. Obstructive bronchiolitis is a structural narrowing of the small airways while emphysema is the destruction of lung parenchyma leading to a decrease in lung elastic recoil. Both disease processes are thought to be caused by chronic inflammation[13]. Due to the complexity and chronic nature of COPD, underlying mechanisms remain elusive and current therapies, such as corticosteroid treatment, are still largely ineffective[19].

1.2.2. COPD-associated lung pathologies

Lung function is decreased in COPD patients by the relative contributions of obstructive bronchiolitis and emphysema. Obstructive bronchiolitis is characterized by fibrosis in the bronchioles, with increased thickness of the airway wall (epithelial metaplasia, increased smooth muscle, goblet cell hyperplasia, and submucosal gland hypertrophy). At the same time, inflammatory exudate accumulates in the lumen, consisting of neutrophils, macrophages, T lymphocytes, and B cells. The levels of these inflammatory cells increase with disease progression[20,21]. The resulting narrowing of the airways causes airflow obstruction.

On the other hand, emphysema in COPD patients is characterized by the destruction of lung parenchyma and can be either panacinar or centrilobular[22]. Destruction of lung tissue, specifically elastin, impairs lung elasticity and contributes to airflow limitation[23]. The progression of both obstructive bronchiolitis and emphysema in COPD is thought to be related to an amplification of the pulmonary inflammatory response normally elicited by cigarette smoke exposure in a subset of smokers[24,25]. However, the process by which smokers develop COPD is incompletely understood and remains an area of intense research.

1.2.3. Inflammatory processes associated with smoking

COPD develops in an estimated 15% of smokers, although this proportion has been suggested to be higher[24,26]. A more recent study found the development of airflow limitation in 33% of male and 24% of female continuous smokers[27]. Smoking, even in healthy individuals, increases the total cell number recovered from the bronchoalveolar lavage (BAL), with an increase in the levels of macrophages and neutrophils.

Correspondingly, numerous inflammatory mediators are also increased, including monocyte chemotactic protein (MCP)-1, interleukin (IL)-8[28,29], IL-1β, IL-6[29], and the neutrophil survival promoting granulocyte macrophage colony stimulating factor (GMCSF)[30,31].

The inflammatory response induced by cigarette smoking leads to lung tissue damage. Neutrophils release neutrophil elastase (NE), which degrades connective tissue. Higher concentrations of elastase are found in the induced sputum of smokers, correlating with the increased proportion of neutrophils[32]. Smokers have also been shown to have increased plasma levels of both NE and the fibrinopeptide A-containing fragment (A-alpha-1-21), a specific product of NE, suggesting higher levels of NE activity[33,34]. Other proteases increased in smokers include the extracellular matrix degrading enzymes matrix metalloproteinases (MMPs)[35]. Smokers have higher induced sputum concentrations of MMP-9 as compared to controls, with a simultaneous decrease in the tissue inhibitor of metalloproteinase (TIMP) -1[36]. Lastly, cigarette smoke exposure induces oxidative stress in the lungs as assessed by higher levels of 8-isoprostane in both induced sputum and exhaled breath condensate[37,38]. A higher 8-isoprostane level is considered a measure of lipid peroxidation by reactive oxygen species (ROS) and an indication of oxidative injury[39]. The inflammatory response elicited by cigarette smoke exposure is further amplified in COPD patients with contribution from both innate and adaptive immune processes.

1.2.4. Innate immune processes associated with COPD

Alveolar macrophages (AMs) are resident innate immune cells of the lungs and are directly exposed to the external environment. Thus they are considered the first line of

defence against invading pathogens and respond to stimuli through the production of critical inflammatory mediators. AMs also carry out the phagocytosis of bacteria and apoptotic cells[40]. However, AMs are considered an important source of inflammatory mediators, such as TNF-α, IL-8, CXC chemokines, MCP-1, LTB_4, and ROS, that contribute to COPD pathogenesis[25]. AMs isolated from COPD patients also degrade more elastin through cysteine and serine proteases, as well as MMPs[43]. Of note, MMP-1, MMP-9, and MMP-12 are elevated in COPD patients[44–46]. COPD patients with emphysema have higher macrophage numbers in both the air space and lung tissue as compared to healthy smokers[41]. The number of macrophages in the airways also correlates with disease severity[42]. Thus AMs are thought to be a critical source of inflammatory mediators that simultaneously amplify cellular inflammation while causing lung tissue damage.

It is thought that chemokines released by AMs in response to cigarette smoke recruit neutrophils, a hallmark of COPD[47]. Neutrophil recruiting chemotactic factors in COPD include leukotriene B4 (LTB4), IL-8, and related CXC chemokines such as CXCL-1 and CXCL-5[25,48,49]. Normally, neutrophils are rapidly recruited to bacterial infection sites to phagocytose and destroy pathogens via ROS generation and the release of NE, cathepsins, and antibacterial proteins[50]. However, in the case of COPD, neutrophils contribute to tissue destruction through the release of NE, cathepsin G, proteinase-3, MMP-8, and MMP-9[25]. Both sputum IL-8 and NE concentrations have been shown to correlate with disease severity as measured by airflow limitation[32,51]. Similarly, disease severity is associated with neutrophil numbers in bronchial biopsies[42]. An increase in sputum neutrophil levels also correlated with a rapid decline in lung

function as determined by FEV_1[52]. Additionally, neutrophils accumulated in the lungs of COPD patients are activated, as indicated by the presence of myeloperoxidase and neutrophil lipocalin in the sputum supernatant[53]. Myeloperoxidase contributes to tissue-damaging oxidative stress by generating hypochlorous acid and nitrating tyrosine residues[25,54,55]. Lastly, depletion of neutrophils in cigarette smoke-exposed mice prevented the increase of the elastin and collagen breakdown markers, desmosine and hydroxyproline respectively, further supporting a role for neutrophils in smoke-induced lung damage[56].

Macrophages and neutrophils recruited to the lungs in COPD patients produce ROS such as superoxide anions ($O2^{\cdot-}$), hydrogen peroxide (H_2O_2), hydroxyl radicals ($^{\cdot}OH$), and peroxynitrite[57]. The resulting oxidative stress contributes to lipid, protein, and DNA damage[25]. COPD patients have higher levels of oxidative stress than healthy asymptomatic smokers, as assessed by 8-isoprostane measurements in the sputum and H_2O_2 levels in the exhaled breath condensate. 8-Isoprostane levels also correlates with sputum neutrophil counts, smoking history, and COPD severity[37,58]. Additionally, ROS activate the pro-inflammatory transcription factor NF-κB, and may further amplify established cigarette smoke-induced inflammation[59].

1.2.5. Adaptive immune processes associated with COPD

Adaptive immune responses become more prominent in severe COPD, with an increase in T cells and B cells and the appearance of lung lymphoid aggregates[60]. There are more $CD8^+$ than $CD4^+$ T cells in patients with COPD, and a T lymphocyte accumulation in the lung tissue is mostly observed in smokers with emphysema rather than asymptomatic smokers[61,62]. $CD8^+$ T cells, likely recruited by epithelial CXCL-10

expression, potentially contribute to lung damage and subsequent emphysema through the release of perforins and granzyme-B which cause cytolysis and apoptosis of epithelial cells[25,63,64]. In support of this hypothesis, T-cells isolated from cigarette smoke-exposed mice mediated antigen-dependent tissue destruction reflective of emphysema when transferred to naive mice[65]. B cells are also markedly increased in late stage COPD, corresponding with the appearance of lymphoid aggregates[60,66]. These structures in COPD patients are described to contain mainly B cells, with some follicular dendritic cells scattered throughout, and surrounded by mostly $CD4^+$ T cells. Moreover, markers of cell proliferation (Ki-67) and activation (CD40) suggest early germinal center activity[66]. Possible sources of antigens for adaptive immune responses may be microbial derived, as COPD patients become colonized with bacteria[67]. Cigarette smoke itself also contains immunogenic proteins[68]. Additionally, breakdown products from the extracellular matrix, such as elastin fragments, may stimulate antibody responses[69].

1.3. Cigarette smoke-induced inflammation

1.3.1. Animal models

Current treatment options for COPD remain largely ineffective. A further understanding of the mechanisms underlying cigarette smoke-induced inflammatory responses may contribute to the development of novel and more effective therapeutic intervention strategies. However, COPD is a chronic and heterogeneous disease associated with decades of cigarette smoke exposure in humans. Further complications arise from co-morbidities such as cardiovascular disease, diabetes, and lung cancer[70]. For these reasons, it has been difficult to reproduce all aspects of COPD in cigarette smoke-

exposed animal models. Nevertheless, some key features of COPD can still be modeled and studied to dissect underlying mechanisms.

The mouse model is the most widely used for several reasons including the well-studied mouse genome, low cost, easy management, and the availability of transgenic strains, as well as antibodies and reagents. Evidence of airway damage and remodelling, vascular remodelling, and lymphoid aggregate formation has been observed in mice following long term cigarette smoke exposure, usually after 6 months[71]. The most profound and consistent feature of mouse models of cigarette smoke exposure, however, is the induction of a lung inflammatory response characterized by increased BAL levels of neutrophils and macrophages. Inflammation induced by our whole body cigarette smoke exposure system manifests as early as 4 days following cigarette smoke exposure[72]. Given that the neutrophilic inflammatory response elicited by cigarette smoke exposure is considered to contribute to lung damage and COPD disease progression[73,74], the mouse model is most suitable for investigating the cellular and molecular mechanisms underlying cigarette smoke-induced inflammation.

1.3.2. Mechanisms of cigarette smoke-induced inflammation

The role of various signalling pathways in cigarette smoke-induced inflammation, including toll-like receptor (TLR) -4, IL-17A, IL-18, and IL-1, have been examined[75–77]. The focus of this thesis is on IL-1 signalling pathway-dependent cigarette smoke-induced inflammation. Activation of the IL-1 receptor 1 (IL-1R1) leads to myeloid differentiation primary response gene 88 (MyD88)-dependent signalling and promotes pro-inflammatory gene transcription through NF-κB and mitogen-activated protein

kinase (MAPK) activation[78]. Two cytokines can activate the IL-1R1, including IL-1α and IL-1β[79]. Precursor IL-1α is biologically active as a 31kDa protein[80]. In contrast, IL-1β is initially synthesized as pro-IL-1β (also 31kDa), which is biologically inactive and requires proteolytic cleavage by the cysteine protease caspase-1 for its activation[81]. Caspase-1 is in turn activated by the inflammasome, a multi-protein complex consisting of a member of the Nod-like receptor (NLR) family and the adaptor protein apoptosis-associated speck-like protein (ASC)[82,83]. Inflammasome activation is triggered by diverse stimuli including microbial components and dying cells[84].

Treatment with an anti-IL-1β antibody in low dose cigarette smoke-exposed mice was sufficient to attenuate macrophage accumulation in the BAL[85]. Cigarette smoke-induced neutrophilia was also shown to be both TLR-4 and IL-1R1 dependent. In addition, cigarette smoke condensate (CSC) stimulation of bone marrow-derived macrophages induced both IL-1α and IL-1β production[75]. Adding to these findings, Churg *et al* found that the cigarette smoke-induced markers of lung damage, desmosine and hydroxproline, were reduced in IL-1R1 knockout (KO) mice and that administration of a caspase-1 inhibitor attenuated both cigarette smoke-induced neutrophilia measured in the BAL and serum IL-1β levels[86]. These data suggest that the initiation of cigarette smoke-induced inflammation is dependent on IL-1 signalling, although it is unclear whether the process is IL-1α or IL-1β dependent. Using anti-IL-1α and anti-IL-1β antibodies, a role for both IL-1 cytokines was demonstrated in cigarette smoke-induced neutrophilia, although the process was unaffected in Nlrp3 KO or caspase-1 KO mice[87]. This suggested the possible role of IL-1α in cigarette smoke-induced inflammation. Our laboratory had shown that although both IL-1α and IL-1β were increased in COPD

patients and cigarette smoke-exposed mice, only anti-IL-1α, and not anti-IL-1β, antibody treatment attenuated cigarette smoke-induced neutrophilia in mice. This indicated, for the first time, that cigarette smoke-induced inflammation may be exclusively IL-1α dependent, although further confirmation studies are warranted. IL-1R1 chimeric mouse data from the same study also suggest that it is IL-1R1 activation within the structural cell compartment, likely the epithelium, that mostly contributes to cigarette smoke-induced neutrophilia[88]. However, the cellular source of IL-1α acting on the epithelium remains to be elucidated.

1.4. COPD and bacterial infection

1.4.1. Cigarette smoke and lung bacterial colonization

Cigarette smoke exposure is thought to alter bacterial-host interactions to facilitate lung bacterial colonization and inflammation in smokers and patients with COPD. 42% of healthy smokers were found to be culture positive for potentially pathogenic bacteria from either the BAL or bronchial brushings, while non-smokers were culture negative. Moreover, the presence of these pathogens was associated with increased levels of TNF-α, IL-8, and increased percentages of neutrophils in the BAL[89]. Similar to smokers, 40% of COPD patients were found to be colonized with potentially pathogenic bacteria in their lungs by culturing methods, most frequently with *Haemophilus influenzae*, *Streptococcus pneumoniae*, and *Moraxella catarrhalis*[90]. Although lung microbiota analyses found no significant differences overall between smokers and non-smokers[91,92], the lung microbiota profile of COPD patients is altered, with an increase in bacteria from the phyla Firmicutes and Proteobacteria, which contain potential

pathogens[92–94]. Mechanistically, cigarette smoke-induced mucus hypersecretion and plugging may trap aspirated bacteria in the lungs, allowing more bacterial colonization in the lungs[20,95]. Bacterial persistence could also be due to a decreased ability of AMs to phagocytose and mount appropriate cytokine responses to bacterial pathogens[96,97]. It has been hypothesized that potential pathogenic bacteria such as *H. influenzae* induce a more robust overall inflammatory response than commensal organisms that may drive chronic inflammation in smokers and patients with COPD[95,98]. Indeed, the presence of these bacteria in stable COPD patients is associated with increased lung neutrophilic inflammation compared with COPD patients without bacterial colonization[99]. Furthermore, airway inflammation increased with higher bacterial load, attributable to *H. influenzae* presence[100].

1.4.2. Bacterial exacerbations of COPD

The normal course of COPD is punctuated by periods of exacerbations, which accelerate disease progression as measured by the degree of airflow limitation[101,102]. Clinically, COPD exacerbations are defined as periods of worsened disease symptoms, such as dyspnea, cough, and sputum production, beyond day to day variation requiring a change in current medication. Exacerbations are characterized by increased neutrophilia, as well as sputum concentrations of the neutrophil recruiting inflammatory mediators IL-8 and LTB_4, above levels of stable disease[103,104]. Exacerbations have been associated with environmental pollutants, as well as viral and bacterial infections[105]. Chronic lung bacterial colonization increases the frequency of acquiring exacerbations, and more frequent exacerbations correlated with faster lung function decline[67,101]. Bacterial infection accounts for 50% of exacerbation cases, with *H. influenzae* the most

frequently identified bacteria at 20-30% of exacerbations, followed by *S. pneumoniae* and *M. catarrhalis*[106]. However, the lung microbiota composition during stable COPD and exacerbations were comparable[107]. It is thought that the acquisition of new strains of *H. influenzae*, *S. pneumoniae*, and *M. catarrhalis*, rather than changes in the lung bacterial community, cause disease exacerbation[95,108]. Exacerbations associated with these new bacterial strains had higher levels of sputum inflammatory markers, including TNF-α and NE[109]. These observations highlight that bacterial lung infection can further amplify the inflammatory response already present, leading to increased lung damage that accelerate irreversible airflow limitation.

The evidence presented above suggests that amplified neutrophilia beyond levels observed during stable disease occur in bacterial exacerbations of COPD. Furthermore, the degree of the neutrophilic response often correlates with lung damage and disease severity in COPD. Our laboratory has previously established a mouse model where cigarette smoke exposure exacerbated the lung neutrophilic response to nontypeable *Haemophilus influenzae* (NTHi) infection[110]. In chapter 3.1 of this thesis, we investigated the specific mechanisms underlying this exacerbated inflammation. Of particular interest is the previously established role of IL-1α, which acts on IL-1R1 in the structural cell compartment, likely epithelial cells, to drive the neutrophilic inflammatory response induced by cigarette smoke exposure alone[88]. Given the important role of AMs as both lung resident immune cells and a crucial source of inflammatory mediators for COPD disease pathogenesis, we first hypothesize that the cellular source of IL-1α induced by cigarette smoke exposure is the AM. Previous studies from our laboratory also observed a skewed inflammatory mediator expression profile of AMs from cigarette

smoke-exposed mice upon bacterial ligand challenge[111]. We next hypothesize that AM IL-1α expression is further amplified in cigarette smoke-exposed mice following NTHi challenge, and that the observed exacerbated neutrophilia in response to both stimuli is IL-1α dependent. Data included in chapter 3.1 increase our understanding of an important process that drive COPD disease progression, and may contribute to the development of novel intervention strategies.

1.5. Cigarette smoking and risk of bacterial infection

Established lung bacterial infections contribute to COPD exacerbations and accelerate disease progression. However, COPD patients are additionally at increased risk of acquiring bacterial infection. The epidemiological evidence for cigarette smoking as a risk factor for various bacterial infections is overwhelming. Cigarette smoking has long been associated with community acquired pneumonia (CAP), with an increase in the odds ratio for developing CAP dependent on the number of cigarettes smoked per day[112]. Smokers are also at increased risk of Legionnaires disease and tuberculosis[113,114]. Moreover, the increased risk for bacterial infection extends beyond the respiratory tract as cigarette smoking is also found to be associated with meningococcal disease, otitis media, periodontal disease, bacterial vaginosis, and invasive pneumococcal disease (IPD)[115–119]. Cigarette smoking may increase the incidence of bacterial infectious disease by altering the upper respiratory tract (URT) host defence, and colonization resistance provided by the nasal microbiome, although underlying mechanisms are complex and remain incompletely understood.

1.5.1. Bacterial colonization of the upper respiratory tract

It has been established that the lungs are not sterile, even in healthy individuals. Moreover, bacterial populations found in the lungs resemble that of the URT, with a lower biomass, suggesting that microbes are constantly being introduced to the lungs from the URT[120]. The URT is colonized by a commensal bacterial microbiome that frequently includes opportunistic pathogens, such as *H. influenzae* and *S. pneumoniae*, even in healthy individuals[121,122]. Not surprisingly, the increased incidence of lung colonization by potentially pathogenic bacteria found in smokers is mirrored by higher recovery rates of the same bacteria colonizing their nasopharynx[123]. Nasal colonization by some opportunistic pathogens, such as *S. pneumoniae*, are clinically asymptomatic, but disease is established when bacterial invasion into other tissue sites, such as the lungs, occur[124]. Physical and mechanical barriers, as well as the pathogen-induced nasal inflammatory response are critical to the containment of pathogenic bacterial colonization at the URT. A compromised URT host response may therefore explain how smokers and COPD patients are at increased risk of acquiring lung bacterial infections, which cause exacerbations in COPD patients with detrimental consequences. Despite this, the impact of cigarette smoke exposure on the URT inflammatory response to bacteria remain largely unexplored, and further studies are warranted.

1.5.2. Cigarette smoking and the upper respiratory tract host defence

A critical first line of defence against bacterial infection from colonizing pathogens is the physical barrier of the respiratory tract, consisting of a mucus layer, the respiratory epithelium of columnar cells with and without cilia, goblet mucus cells and basal cells, and the basement membrane[125]. Aside from the nasal entrance, nasopharynx, pharynx,

and larynx that are covered by squamous epithelium, the rest of the upper airways surface is covered by ciliated epithelium. The specialized neuroepithelium of the olfactory area also lack cilia[126]. Epithelial cells are physically connected through tight and adherence junctions that prevent pathogen entry across the epithelium[127]. Cigarette smoke exposure decreases tight junction protein transcription and disrupts cell-cell contacts, compromising the epithelial barrier integrity which may facilitate paracellular pathogen invasion[128,129].

Ciliated regions of the airways contain goblet cells and submucosal glands that secrete mucus, a viscous mixture composed of glycoproteins, proteoglycans, lipids, and other proteins[126,130]. Mucus forms a layer over the epithelium to trap noxious substances, particles and microbes, preventing contact of infectious microbes with the epithelium. Mucus trapping of pathogens also limits their access to the lower respiratory tract and allows for ciliary transport towards the nasopharynx, where microbes can be swallowed[125,131]. The synchronized beating of cilia and mucus production at the airway epithelium together contribute to mucociliary clearance, a critical aspect of the respiratory host defence against microbial infection[132]. The efficiency of mucociliary clearance is dependent on the amount and composition of mucus produced, cilia length and density, as well as ciliary beat frequency[126]. Therefore, any perturbation of mucus production and cilia function may increase the time period of contact between the nasal mucosa and potential infectious microbes, increasing the risk of pathogen colonization and subsequent infection.

There is evidence to suggest that cigarette smoke exposure alters many properties of respiratory mucociliary function that may lead to impaired nasal clearance

of pathogenic bacteria. Smokers develop goblet cell hyperplasia and are prone to developing chronic mucus hypersecretion[133,134]. In addition, mucus from smokers are more dehydrated compared to non smokers, possibly due to cigarette smoke's effects on airway ion channel function and mucin production, which modulate mucus rheology[135–137]. This increase in mucus viscosity makes it more difficult to transport by ciliary clearance and causes mucus stasis[136]. Exposure to cigarette smoke extract *in vitro* decreases both mouse nasal septal epithelium cell ciliogenesis and cilia length[138]. Not only is there a loss of ciliated epithelial cells, smokers also have significantly decreased nasal ciliary beat frequency[139,140]. Finally, functional tests show impaired mucociliary clearance in smokers as assessed by saccharin nasal transit time, defined as the amount of time it took for saccharin placed on the inferior nasal turbinate to be tasted following transport via nasal clearance[141]. Thus, mucus stasis induced by cigarette smoking is thought to facilitate bacterial colonization of the respiratory epithelium and increase the risk of bacterial infections. Indeed, a mouse model of mucus stasis show increased susceptibility to respiratory tract infection[142].

In addition to increasing the time period of contact between potential bacterial pathogens and the epithelium by causing mucus stasis, cigarette smoke exposure also increases direct bacterial adherence to host cells, and may thus facilitate the establishment of pathogen colonization[143,144]. For example, *S. pneumoniae* is known to bind several host receptors including the platelet activating factor receptor (PAFR)[145–147], the expression of which is increased in the lungs of smokers and cigarette smoke-exposed mice[148]. *S. pneumoniae* interacts with the PAFR via a phosphorycholine moiety (ChoP) that mimics the molecular structure of platelet activating factor, the

endogenous ligand to PAFR[149]. After adherence, *S. pneumoniae* has been shown to invade host cells through the PAFR following cell activation by several cytokines, including IL-1α. Moreover, IL-1 administration to rabbits increased lung pneumococcal burden in a PAFR-dependent manner[147]. Pre-treatment with a PAFR antagonist also attenuated lung infection with ChoP-containing strains of *Pseudomonas aeruginosa* in mice[150].

1.5.3. Cigarette smoking and pneumococcal infection

Much interest has been placed in the nasally colonizing opportunistic pathogen *S. pneumoniae*, or the pneumococcus, which is the second most frequently isolated bacteria associated with COPD exacerbations[106]. *S. pneumoniae* is also a leading cause of CAP, and associated with invasive infections such as bacteraemia and meningitis, contributing significantly to morbidity and mortality worldwide [151–153]. This Gram-positive bacteria behaves as a commensal in the URT, colonizing the nasal mucosa of up to 18% of adults[154]. The bacteria can persist for weeks before clearance but nasal colonization alone does not lead to disease[155]. However, nasal colonization is considered a requirement for bacterial dissemination into other tissue sites and the subsequent development of pneumonia and IPD[124]. Smokers are at increased risk of acquiring CAP and cigarette smoking is a strong, independent risk factor for the development of IPD[112,119,156,157]. Smokers are over-represented in a population of IPD patients at 58%, as compared to 24% of control healthy individuals[119]. Interestingly, there is a dose-dependent relationship between the number of cigarettes smoked per day and the odds ratio for acquiring both CAP and IPD[112,119]. The susceptibility of

smokers to pneumococcal infections may be explained by the impact of cigarette smoke exposure on the URT host defence.

S. pneumoniae activates TLR-2 signalling that is thought to initiate nasal inflammatory responses. TLR-2 deficiency significantly decreased survival following nasal pneumococcal colonization in mice[158]. Pneumococcal nasal colonization in mice induces rapid neutrophil recruitment to the nasal spaces. However, this neutrophilic response is not sufficient to clear the colonizing pneumococci, likely due to the presence of the pneumococcal capsule that resists neutrophil killing[159,160]. Following the resolution of neutrophilia, there is a consistent and prolonged macrophage recruitment which is critical for the control and clearance of pneumococci over the course of several weeks. Macrophage recruitment was found to be both TLR-2 and Th17-dependent[161]. Although the impact of cigarette smoke exposure on the bacterial host response has been studied extensively in the lungs, little is known about cigarette smoke's effects on the URT. It remains to be investigated whether cigarette smoke impacts nasal inflammatory responses against *S. pneumoniae* that may impair the control of pneumococcal colonization at the nasal mucosa, predisposing to bacterial dissemination into other tissue sites such as the lungs.

Despite the well-documented association between cigarette smoking and pneumococcal infections, underlying mechanisms remain elusive, partly due to a lack of animal models incorporating nasal pneumococcal colonization with cigarette smoke exposure. In chapter 3.2, we sought to establish a mouse model of cigarette smoke exposure over the course of nasal pneumococcal colonization. This model allowed us to investigate mechanisms predisposing smokers to pneumococcal infections by

examining the progression from an asymptomatic pneumococcal carrier state to the establishment of infectious disease. We hypothesize that cigarette smoke exposure attenuates nasal inflammatory responses normally induced by *S. pneumoniae* and predisposes mice to bacterial invasiveness into the lungs. Additionally, we postulate that the increased incidence of pneumococcal lung invasion in cigarette smoke-exposed mice to be dependent on increased PAFR expression and associated with decreased nasal mucociliary clearance. Data included in chapter 3.2 increase our understanding of cigarette smoke's effects on the bacterial host defence of the upper respiratory tract and will help guide future efforts to reduce pneumococcal disease burden.

1.6. The nasal bacterial microbiome

We are now increasingly aware of the importance of the human bacterial microbiota in health and disease. A variety of bacteria colonize the skin as well as mucosal surfaces of the body including the oral cavity, gut, vagina, upper respiratory tract, and lungs[162–165]. These microbes react to and influence the microenvironment that they occupy as they interact with each other and the host, with some beneficial outcomes for the host[166,167]. The microbiota plays an important role in food metabolism, modulates the host immune system, and offers protection from pathogen invasion, termed "colonization resistance"[168–170]. Smokers have been observed to have increased pathogen acquisition in the URT[123]. Although this can be explained in part by cigarette smoke's impact on the respiratory host defence, another mechanism that may contribute to increased pathogen acquisition is perturbation of the nasal microbiota. Of note, bacteria are also exposed to cigarette smoke as they colonize the URT. The

impact of cigarette smoke exposure on nasal bacterial communities, and how this may be related to increased pathogen acquisition, remain unclear.

Microbes establish ecological relationships with each other and the specific environment of their tissue site, which is reflected in the composition of the specific microbial community. For example, although the URT of healthy individuals have been found to usually contain bacteria from the phyla Firmicutes, Proteobacteria, Actinobacteria, and sometimes Bacteroidetes, within-niche variation occurs from individual to individual as a result of microbe-microbe and microbe-host interactions[164]. In the human anterior nares, four distinct microbiota profiles have been observed, each with a predominance of bacteria from the genera *Corynebacterium, Propionibacterium* (both phylum Actinobacteria)*, Moraxella* (phylum Proteobacteria)*, or Staphylococcus* (phylum Firmicutes)[171]. Microbes that share similar physical and chemical growth conditions, or share cooperative relationships such as cross-feeding and co-aggregation, may co-occur in the same niche. Others may exhibit exclusion interactions due to toxin production, an unfavourable environmental impact on other bacterial species, immuno-modulation, or a requirement for similar host adhesion receptors and nutrient resources[147,166,167,172]. An example of co-occurrence is the enrichment of *Propionibacterium acnes* in persistent carriers of *Staphylococcal aureus*[173]. An explanation for this is that *Propionibacterium*, which can hydrolyse sebum lipids from glands of the anterior naris keratinized squamous epithelium to generate short-chain free fatty acids, lowers the pH of the surrounding microenvironment, favouring *Staphylococcus* and *Corynebacterium* growth[174,175]. On the other hand, competitive interactions between bacteria, such as the production of bacteriocins (secreted bacterial

peptides that are active against other bacteria), are emerging as an area of interest as they can potentially be applied to prevent pathogen outgrowth[176]. *E. coli* H22 has been observed to produce several bacteriocins that inhibit *Klebsiella pneumoniae* and *Salmonella in vitro*, and may be responsible for the reduction of gut *Shigella flexneri* levels in germ free mice[177]. The URT is constantly exposed to new microbes with colonizing potential from both the environment, including airborne or food associated microbes, and other tissue sites, such as drainage from the middle ear, sputum from the lungs, and regurgitation from the stomach. It is thought that colonization resistance provided by competitive interactions of the local microbiota help contain both acquired and resident opportunistic pathogens at the URT[175].

The diverse composition of the microbiota, encompassing both richness (species number) and evenness (species distribution), is a feature associated with ecological stability over time and health of the host[121,175]. This association may be related to the idea that more taxa add ecological function to the community and also increases the redundancy of specific functions. A highly diverse community may therefore be more resilient to environmental stress as it has a higher probability of containing a taxon resistant to that particular stress and thus more likely to retain that ecological function[166]. Along these lines, a highly diverse ecosystem was observed to be more stable over time[178]. Diversity may be important to the ability of the microbiota to resist pathogen acquisition[121]. Thus a perturbation of microbial diversity may compromise colonization resistance. Indeed, dysbiosis, an imbalance of the microbiota composition, is associated with many diseases. Children with mild URT infections and colonized with the potential pathogens *S. pneumoniae*, *M. catarrhalis*, and *H. influenzae* have

decreased nasal microbial diversity, with less abundance of the commensals *Lactococcus, Anoxybacillus, Corynebacterium and Dolosigranulum*, as compared to controls[179]. Similarly, both nasal microbial richness and evenness was decreased in children with acute otitis media when compared to healthy children[180]. Lastly, depletion of the resident sinus microbiome in mice was associated with more severe features of chronic rhinosinusitis upon administration of the disease associated bacterium *Corynebacterium tuberculostearicum*[181]. These data suggest that maintaining microbiota diversity may be part of the first line of defence to both resist new pathogen acquisition and contain resident pathogenic bacteria.

1.7. Cigarette smoking and the nasal microbiome

Cigarette smoke exposure is an environmental stress that may perturb the balanced ecological composition of the URT microbiota. Smokers are reported to have microbial dysbiosis that could compromise colonization resistance. In a study examining nasopharyngeal bacterial cultures from 20 smokers and 20 non-smokers, increased recovery of potential pathogens, including *S. pneumoniae*, *H. influenzae*, *M. catarrhalis*, and *S. pyogenes*, were observed in smokers. Additionally, less bacterial isolates (including α-hemolytic streptococci, nonhemolytic streptococci, *Prevotella*, and *Peptostreptococcus*) capable of competing with the growth of these potential pathogens *in vitro* were found in the resident microbial flora of smokers, with fewer instances of interference as compared to non-smoker microbiota[123]. Highly sensitive, global sequencing approaches also confirm an increase in the presence of potential pathogens such as *S. aureus* and *Haemophilus* in the URT of smokers. Other Firmicutes, including *Streptococcus*, have increased abundance in both the nasopharynx and the middle

meatus of smokers while a reduction in Actinobacteria, such as *P. acnes* and *Corynebacterium* was observed[164,182]. Of note, *Corynebacterium* presence may be protective for otitis media and was associated with decreased *S. pneumoniae* URT colonization[183]. In addition, smokers who underwent smoking cessation for 12-15 months had reduced occurrences of nasopharyngeal pathogen isolation and restored presence of pathogen-interfering microbial flora bacterial isolates, further suggesting an effect of cigarette smoke on nasal microbiota composition[184]. It is plausible that cigarette smoke may facilitate pathogen colonization by introducing microbiota dysbiosis and compromising colonization resistance at the URT. Increased incidences and duration of nasal pathogen colonization, in turn, may contribute to the increased risk of bacterial infectious disease, such as IPD, observed in smokers.

There are multiple reports that cigarette smoke exposure increases the risk of pneumococcal nasal colonization in humans[185–187]. Although this may be attributable to the nasal microbiota dysbiosis observed in smokers, current studies (outlined above) are mostly descriptive and cross-sectional. For example, the URT microbiota analysis of smokers mostly assess microbial composition when the pathogen acquisition event has already taken place. Hence, it is unclear whether the microbial dysbiosis (as compared to non-smokers without pathogen acquisition) is present prior to pathogen exposure in smokers, therefore linking microbial dysbiosis with increased risk of pathogen acquisition, or if changes in microbiota composition actually occurred as a consequence of the establishment of pathogen colonization. Thus the impact of cigarette smoke exposure on the URT microbiota composition is difficult to interpret without appropriate controls to assess the impact of pneumococcal exposure alone. Along these lines, a

human experimental nasal pneumococcal carriage model showed that pneumococcal challenge alone was sufficient to decrease *Corynebacterium* abundance in the nasal wash as compared to baseline microbial composition prior to pneumococcal exposure[188]. Furthermore, a loss of nasal microbiota diversity was observed in mice upon nasal pneumococcal colonization, with a transient dominance of pneumococci[189]. Although highly informative, other limitations of descriptive, cross-sectional studies include the inability to control for differences in environmental exposure and timing of pathogen acquisition between individuals. Therefore, experimental models to investigate nasal pneumococcal colonization and microbiota composition in the context of cigarette smoke exposure are warranted.

In chapter 3.2, we characterized a model of nasal pneumococcal colonization in cigarette smoke-exposed mice, which allows us to control the duration of cigarette smoke exposure and timing of colonization. This model provides us with a powerful tool to understand the relationship between nasal microbiota composition and pneumococcal colonization in the context of cigarette smoke exposure. In chapter 3.3, we hypothesize that cigarette smoke exposure causes nasal microbiome dysbiosis in mice associated with increased nasal pneumococcal colonization upon experimental nasal pneumococcal challenge. To our knowledge, this is the first study to investigate the link between nasal microbiome dysbiosis and nasal pathogen colonization in the context of cigarette smoke exposure. The studies presented in chapter 3.3 increase our understanding of the impact of cigarette smoke exposure on bacterial community interactions, and may contribute to the continued efforts to reduce infectious disease burden.

1.8. Central paradigm

Cigarette smoke exposure is well documented to predispose to bacterial infections. Furthermore, once acquired, lung bacterial infections accelerate progression of the smoking-related respiratory disease COPD by further amplifying the pre-existing inflammatory response. Acquired lung infections in smokers may be related to an inability to control colonizing bacterial pathogens at the URT. Of note, smokers also have an increased incidence of pathogen acquisition that may be related to perturbations of the nasal microbiota. We postulate that cigarette smoke exposure alters bacterial-host interactions, as well as bacterial community interactions, to promote infection and disease. To address these ideas, we present the following specific hypotheses and studies.

1.9. Specific hypotheses

1. We hypothesize that cigarette smoke exposure exacerbates the neutrophilic response to NTHi lung infection by skewing the lungs towards amplified IL-1α expression.

2. We hypothesize that cigarette smoke exposure attenuates nasal inflammatory responses normally induced by *S. pneumoniae* and predisposes mice to bacterial invasiveness into the lungs. Additionally, we postulate that the increased incidence of pneumococcal lung invasion in cigarette smoke-exposed mice to be dependent on increased PAFR expression and associated with decreased nasal mucociliary clearance.

3. We hypothesize that cigarette smoke exposure causes nasal microbiome dysbiosis associated with increased pneumococcal nasal colonization in mice.

1.10. Study summaries

Chapter 3.1: We confirmed that cigarette smoke-induced neutrophilia is IL-1α, and not IL-1β, dependent utilizing mice deficient in these specific cytokines. Utilizing IL-1α chimeric mice, we also showed that IL-1α from the hematopoietic cell compartment, likely the AM, is critical to cigarette smoke-induced neutrophilia. We observed AMs from cigarette smoke-exposed mice to have an altered inflammatory mediator expression profile with increased IL-1α expression in response to NTHi stimulation. Cigarette smoke exposure primed the lungs towards exacerbated neutrophilia upon NTHi infection. Repeated NTHi infection in cigarette smoke-exposed mice increased lung compliance and airspace size, suggesting the exacerbated neutrophilia to cause lung damage, consistent with COPD disease progression following an exacerbation. The amplified inflammatory response to bacteria was dependent on IL-1R1 and IL-1α, but not IL-1β. Downstream of IL-1 signalling, exacerbated neutrophilia correlated with levels of CXCL-5 and was CXCR2 dependent. We conclude that cigarette smoke-induced inflammation is driven by IL-1α likely expressed by AMs, and that cigarette smoke exposure primes the lungs towards amplified IL-1α expression upon NTHi infection, leading to an exacerbated neutrophilic response. Our study suggests IL-1α may be a relevant therapeutic target for controlling inflammation during bacterial exacerbations of COPD. The study presented in chapter 3.1 has been published in the *Journal of Immunology*.

Chapter 3.2: Cigarette smoke exposure attenuated nasal inflammatory mediator expression induced by nasal pneumococcal colonization, including TNF-α, CXCL-1, and CXCL-2. Furthermore, while *S. pneumoniae* elicited a significant increase in nasal neutrophil levels in room air-exposed mice, there was no significant increase in smoke-exposed mice, suggesting that the ability to recruit additional neutrophils may be impaired by cigarette smoke exposure. Continuous cigarette smoke exposure over the course of nasal pneumococcal colonization predisposed mice to mortality associated with IPD. Bacteraemia associated with leukopenia, serum IL-6 presence, and inflammatory infiltrates at the meninges indicated mice developed sepsis and meningitis. Interestingly, we observed pneumococci in the spleen, but not BAL, in some mice. In addition, mice did not show overt signs of pulmonary inflammation, suggesting the absence of pneumonia. Imaging studies utilizing a radioactive ligand showed that short term cigarette smoke exposure did not compromise nasal clearance or epithelial barrier integrity. PAFR or IL-1α deficiency also did not rescue cigarette smoke-exposed mice from IPD associated mortality. Mice were completely rescued from IPD following smoking cessation during nasal pneumococcal colonization. This was associated with increased nasal CXCL-2 and neutrophil levels in the cessation group. Our data suggest that cigarette smoke exposure may increase the risk of not only pneumonia, but also occult pneumococcal bacteraemia. Mechanistically, we propose cigarette smoke to attenuate a pro-inflammatory environment at the nasopharynx normally induced by *S. pneumoniae*, which hinders recruitment of crucial cellular effectors required for the prevention of IPD. The study presented in chapter 3.2 has been published in *Infection and Immunity*.

Chapter 3.3: We observed that cigarette smoke exposure alone did not impact nasal microbiome composition in mice. Microbiome composition was also unchanged at an early time point (12 h) following low dose nasal pneumococcal inoculation in cigarette smoke-exposed mice, suggesting that cigarette smoke exposure did not impair the ability of the microbiome to resist initial nasal pneumococcal acquisition. However, established high dose nasal pneumococcal colonization in cigarette smoke-exposed mice was associated with nasal microbiome dysbiosis. Notably, we observed an enrichment in other potential pathogens including *Fusobacterium*, *Gemella*, and *Neisseria*. Our findings suggest that clinical observations of nasal microbiome dysbiosis in smokers may occur as a consequence of increased pathogen colonization. Thus, cigarette smoke exposure may increase nasal pneumococcal colonization by impacting other aspects of bacterial-host interactions independent of nasal microbiome composition. The study presented in chapter 3.3 is in preparation for submission to *Infection and Immunity*.

CHAPTER 2. MATERIALS AND METHODS

2.1. Animals

6-8 week old female BALB/c and C57BL/6 mice were purchased from Charles River Laboratories (Saint-Constant, PQ, Canada) and the Jackson Laboratory (Bar Harbor, ME) for experiments presented in Chapter 3.1. For all *S. pneumoniae* studies, 10-12 week old female C57BL/6 mice were from The Jackson Laboratory only. CXCR2 knockout (KO) mice on a BALB/c background and IL-1R1 KO mice on a C57BL/6 background were acquired from the Jackson Laboratory. PAFR deficient mice on a C57BL/6 background were a kind gift from Dr. Elaine Tuomanen[190]. IL-1α KO mice and IL-1β KO mice on a C57BL/6 background were a kind gift from Dr. Yoichiro Iwakura (University of Tokyo)[191] and were bred in house. Mice were housed under specific pathogen-free conditions with a light-dark cycle of 12 hours and *ad libitum* access to food and water. All experimental procedures were approved by the Animal Research Ethics Board of McMaster University.

2.2. Cigarette smoke exposure

Mice were exposed to the mainstream smoke from 12 3R4F reference cigarettes (Tobacco and Health Research Institute, University of Kentucky, Lexington, KY), with filters removed, for 50 minutes, twice daily, at 5 days per week using a whole body cigarette smoke exposure system (SIU-48, Promech Lab AB (Vintrie, Sweden)) as reported previously[72]. Prior to cigarette smoke exposure, mice were acclimatized to the restrainers for 20 minutes on the first day, 30 minutes on the second day, and 50 minutes on the third day. Control mice were exposed to room air only.

2.3. Bacterial preparation

The nontypeable *Haemophilus influenzae* (NTHi) strain 11P6 is a clinical strain isolated from the sputum of a COPD patient experiencing an exacerbation and provided to us by Dr. Sanjay Sethi (VA Medical Research, Buffalo, NY). NTHi was streaked on chocolate agar plates containing 1% IsoVitaleX (BD Biosciences, Franklin Lakes, NJ). Single colonies were picked and grown to log phase in brain-heart infusion (BHI) broth (Difco, Fisher Scientific, Ottawa, ON, Canada) supplemented with Hemin and nicotinamide adenine dinucleotide (NAD) (Sigma, Oakville, ON, Canada). The inoculated BHI + Hemin+ NAD broth was maintained on a rotary shaker at 37ºC until an OD value of 0.7-0.8 was obtained at a 600nm wavelength. Colony forming units (CFU) were predicted from the OD value based on a previously generated standard curve. NTHi was washed three times with PBS, re-suspended in RPMI and diluted to a ratio of 10 CFU/cell (for alveolar macrophage culture), or to 10^6 CFU in 35µl PBS (for intranasal challenge in mice).

Stocks of *S. pneumoniae* P1547, a serotype 6A virulent clinical isolate[192,193], and *S. pneumoniae* TIGR4, a serotype 4 clinical isolate[194,195], were streaked on tryptic soy agar (BD Biosciences, Franklin Lakes, NJ) supplemented with 5% sheep's blood (Cedarlane, Burlington, ON, Canada) and neomycin (Sigma-Aldrich, Oakville, ON, Canada), at 10µg/ml for P1547 and 5µg/ml for TIGR4. Single colonies were picked and grown to log-phase in tryptic soy broth (BD Biosciences, Franklin Lakes, NJ) containing neomycin. CFU were predicted from the OD value at 600 nm based on a previously generated standard curve. The bacteria were washed three times with PBS, re-suspended and diluted to the indicated dose in PBS for nasal inoculation into mice.

2.4. NTHi lung challenge in mice

Following the final cigarette smoke exposure, mice were anesthetised with isoflurane and administered 10^6 CFU NTHi in 35µl PBS intranasally. Mice were sacrificed 12 hours post-infection for sample collection.

2.5. Nasal pneumococcal colonization

Mice were room air- or cigarette smoke-exposed for 1 week prior to nasal pneumococcal colonization. Following cigarette smoke exposure on day 1 of the second week, mice were intranasally inoculated, in the absence of anaesthesia, with 10µl containing the indicated strain and dose (CFU) of *S. pneumoniae*. Mice continued to be cigarette smoke-exposed post-nasal colonization without interruption. Mice were given HydroGel® and placed on heating pads following each cigarette smoke exposure for the first 3 days post bacterial inoculation to facilitate establishment of nasal colonization.

2.6. Survival studies

According to the Canadian Council on Animal Care Guidelines, the death of experimental animals is considered unethical. Therefore, mice were subjected to endpoint monitoring based on criteria predetermined in our Animal Utilization Protocol. Briefly, animals were scored based on appearance, behaviour, hydration status, and clinical signs, as reported in detail previously[196]. Mice were considered to be at endpoint when presenting with a score higher than 9 or greater than 20% weight loss at two consecutive readings 4 hours apart. Mice reaching endpoint were sacrificed for sample collection for the indicated duration of the survival study. Surviving mice were sacrificed on the indicated end date of the study.

2.7. Sample collection

Mice were sacrificed for the collection of nasal wash, complete nasal turbinates (CNT), and bronchoalveolar lavage (BAL), as well as the generation of lung, brain and spleen homogenates. Briefly, the trachea was canulated and nasal wash collected from the nares by instilling 200µl PBS through the trachea. The multi-lobe right lung was tied off prior to BAL collection. To generate BAL, the left lung lobe was instilled with 250µl, then 200µl of PBS. Lung homogenates were generated in 1ml of PBS from the unlavaged right lung lobes using a Polytron PT 2100 homogenizer (Kinematica, Switzerland) at 21,000-25,000 rpm for 3-6 seconds. Similarly, brain and spleen homogenates were generated using the entire organ.

2.8. Bacterial burden determination

To assess NTHi burden, samples were plated on chocolate agar containing 1% IsoVitaleX. To assess *S. pneumoniae* burden, samples were plated on tryptic soy agar supplemented with sheep's blood (5%) and neomycin (10µg/ml for strain P1547, 5µg/ml for strain TIGR4). Bacterial CFU were counted following 24 hour incubation at 37ºC.

2.9. Determination of cellular inflammation

Total cell numbers in the BAL and blood were determined using a haemocytometer. BAL cytospins and blood smears were generated and stained with Hema 3 (Biochemical Sciences, Swedesboro, NJ). 500 and 200 cells were counted per slide to determine the relative proportion of mononuclear cells and neutrophils in the BAL and blood, respectively.

2.10. Cytokine measurement by ELISA

Cytokine levels in the BAL fluid (CXCL-1 and CXCL-2), lung homogenates (IL-1α and IL-1β), AM cell supernatants (IL-1α, IL-1β, and TNF-α), and serum (TNF-α and IL-6) were determined by enzyme-linked immunosorbent assay (ELISA) (R&D Systems, Minneapolis, MN) as per the manufacturer's instructions.

2.11. Taqman real-time RT-qPCR

Nasal wash was performed with RLT lysis buffer (Qiagen, Mississauga, ON, Canada) as previously described[158]. Lung tissue and precision cut lung slices were homogenized in RLT lysis buffer. AM cell lysates were also generated with RLT lysis buffer. RNA was isolated from samples using the RNeasy Mini Kit with optional DNase step (Qiagen). cDNA was synthesized with Superscript II Reverse Transcriptase (Invitrogen, Grand Island, NY) and TaqMan real-time RT-quantitative PCR (qPCR) was performed with the StepOnePlus™ Real-Time PCR System (Life Technologies Inc., Burlington, ON, Canada). *Tnfa*, *Cxcl1*, *Cxcl2*, *Cxcl5, Ptafr*, and *Il1a* expression were determined using the ΔΔCt method. Target gene expression was first normalized to the housekeeping gene *Gapdh* of the same sample and subsequently expressed as fold change over the indicated control group.

2.12. Macrophage isolation and culture

BAL fluid was collected after instilling the whole lung with 1 ml PBS. This process was repeated 5 times to maximize cell recovery. BAL cells were re-suspended in 500µl fresh PBS. AMs were identified and counted using a haemocytometer. BAL cells were re-suspended in RPMI supplemented with 10% FBS (Sigma-Aldrich, Oakville, ON,

Canada), 1% L-glutamine, 1% penicillin/streptomycin (Invitrogen, Grand Island, NY), and 0.1% β-mercaptoethanol (Invitrogen) and cultured in polystyrene flat-bottomed 96 well plates at 50,000 AMs per well. AMs were incubated at 37ºC and 5% CO_2 for 1 hour to facilitate adherence. Non-adherent cells were removed by washing three times with warm PBS. AMs were cultured for 24 hours with RPMI alone, in the presence of 1μg/ml Pam3CSK4, 1μg/ml LPS (Invivogen, San Diego, CA), or 10CFU/AM of NTHi. AM supernatants were collected for cytokine measurement by ELISA. To determine IL-1α mRNA expression, AMs were cultured with LPS for 4 hours, and cells were collected in RLT lysis buffer for subsequent RNA isolation and Taqman real-time RT-qPCR.

2.13. Immunohistochemistry

Lungs were fixed at 30 cm H_2O pressure in 10% formalin after BAL collection. Samples were further fixed with formalin for at least 24 hours. The lungs were paraffin embedded and 4-μm slices were generated. Tissues were treated in 0.01 M citrate buffer for 45 minutes to retrieve antigen and incubated for 1 hour with either anti–IL-1α polyclonal goat Ab or anti-CXCL5 polyclonal rabbit Ab (R&D Systems) diluted in UltrAb diluent (Thermo Scientific, Rockford, IL) at 7 mg/ml. Immunohistochemistry was developed with goat on rodent HRP probe (Biocare, Concord, CA) or anti-rabbit Dakocytomation HRP (Dako Canada, Burlington, ON, Canada) and counterstained with Meyer's solution.

2.14. Precision cut lung slice culture

Lung slices were generated as previously described[88]. Lungs were inflated with warmed (37ºC) 2% agarose (Sigma-Aldrich) in HBSS supplemented with HEPES (Sigma-Aldrich). After cooling, the lungs were dissected and maintained in an ice-cold HBSS

solution prior to and during slicing. Slices at 120 µm were generated using a vibratome (Leica Microsystems, Concord, ON, Canada). We were able to generate approximately 40 slices from each mouse lung, which were then cultured in Dulbecco's Modified Eagles Medium (DMEM)/F12 (Gibco, Burlington, Canada) supplemented with 35 mg/ml L-ascorbic Acid (Sigma-Aldrich), 5 mg/ml transferin (Gibco), 2.85 mg/ml Insulin (Sigma-Aldrich), and 3.25 ng/ml selenium (atomic absorption standard solution; Sigma-Aldrich). Following 0.22 mm filter-sterilization, the DMEM/F12 solution was additionally supplemented with 250 ng/ml amphotericin B (Sigma-Aldrich) and 1% penicillin/streptomycin. To wash the lung slice culture, media was replaced every hour for 3 hours. Lung slices were cultured overnight and stimulated the following day with NTHi for 6 hours. Samples were collected in RNA later (Ambion, Austin, TX) and stored at -80ºC for RNA isolation.

2.15. Lung function measurement and assessment of pathology

Forced oscillation measurements were performed using the FlexiVent ventilator system (SCIREQ, Montreal, QC, Canada). Mice were anesthetised with 10mg/kg xylazine (BayerHealthcare, Berlin, Germany) and 30 mg/kg sodium pentobarbital (Ceva, Lenexa, KS) by intraperitoneal injection. Mice were then immobilized by intraperitoneal injection of 10 mg/kg rocuronium bromide (V Laboratories, Montreal, QC, Canada). Tracheostomy was performed using a blunted 18-gauge needle. Oxygen saturation and heart rate were continuously monitored using an infrared pulse oxymeter (Biox 3700; Ohmeda, Boulder, CO). The animal was connected to a computer-controlled Flexivent ventilator. All mice were ventilated with 150 breaths/minute, with an applied pressure limit of 30 cm H_2O. A snapshot perturbation manoeuvre was performed with forced

oscillation perturbation consequently applied. Maximal pressure-regulated pressure-volume loops were generated to obtain maximal vital (total) lung capacity and static compliance. Animals were removed from the ventilator and immediately euthanized following data collection.

Lungs were formalin fixed and paraffin embedded to generate H&E-stained slides. Three lung slices were generated for each sample. Each lung section was imaged in its entirety, and the airspace size was quantified by Pneumometrics Software (version 1) as described[197].

2.16. Pathology

Mice reaching endpoint were anesthetised by intraperitoneal injection with an overdose of pentobarbital. The chest cavity was opened to expose the heart and 50 U of heparin was injected into the heart apex. Mice were perfused through the heart with lactated ringer's solution first, then with 10% formalin to fix all organs. The heart and brain were collected and fixed in formalin for at least 24 hours. In a separate experiment, the single lobe lung was fixed at 30cm H_2O pressure in 10% formalin following the collection of BAL. After fixation in formalin for at least 24 hours, tissues were paraffin embedded, sectioned, stained with H&E, and examined by a trained pathologist.

2.17. Gram stain

Gram stain was performed on heart microlesions based on the Brown and Hopps method. Briefly, sections were treated with crystal violet, decolourized so that the blue-violet stain from Gram-negative bacteria was removed, and counterstained with Fuchsin to dye Gram-negative bacteria red.

2.18. Flow cytometry

Nasal wash samples were stained with fluorescent antibodies by incubation at 4ºC and assayed with a BD LSRII flow cytometer on the same day. Data were gathered with FACSDiva software (BD) and analyzed with FlowJo software (TreeStar).

2.19. Imaging

Room air or cigarette smoke-exposed mice were anesthetised by intraperitoneal injection with ketamine/xylazine and nasally inoculated with ^{99m}Technetium-diethylene triaminepentaacetic acid (^{99m}Tc-DTPA) (Lantheus Medical Imaging, North Billerica, MA) at a time point corresponding to day 3 post-nasal colonization. Dynamic images of mice were obtained by SPECT every 30 seconds for 20 minutes to observe distribution of the radioligand (X-SPECT system, GammaMedica-Ideas, Northridge, CA). The mean count from the nasal region of interest was converted to percent of the highest count (obtained in the first frame) for each mouse and expressed as percent maximal activity. A whole body scan was performed 30 minutes post-nasal inoculation followed by a whole body CT. The upper airway dose of ^{99m}TC-DTPA as a percentage of the whole body distribution was compared between room air and cigarette smoke-exposed mice.

2.20. Bacterial genomic DNA extraction and nested PCR amplification

Mouse CNT was added to 800µl of 200mM monobasic Sodium Phosphate and 100µl of guanidine thiocyanate-ethylenediaminetetraacetic acid-Sarkosyl and homogenized with 0.2 g of 0.1mm glass beads (Mo Bio, Carlsbad, CA) for 3 minutes at 300rpm. DNA was extracted using MagMAX™ Express technology and the MagMAX™ DNA Multi-Sample Kit according to the manufacturer's instructions (ThermoFisher Scientific, Waltham,

MA). Briefly, homogenized samples were mixed with DNA binding beads in 96 well plates. Bound DNA was washed, treated with RNAse A, washed again and eluted from the beads with elution buffer.

Prior to 16S rRNA gene sequencing, nested PCR was performed with *Taq* polymerase (Life Technologies, Carlsbad, CA) to amplify the variable 3 (v3) region of the 16S rRNA gene. The first PCR amplification (15 cycles: 94°C - 30 seconds, 56°C- 30 seconds, 72°C - 60 seconds) targeted the v1-v5 region of the 16S rRNA gene using specific primers 8F (AGAGTTTGATCCTGGCTCAG) and 926R (CCGTCAATTCCTTTRAGTTT). Product from the first PCR was amplified again in a second PCR run (30 cycles: 94°C - 30 seconds, 47°C - 30 seconds, 72°C - 40 seconds) to amplify the v3 region, which is the region examined for Illumina MiSeq sequencing. The V3R primer used is identical across samples while V3F primers contained individual barcodes unique to each CNT sample to allow for multiplex amplification. Primer sequences were adapted from Bartram *et al*[198]. The PCR reaction was performed in triplicate to avoid PCR bias.

2.21. 16S rRNA gene sequencing, processing, and data analysis

Products from the nested PCR reactions were sequenced with the Illumina MiSeq platform according to the manufacturer's instructions at the McMaster University DNA Sequencing Facility. Sequencing data were processed as previously described[199,200]. Briefly, reads greater than the length of the 16S rRNA gene v3 region were trimmed using Cutadapt[201]. PANDASeq[202] was used to align paired-end reads and AbundantOTU+[203] was used to cluster reads into Operational Taxonomic Units (OTUs) based on 97% similarity. The Ribosomal Database Project classifer[204] was used against

the Greengenes[205] (February 4, 2011 release) reference database to assign taxonomy. Single sequence OTUs (i.e. singletons) were removed using Quantitative Insights into Microbial Ecology (QIIME)[206]. On average, there were 11,010 reads per sample (range 1,201-90,900) and 250 OTUs (range 94-582).

Data were analysed with various software. β-diversity between samples were assessed with Phyloseq[207] using the Bray Curtis distance metric and visualized by Principal Coordinates Analysis (PCoA) ordination. Differences between whole bacterial communities were tested for significance with vegan's[208] implementation of permutational multivariate analysis of variance (PERMANOVA) in the adonis command. R was used to generate taxonomic summaries. Differences in specific bacterial genera were computed with DESeq2[209]. A p-value of less than 0.01 was considered significant following DESeq2's implementation of the Benjamini-Hochberg multiple testing adjustment procedure.

2.22. *LytA* measurement by real-time RT-qPCR

Real-time RT-qPCR was performed with GoTaq qPCR Master Mix (Promega, Madison, WI) and the StepOnePlus™ Real-Time PCR System (Life Technologies Inc., Burlington, ON, Canada) following isolation of CNT genomic DNA to assess levels of the *S. pneumoniae* specific gene *LytA* as previously described[210]. *LytA* abundance was normalized to levels of the host housekeeping gene *Gapdh*. Forward and reverse primers used for *LytA* were: forward, 5'-AGTACCAGTTGCCGTCTGTG-3'; reverse, 5'-AAATGGGGCATTAGCCGTGA-3'. Forward and reverse primers used for mouse *Gapdh* were: forward 5'-GCACAGTCAAGGCCGAGAAT-3'; reverse 5'-GCCTTCTCCATGGTGGTGAA-3'.

2.23. Statistical analysis

Data are expressed as mean ± SEM. GraphPad Prism 5 (GraphPad Software Inc., San Diego, CA) and SPSS Software (IBM, Armonk, NY) were utilized for statistical analysis. Levene's test for equality of variances was used to account for differences in data variability between groups. Independent *t* tests were used for comparisons between two groups. As indicated, the Univariate General Linear Model was used prior to independent *t* tests for some experiments. Log-rank test was used for comparison of Kaplan-Meier survival curves. Differences of $p < 0.05$ were considered statistically significant. Inflammatory cell count data for key experiments in chapter 3.1 were pooled from 2 independent experiments.

CHAPTER 3. RESULTS

3.1. Cigarette smoke exposure primes the lungs towards exacerbated neutrophilia in response to NTHi challenge dependent on IL-1α

The study presented in chapter 3.1 (published in the *Journal of Immunology*) increased our understanding of the role of IL-1 signalling in bacterial exacerbations of cigarette smoke-induced inflammation. These data contributed to the decision process to pursue a phase 2 clinical trial investigating anti-IL-1R1 antibody therapy as a potential intervention strategy in COPD patients[211].

3.1.1. Cigarette smoke-induced neutrophilia is dependent on IL-1α from the hematopoietic cell compartment

To determine whether cigarette smoke-induced neutrophilia is IL-1α or IL-1β dependent, we cigarette smoke-exposed IL-1α KO and IL-1β KO mice for 4 days. Cigarette smoke exposure significantly increased IL-1α protein levels in the lung homogenate (Figure 1A). Cigarette smoke-induced neutrophilia in the BAL fluid was almost completely abolished in IL-1α KO mice, which was associated with a significant decrease in the neutrophil recruiting chemokines CXCL-1 and CXCL-5. IL-1β was also increased in the lung homogenate following cigarette smoke exposure, although cigarette smoke-induced neutrophilia was not decreased in IL-1β KO mice (Figure 1B). Additionally, although CXCL-1 levels in the BAL fluid were decreased in response to smoke by IL-1β deficiency, CXCL-5 levels remained unchanged. These data suggest cigarette smoke-induced neutrophilia is dependent on IL-1α, not IL-1β. We further investigated the cellular source of IL-1α contributing to cigarette smoke-induced inflammation. Chimeric

mice with IL-1α deficiency in either the structural (wild type donor bone marrow cells given to IL-1α KO recipients) or the hematopoietic (IL-1α KO donor bone marrow cells given to wild type recipients) cell compartments were generated and cigarette smoke-exposed for 4 days. We observed decreased neutrophilia only in the KO to wild type group, suggesting that cigarette smoke-induced neutrophilia was dependent on IL-1α derived from hematopoietic cells (Figure 1C). As our lab has previously observed intense IL-1α staining by immunohistochemistry on AMs from cigarette smoke-exposed mice[88], our findings suggest that cigarette smoke-induced neutrophilia is dependent on IL-1α derived from this cell type.

3.1.2. Cigarette smoke exposure primes AMs to produce IL-1α in response to bacteria

As AMs are involved in cigarette smoke-induced neutrophilia, we further investigated this cell type. Cigarette smoke exposure significantly increased mononuclear cell accumulation in the BAL fluid (Figure 2A). This was accompanied by an altered macrophage phenotype. As previously observed, macrophages from the BAL fluid of cigarette smoke-exposed mice had increased size, irregular shape and contained vesicle structures (Figure 2B)[110]. Furthermore, we showed that AMs cultured from cigarette smoke-exposed mice to produce increased IL-1α at baseline. IL-1α production by AMs cultured from cigarette smoke-exposed mice was further amplified following stimulation with Pam_3CSK_4, LPS, and NTHi (Figure 2C). A corresponding increase in IL-1α mRNA expression in AMs isolated from cigarette smoke-exposed mice was also observed following LPS stimulation (Figure 2D). On the other hand, TNF-α levels were significantly decreased in response to Pam_3CSK_4, LPS, and NTHi stimulation in AMs

isolated from cigarette smoke-exposed mice (Figure 2E). Lastly, IL-1β levels, although induced by bacterial stimulation in AMs isolated from cigarette smoke-exposed mice, were barely detectable and below the limit of quantification by ELISA (Figure 2F). These observations indicate that cigarette smoke exposure increased macrophage accumulation in the lungs and altered the AM towards a skewed inflammatory mediator expression profile, with exaggerated IL-1α expression in response to bacterial stimulation.

3.1.3. Cigarette smoke exposure primes the lungs towards exacerbated neutrophilia associated with increased CXCL-5 expression

To investigate the impact of cigarette smoke exposure on the pulmonary inflammatory response to bacteria, we challenged 8 week cigarette smoke-exposed mice intranasally with NTHi. Cigarette smoke exposure significantly increased BAL fluid mononuclear and neutrophil cell number as compared to room air control in response to NTHi challenge (Figure 3A). Neutrophilia induced by the combination of cigarette smoke exposure and NTHi infection was severely attenuated in CXCR2 KO mice (Figure 3B), confirming a role for this receptor in cigarette smoke-induced neutrophil recruitment[212]. We further observed that exacerbated neutrophilia in response to NTHi in cigarette smoke-exposed mice was associated with increased CXCL-5, but not CXCL-1 levels in the BAL fluid (Figure 3C). Immunohistochemistry show staining for CXCL-5 at the lung epithelium in NTHi-infected, cigarette smoke-exposed mice (Figure 3D). AMs cultured from 8 week cigarette smoke-exposed mice did not produce CXCL-5 in response to NTHi challenge (data not shown). However, precision cut lung slices generated from 8-week cigarette smoke-exposed mice, which contain epithelial cells, had increased CXCL-5 mRNA

expression as compared to room air control in response to NTHi stimulation in culture (Figure 3E). Overall, these findings show that cigarette smoke exposure exacerbates the lung neutrophilic response to NTHi infection dependent on CXCR2 and that the most important CXCR2 ligand may be CXCL-5.

3.1.4. Cigarette smoke exposure primes the lungs towards exacerbated neutrophilia dependent on IL-1R1

Given the importance of IL-1 signalling in cigarette smoke-induced inflammation, and our previous observations that cigarette smoke exposure primed AMs towards higher IL-1α expression in response to bacteria, we further investigated the role of IL-1R1 in the exacerbated neutrophilic response to NTHi in cigarette smoke-exposed mice. The increase in BAL fluid mononuclear and neutrophil cell numbers induced by NTHi in cigarette smoke-exposed mice was significantly attenuated with IL-1R1 deficiency (Figure 4A). Corresponding to decreased NTHI-induced neutrophilia in cigarette smoke-exposed IL-1R1 KO mice, CXCL-5 levels were also attenuated. Interestingly, we observed an increase in CXCL-1 levels in the same mice (Figure 4B). These data show that cigarette smoke exposure primes the lungs towards exacerbated neutrophilia dependent on IL-1 signalling, with a possible role for CXCL-5.

3.1.5. Cigarette smoke exposure primes the lungs towards exacerbated neutrophilia dependent on IL-1α

To further elucidate underlying mechanisms of the exacerbated neutrophilic response to NTHi in cigarette smoke-exposed mice, we assessed the relative contributions of IL-1α and IL-1β. We found significantly increased levels of IL-1α, but not IL-1β in the lung

homogenates of cigarette smoke-exposed mice following NTHi infection as compared to levels induced by NTHi infection alone (Figure 5A). Moreover, immunohistochemistry showed IL-1α staining to be mainly localized to the AM (Figure 5B), which is in agreement with our previous observations in Figure 2 that cigarette smoke exposure primes the AM towards amplified IL-1α expression in response to NTHi stimulation. To determine whether exacerbated neutrophilia in response to NTHi was IL-1α or IL-1β dependent in cigarette smoke-exposed mice, we repeated our bacterial infection model utilizing IL-1α KO and IL-1β KO mice. 8 week cigarette smoke-exposed IL-1α KO (Figure 5C), but not IL-1β KO mice (Figure 5D), showed significantly attenuated BAL fluid mononuclear and neutrophil cell numbers as compared to wild type control in response to NTHi challenge. These data provide strong evidence that cigarette smoke exposure primes the lungs towards exacerbated neutrophilia dependent on IL-1α, not IL-1β.

3.1.6. Targeting exacerbated neutrophilia may compromise bacterial clearance in cigarette smoke-exposed mice

To investigate the consequences of attenuating the excessive inflammatory response on bacterial clearance, we assessed bacterial burden in the lung homogenates of 8-week cigarette smoke-exposed IL-1R1 KO, CXCR2 KO, and IL-1α KO mice following NTHi infection (Figure 6). Both IL-1R1 and CXCR2 deficiency significantly increased the amount of NTHi cultured from lung homogenates of cigarette smoke-exposed mice, as compared to their wild type counterparts. In contrast, IL-1α deficiency did not increase NTHi burden in cigarette smoke-exposed mice. These data suggest that targeting IL-1α

during bacterial exacerbations may attenuate excessive neutrophilia without compromising lung bacterial clearance.

3.1.7. Repeated NTHi infections increases lung compliance and airspace enlargement in cigarette smoke-exposed mice

To investigate whether the exacerbated response to bacteria in cigarette smoke-exposed mice is associated with lung function decline, we assessed the effect of repeated NTHi infection over the course of long term cigarette smoke exposure on lung physiology and pathology in mice (Figure 7A). Using FlexiVent technology, pressure volume curves were generated. We observed a greater volume at lower pressures in the lungs of cigarette smoke-exposed mice as compared to room air control. This increase was even greater in the lungs of cigarette smoke-exposed mice that received repeated NTHi infections (Figure7B). For quantification, compliance of the lungs (Figure 7C) was calculated utilizing the data from Figure 7B. Airspace size was also quantified in lung histology slides generated from the same experiment. Airspace enlargement was significantly increased by cigarette smoke exposure and repeated NTHi infection as compared to cigarette smoke exposure alone, suggesting that increased lung damage is associated with the exacerbated inflammatory response to bacteria (Figure 7D). These data suggest that exacerbated neutrophilia in response to repeated bacterial infection and prolonged cigarette smoke exposure may contribute to lung function decline, consistent with COPD patients experiencing exacerbations.

In summary, data presented in chapter 3.1 suggest that cigarette smoke induces AMs to express IL-1α, which leads to neutrophil recruitment associated with increased CXCL-1 and CXCL-5 production. Cigarette smoke exposure also alters the AM

phenotype, priming them towards excessive IL-1α production in response to NTHi stimulation. IL-1α plays a critical role in the subsequent exacerbated neutrophilic response to NTHi associated with a further increase in CXCL-5 production (Figure 8). In association with this exacerbated neutrophilic response, repeated NTHi challenge in cigarette smoke-exposed mice led to increased lung damage. Thus, repeated exposure to bacteria over time in smokers may contribute to decline in lung function.

3.2. Cigarette smoke exposure attenuates the nasal host response to *S. pneumoniae* and predisposes mice to IPD

The study presented in chapter 3.2 (published in *Infection and Immunity*) investigated how cigarette smoke exposure impacts nasal pneumococcal colonization. This study is, to our knowledge, the first to document the progression from asymptomatic pneumococcal colonization to IPD in the context of cigarette smoke exposure. We showed that cigarette smoke exposure was associated with an attenuation of the nasal inflammatory response to *S. pneumoniae* and these data suggest that smokers may be at increased risk of occult bacteraemia. These findings have contributed to our understanding of the impact of cigarette smoke exposure on nasal pneumococcal colonization and may help future efforts to reduce the incidence of IPD.

3.2.1. Cigarette smoke exposure compromises the nasal host response following pneumococcal colonization

We investigated the effect of cigarette smoke exposure on nasal pneumococcal colonization. 1-week cigarette smoke-exposed mice were nasally colonized with *S. pneumoniae* and sacrificed on day 2 post-colonization. While the nasal pneumococcal

burden was comparable to room air control (Figure 9A), we observed an attenuation of nasal TNF-α, CXCL-1, and CXCL-2 expression in cigarette smoke-exposed mice (Figure 9B). Correspondingly, room air control mice had a significant increase in nasal neutrophils following pneumococcal colonization as assessed by flow cytometry (Figure 9C). However, there was no significant increase in response to pneumococcal colonization in cigarette smoke-exposed mice, suggesting that the ability to recruit additional neutrophils may be impaired. Lastly, cigarette smoke exposure did not impact nasal CCL2 expression (Figure 9B) or the proportion of macrophages (Figure 9C). Our findings suggest that cigarette smoke exposure may impair the host response to *S. pneumoniae* at the nasal mucosa.

3.2.2. Cigarette smoke exposure predisposes mice to IPD and mortality following nasal pneumococcal colonization

To investigate the consequences of a compromised nasal host response, the health status of mice was monitored for 16 days post-nasal colonization over the course of continuous cigarette smoke exposure. Mice assessed to be at endpoint, as determined by appearance and behaviour, were euthanized over the course of the study. Cigarette smoke exposure increased the frequency of mice reaching endpoint (60%), compared to room air control (10%) (Figure 10A). Rapid weight loss was observed in endpoint mice (Figure 10A). To determine if mortality was associated with IPD, we cultured for pneumococci in the lungs, spleen, and brain. Nasal wash cultures indicated successful colonization (Figure 10B and C). In addition, we detected pneumococci in the BAL, lungs, spleen, and brain of endpoint mice (Figure 10B). Interestingly, two endpoint mice had pneumococci in the lung homogenate, but not BAL. While surviving room air control

mice remained nasally colonized, no bacteria were cultured from other tissues (Figure 10C). Cigarette smoke-exposed mice surviving to day 16 had higher nasal bacterial burden than control mice. Of note, some surviving cigarette smoke-exposed mice also had pneumococci in the brain, and IPD may have developed if the study had continued longer (Figure 10C).

Mortality following cigarette smoke exposure occurred over a range of initial bacterial inoculation doses (Figure 11). At the low (10^5 CFU) and intermediate (10^6 CFU) bacterial doses, cigarette smoke-exposed mice reached endpoint at a rate that was significantly higher than room air-exposed mice. Mortality was delayed and occurred over a longer span of time in mice inoculated with the low bacterial dose. At the high bacterial dose (10^7 CFU), both room air and cigarette smoke-exposed mice reached endpoint. Although the low bacterial dose group appeared to have higher mortality rates compared to the intermediate and high dose groups, the survival curves of cigarette smoke-exposed mice at these three doses were not significantly different from each other as assessed by log rank test ($p=0.7294$). Our results show mortality in cigarette smoke-exposed mice over a range of initial pneumococcal inoculum doses. Overall, these data provide strong evidence that cigarette smoke exposure following nasal pneumococcal colonization increases the incidence of IPD and mortality in mice.

3.2.3. Endpoint mice show characteristics of sepsis and meningitis

Given the presence of pneumococcal bacteraemia in endpoint mice, we looked for abnormalities characteristic of sepsis. Total blood leukocyte number was lower in all endpoint mice compared to both vehicle control and surviving mice. Differential cell counting showed reduced mononuclear cells, but not neutrophils (Figure 12A).

Moreover, we detected IL-6 in the serum of endpoint mice (Figure 12B). The presence of serum cytokines, combined with blood leukopenia and evidence of bacteraemia (Figure 10B), indicate that endpoint mice developed sepsis.

We next assessed the histopathology of endpoint mice and observed neutrophilic inflammation at the meninges, characteristic of meningitis (Figure 12C and F). Endomyocarditis was also noted, with an area of intense neutrophil accumulation in one case (Figure 12D and G). Notably, microlesions were present within the myocardium (Figure 12E), which stained Gram positive (Figure 12H), likely due to pneumococcal presence. Strikingly, the lungs of cigarette smoke-exposed endpoint mice were without evidence of overt inflammation and tissue consolidation (Figure 13A), and comparable to those of cigarette smoke-exposed surviving mice (Figure 13B). The lack of inflammation was also reflected in the BAL cell counts of endpoint mice (Figure 13C). Our observations suggest that endpoint mice develop IPD in the absence of pneumonia, leading to meningitis, sepsis, endomyocarditis and cardiac damage.

3.2.4. Invasive infection occurs rapidly into the blood and brain of cigarette smoke-exposed mice

To characterize the pattern of bacterial dissemination from nasal colonization, we sacrificed cigarette smoke-exposed mice daily post-nasal colonization and assessed pneumococcal burden in the BAL, spleen, and brain. Mice reaching endpoint outside of the indicated time points were excluded from the study. Widespread bacterial dissemination occurred on days 3 and 4, as shown by the percentage of mice with pneumococci in various tissues (Figure 14A). Of note, the majority of mice showed no obvious change in health status (Figure 14A). In some mice, bacteria were detected in

the spleen only, the brain only, or simultaneously in the brain and spleen without presence in the BAL (Figure 14B). Interestingly, there was no case of pneumococcal detection in the BAL only, and we observed no increased BAL cellular inflammation in mice with detectable BAL bacteria, as compared to mice without bacterial dissemination (Figure 15A). In addition, nasal bacterial burden was not increased despite widespread bacterial dissemination (Figure 15B). Finally, we observed no bacterial dissemination in room air control mice except in one case (Figure 14C). Overall, these data suggest that more bacterial dissemination occurs in cigarette smoke-exposed mice compared to control, and that the point of dissemination may be the nasopharynx, rather than the lungs.

3.2.5. Cigarette smoke exposure does not compromise nasal clearance or epithelial barrier integrity

To investigate whether cigarette smoke exposure predisposed to IPD by compromising nasal clearance or epithelial barrier integrity, we administered ^{99m}Tc-DTPA intranasally to room air- and cigarette smoke-exposed mice at a time point corresponding to day 3 post-nasal colonization, when bacterial dissemination is first observed. Dynamic images were obtained by SPECT to observe nasal clearance of the radioligand. The activity of ^{99m}Tc-DTPA in the upper airways, measured every 30 seconds, was comparable between room air and cigarette smoke-exposed mice (Figure 16A). Representative images are shown (Figure 16B). To determine whether cigarette smoke exposure compromised nasal epithelial barrier function, we assessed the upper airway dose of ^{99m}TC-DTPA as a percentage of the whole body distribution (outlined in Figure 16C). At 30 minutes post-nasal delivery, the ^{99m}Tc-DTPA was still mainly confined to the upper

respiratory tract (Figure 16D), and there was no significant difference in the upper airway dose of ^{99m}TC-DTPA between room air (75.2 ± 1.3%) and cigarette smoke-exposed animals (73.9 ± 0.34%) as a percentage of whole body distribution. These data suggest that short-term cigarette smoke exposure alone does not impact either nasal clearance or epithelial barrier integrity in the upper airways.

3.2.6. PAFR or IL-1α deficiency does not rescue cigarette smoke-exposed mice from mortality following nasal pneumococcal colonization

S. pneumoniae is known to bind several host receptors including the PAFR[145–147], which may facilitate bacterial invasion independent of epithelial barrier function. Of particular interest, *S. pneumoniae* has been shown to adhere to and invade host cells activated by cytokines such as TNF-α and IL-1α, in a PAFR-dependent manner[147]. Moreover, both PAFR and IL-1α are increased in the lungs of smokers and COPD patients[88,148,213]. Therefore, cigarette smoke exposure may predispose to IPD by inducing PAFR expression in an IL-1α-dependent manner. In support of this hypothesis, we found that cigarette smoke exposure significantly up-regulated lung mRNA expression of both PAFR and IL-1α. Furthermore, the cigarette smoke-induced increase in lung PAFR mRNA expression was IL-1α dependent (Figure 17A). In contrast, cigarette smoke exposure attenuated PAFR and IL-1α expression at the nasopharynx (Figure 17B). Functionally, IL-1α or PAFR deficiency did not rescue cigarette smoke-exposed mice from mortality (Figure 17C). PAFR or IL-1α deficiency also did not significantly affect the survival of corresponding room air controls as compared to wild type mice (data not shown). Our findings show differential regulation of PAFR and IL-1α by cigarette smoke exposure between the upper and lower respiratory tract. Furthermore, the increased

susceptibility to IPD caused by cigarette smoke exposure occur independently of PAFR and IL-1α.

3.2.7. Smoking cessation fully protects mice from mortality following nasal pneumococcal colonization

Mice were completely rescued from IPD if cigarette smoke exposure was stopped following nasal pneumococcal colonization, suggesting that smoking cessation may be the most effective intervention strategy (Figure 18A). The increased survival rate was associated with an increase in nasal neutrophils in the cessation group (Figure 18B). Although smoking cessation did not impact the nasal expression of TNF-α as compared to cigarette smoke-exposed mice, we did observe an increase in CXCL-1 and CXCL-2 expression (Figure 18C). These data suggest that the increased incidence of IPD following cigarette smoke exposure is reversible and smoking cessation may recover nasal CXCL-1 and CXCL-2 expression, as well as neutrophil recruitment.

In Chapter 3.2, we show a mouse model that closely reflect clinical observations of cigarette smoke exposure as a risk factor for the development of IPD. Mechanistically, we propose that cigarette smoke exposure attenuates nasal inflammation normally elicited by *S. pneumoniae*, which hinders recruitment of crucial cellular effectors required for the prevention of IPD. Our data also suggest that smoking cessation may be the most effective intervention strategy to reduce the incidence of IPD. However, given the high prevalence of cigarette smoking, understanding inflammatory processes at the nasal mucosa in the context of cigarette smoke exposure is also warranted.

3.3. Cigarette smoke exposure does not alter the nasal microbiome in the absence of nasal pneumococcal colonization in mice.

The study presented in chapter 3.3 (manuscript in preparation, planned submission to *Infection and Immunity*) is, to our knowledge, the first to investigate the impact of cigarette smoke exposure on the nasal microbiome in mice. Utilizing a mouse model has allowed us to assess nasal microbiome composition in the absence and presence of nasal pneumococcal colonization. Importantly, we show that cigarette smoke exposure alone does not impact microbiome composition. However, we observed nasal microbiome dysbiosis as a consequence of established nasal pneumococcal colonization. These findings have advanced our understanding of bacterial community interactions in smokers.

3.3.1. Cigarette smoke exposure increases nasal pneumococcal colonization

To investigate how cigarette smoke exposure impacts the nasal microbiome during pneumococcal colonization, we established a non-invasive model of *S. pneumoniae* colonization using strain TIGR4 (a serotype 4 clinical isolate) to avoid survival bias[194,195]. Continuous cigarette smoke exposure of mice post-nasal inoculation with 10^7 CFU of TIGR4 had minimal impact on survival compared to room air control (Figure 19A). To assess whether cigarette smoke exposure increased nasal pneumococcal colonization, we cultured for *S. pneumoniae* presence in the nasal wash of cigarette smoke-exposed mice at 12 hours post-nasal colonization with a very low pneumococcal dose (10^3 CFU). Cigarette smoke exposure increased the incidence of pneumococcal detection in the nasal wash, although this difference was not statistically significant (Figure 19B). However, when the nasal pneumococcal inoculation dose was increased

to 10^4 CFU, we observed a significantly higher nasal wash bacterial burden in cigarette smoke-exposed mice as compared to room air control at 12 hours post-colonization. Nasal wash bacterial burden between room air and cigarette smoke-exposed mice was comparable by day 2 and day 3 post-nasal pneumococcal colonization (Figure 19C). The *S. pneumoniae* specific gene *lytA* was measured in genomic DNA isolated from complete nasal turbinates (CNTs) to assess nasal pneumococcal burden, as these were the same samples utilized subsequently to examine nasal microbiome composition. Some *lytA* expression was detectable at baseline, likely due to naturally occurring *S. pneumoniae* presence in the nasal microbiome, and was unaltered by cigarette smoke exposure. Surprisingly, we observed no difference in *lytA* levels between room air- and cigarette smoke-exposed mice at 12 hours following low dose (10^4 CFU) nasal pneumococcal colonization in CNT samples (Figure 19D). However, cigarette smoke exposure did increase *lytA* levels at day 3 following high dose (10^7 CFU) nasal pneumococcal colonization, although the increase was not statistically significant (Figure 19E). Overall, these data suggest that cigarette smoke exposure increases nasal pneumococcal colonization in mice.

3.3.2. Cigarette smoke exposure alone does not significantly alter nasal microbiome composition

To investigate the impact of cigarette smoke exposure on nasal bacterial composition, mice were cigarette smoke-exposed for 1 week and nasally inoculated with PBS (to control for nasal pneumococcal colonization). Mice continued to be cigarette smoke-exposed and were sacrificed 1 day (1 week + 1 day smoke exposure) and 3 days (1 week + 3 days smoke exposure) later. Microbiome composition was analyzed in CNT

samples by 16S rRNA gene sequencing. We observed no significant differences in the composition of nasal bacterial communities between room air- and cigarette smoke-exposed mice as assessed by the Bray-Curtis distance and visualized with the principal coordinate analysis (PCoA) plot (Figure 20). Cigarette smoke exposure (1 week + 1 day) also did not impact relative abundances of major bacterial phyla present in the CNTs (Figure 21A) and taxonomic summary plots were similar between room air and cigarette smoke-exposed mice (Figure 21B). Nasal bacterial community composition was also unchanged between room air- and cigarette smoke-exposed mice at 12 hours following low dose nasal pneumococcal inoculation (10^4 CFU), as visualized with the PCoA plot (Figure 22A). Additionally, relative abundances of major bacterial phyla (Figure 22B) and taxonomic summary plots (Figure 22C) were similar between room air and cigarette smoke-exposed mice. These data suggest that cigarette smoke exposure did not compromise the ability of the nasal microbiome to resist initial pneumococcal acquisition. Overall, our findings suggest that cigarette smoke exposure does not alter the nasal bacterial community composition.

3.3.3. The nasal microbiome is altered following established nasal pneumococcal colonization in cigarette smoke-exposed mice

To investigate the impact of cigarette smoke exposure on nasal bacterial composition in the presence of established nasal pneumococcal colonization, mice were cigarette smoke-exposed for 1 week and nasally inoculated with high dose (10^7 CFU) *S. pneumoniae*. Mice were sacrificed at day 3 post-nasal pneumococcal colonization. Microbiome composition was analyzed in CNT samples by 16S rRNA gene sequencing. We observed significant differences in nasal bacterial community composition between

room air and cigarette smoke-exposed mice in the presence of established nasal pneumococcal colonization as visualized by the PCoA plot (Figure 23A). 3 out of the 5 cigarette smoke-exposed mice had very high nasal pneumococcal burden as indicated. Relative abundances of the major bacterial phyla remained similar between room air and cigarette smoke-exposed mice (Figure 23B). Taxonomic summary plots show differences between room air and cigarette-smoke exposed mice (Figure 23C). As indicated, 3 out of the 5 cigarette smoke-exposed mice had very high nasal pneumococcal burden, which is reflected by the height of the *Streptococcus* bar in their taxonomic summary plot. Interestingly, the combination of cigarette smoke exposure and nasal pneumococcal colonization significantly increased the relative abundance of several genera containing potentially pathogenic bacteria, including *Fusobacterium*, *Gemella*, and *Neisseria* (Figure 24). Other bacterial genera with significant differences between room air and cigarette smoke-exposed mice following day 3 nasal pneumococcal colonization are presented in Table 1. These findings suggest that changes in the nasal microbiome observed in smokers may occur as a consequence of established nasal pathogen colonization.

3.3.4. The impact of cigarette smoke exposure and nasal pneumococcal colonization on specific bacterial genera

Corynebacterium and *Lactococcus* were both reported to negatively associate with URT pneumococcal colonization, and smokers were observed to have less abundant *Corynebacterium*[164,179,182]. Thus we further investigated the abundance of these specific bacterial genera. Cigarette smoke exposure did not significantly alter the levels of *Corynebacterium* and *Lactococcus* in the presence of nasal pneumococcal colonization

(Figure 25). These data suggest that commensal bacteria may not be impacted differently by *S. pneumoniae* in the context of cigarette smoke exposure as compared to pneumococcal colonization alone.

We also investigated the abundance of specific genera, including *Haemophilus* and *Staphylococcus*, known to interact with *S. pneumoniae*[214,215]. Cigarette smoke exposure significantly increased *Streptococcus* abundance at the genus level following nasal pneumococcal colonization (Figure 26A). However, we did not observe significant differences in *Haemophilus* and *Staphylococcus* between room air and cigarette smoke-exposed mice following nasal pneumococcal colonization (Figure 26B and C). Of note, there was a significant increase in one *Haemophilus* OTU in cigarette smoke-exposed mice following day 3 post-nasal pneumococcal colonization (data not shown).

Overall, data presented in chapter 3.3 suggest that cigarette smoke exposure alone does not alter the nasal microbiome and that clinical observations of nasal microbiome dysbiosis in smokers may occur as a consequence of nasal pathogen colonization.

CHAPTER 4. DISCUSSION

The focus of this thesis is to elucidate the impact of cigarette smoke exposure on bacterial-host interactions. Data generated show that cigarette smoke exposure alters bacterial-host interactions to promote infection and disease.

4.1. Summary of results

COPD patients are at increased risk of acquiring lung bacterial infections that lead to COPD exacerbations, increasing inflammation and accelerating disease progression. We investigated, in chapter 3.1, mechanisms underlying exacerbated lung inflammatory responses to bacteria in cigarette smoke-exposed mice. We first confirmed our previous observations that cigarette smoke-induced inflammation in the lungs is IL-1α dependent and that the critical cellular source of IL-1α is likely the AM. Importantly, we observed cigarette smoke exposure to skew the AM inflammatory mediator expression profile towards amplified IL-1α expression in response to NTHi. NTHi infection also amplified lung levels of IL-1α, but not IL-1β, in cigarette smoke-exposed mice. Ultimately, cigarette smoke exposure exacerbated the neutrophilic response to NTHi in an IL-1α dependent manner that correlated with CXCL-5 expression. Repeated NTHi infection was also associated with increased lung damage in cigarette smoke-exposed mice. The study presented in chapter 3.1 suggests that cigarette smoke exposure primes the lung environment towards an exacerbated IL-1α response to NTHi, leading to amplified neutrophilia and lung damage upon bacterial infection.

COPD patients and smokers may have increased lung bacterial infection due to a failure to control pathogen colonization at the URT. We next investigated in chapter 3.2 how cigarette smoke exposure affected the course of nasal pneumococcal

colonization in mice. Cigarette smoke exposure attenuated the nasal inflammatory response normally induced by nasal pneumococcal colonization, with decreased CXCL-1, CXCL-2, and TNF-α expression. This was associated with an increased incidence of IPD and mortality in cigarette smoke-exposed mice. We observed evidence of sepsis and meningitis in mice reaching endpoint such as leukopenia and inflammatory infiltrates at the meninges. Surprisingly, contrary to our hypothesis, there were no overt signs of lung inflammation or consolidation that would suggest endpoint mice developed pneumonia. Furthermore, time course experiments showed bacteraemia in all mice with detectable BAL bacterial burden whereas we have detected cases of pneumococcal cultures in the spleen only. It is possible that mice developed bacteraemia without a requirement for prior lung infection in our mouse model. Mechanistically, cigarette smoke-exposed mice did not have impaired nasal clearance or compromised epithelial barrier integrity. Deficiency in PAFR or IL-1α also did not rescue cigarette smoke-exposed mice from IPD. However, smoking cessation completely rescued mice from IPD following nasal pneumococcal colonization, and was associated with an increase in CXCL-2 and neutrophil levels as compared to mice that continued to be cigarette smoke-exposed. We conclude that cigarette smoke exposure impairs the URT host defence and predisposes mice to IPD following nasal pneumococcal colonization.

In addition to compromising the control of colonizing pathogenic bacteria at the URT mucosa, cigarette smoke exposure may also increase pathogen acquisition and colonization by perturbing the nasal microbiome. The last study in chapter 3.3 investigated the link between increased nasal pneumococcal colonization and nasal microbiota dysbiosis in cigarette smoke-exposed mice. We observed that cigarette

smoke exposure alone did not alter the composition of the nasal microbiome in mice. However, nasal microbiome dysbiosis occurred as a consequence of established nasal pneumococcal colonization in cigarette smoke-exposed mice as compared to room air control. Of note, similar to clinical reports in human smokers, we observed an enrichment of potentially pathogenic bacteria such as *Fusobacterium, Gemella*, and *Neisseria* during nasal pneumococcal colonization in cigarette smoke-exposed mice. Our findings in chapter 3.3 indicate cigarette smoke exposure may predispose to pathogen colonization independent of nasal microbiome dysbiosis, and changes in microbiota composition observed in smokers may occur after pathogen colonization.

4.2. General discussion of the experimental approach

Mice were cigarette smoke-exposed using an established whole body smoke exposure system as previously described[72]. Cigarette smoke exposure was well-tolerated in mice, with no change in corticosterone levels between room air and cigarette smoke-exposed mice, and carboxyhemoglobin and cotinine levels in mice were comparable to that of human smokers[72,216]. Cigarette smoke exposure in our mouse model induced lung neutrophilia that is thought to contribute to lung damage and COPD disease progression[73,74]. To study the impact of cigarette smoke exposure on the bacterial host response, we utilized a clinical isolate of NTHi acquired from a COPD patient during exacerbation[108]. Of note, we showed repeated NTHi infection and prolonged cigarette smoke exposure to induce airspace enlargement and increase lung compliance, suggesting lung dysfunction in association with exacerbated neutrophilia in our mouse model. Thus, our mouse model is ideal for investigating the impact of cigarette smoke exposure on bacterial-host interactions.

Responses to experimental conditions may vary dependent on the mouse strain utilized. The experimental mouse strain was chosen according to the availability of transgenic mouse strains. The majority of transgenic mice utilized, including IL-1R1 KO, IL-1α KO, IL-1β KO, and PAFR KO mice were on a C57BL/6 background while CXCR2 KO mice were on a BALB/c background. Therefore the models presented in this thesis were often investigated in C57BL/6 mice, with BALB/c mice utilized as the appropriate controls for studies pursued in CXCR2 KO mice.

The pneumococcal nasal colonization method was adapted from the laboratories of Dr. Jeffrey Weiser and Dr. Dawn Bowdish[194,217]. Both the volume and anaesthesia type used may influence nasal inoculum distribution following intranasal delivery[218,219]. By using a small inoculation volume in the absence of anaesthesia, we are confident that lung bacterial delivery was minimized in our mouse model and that the bacteria was contained in the URT. Our imaging data using ^{99m}Tc-DTPA validated that nasal delivery of the bacteria was contained to the upper respiratory tract. Similar to nasopharyngeal carriage in humans, nasal colonization with several pneumococcal strains in adult mice was largely asymptomatic, and lasted several weeks with few cases of bacteraemia and other invasive infections[155,220]. The *S. pneumoniae* strain P1547 in our study was derived from a clinical blood isolate of a patient with IPD[192,193]. Therefore, we believe our experimental approach is well-suited for investigating the impact of cigarette smoke exposure on the natural progression of invasive bacterial infection from the nasopharynx. Our model holds clinical significance in that smokers continue smoking during asymptomatic nasal pneumococcal colonization.

We investigated the impact of cigarette smoke exposure on the nasal microbiome utilizing a mouse model. The major bacterial phyla present in our model were consistent with those found in the human nasal microbiome and other reports in mice, with a negative association between Firmicutes and Actinobacteria[210,221]. In order to investigate the impact of cigarette smoke exposure on nasal microbiome composition during nasal pneumococcal colonization, we utilized *S. pneumoniae* strain TIGR4 (a serotype 4 clinical isolate)[194,195]. In contrast to the pneumococcal strain P1547 utilized in chapter 3.2, TIGR4 did not significantly increase mortality in cigarette smoke-exposed mice, permitting the study of nasal colonization with minimal IPD and survivor bias. Analysis was carried out in complete nasal turbinates (CNTs), rather than in nasal wash samples, to maximize the collection of bacterial DNA for sequencing. We also assessed nasal pneumococcal burden by PCR measurement of the *S. pneumoniae* specific *lytA* gene, rather than CNT homogenization and culturing on blood agar, to minimize bacterial DNA contamination. Due to the presence of large amounts of host DNA in the CNT samples, nested PCR was utilized to increase the sensitivity of bacterial 16s amplification prior to sequencing. To evaluate the impact of pneumococcal acquisition on the nasal microbiota, we utilized a low pneumococcal inoculation dose (10^4 CFU) and assessed the nasal microbiome at an early time point (12 hours) post-pneumococcal colonization. A low pneumococcal inoculation dose allowed for sub-maximal colonization levels and the detection of nasal pneumococcal burden differences between room air and cigarette smoke-exposed mice. To investigate nasal microbiome changes following established nasal pneumococcal colonization, we inoculated mice with a high dose of *S. pneumoniae* (10^7 CFU) and assessed nasal

microbiome changes on day 3 post-pneumococcal colonization. As before, mice continued to be cigarette smoke-exposed post-nasal pneumococcal colonization without interruption to mimic that smokers continue smoking during asymptomatic nasal colonization.

4.3. Cigarette smoke-induced inflammation in the lungs

We and others have previously established a critical role for IL-1R1 signalling in cigarette smoke-induced lung inflammation[75,88]. However, the specific impact of the two IL-1 cytokines, IL-1α and IL-1β, as well as their cellular source, remain unclear. Reports by others of a role for the IL-1β-activating protease caspase-1 in cigarette smoke-induced inflammation has been contradictory, although these findings generally agree on a role for IL-1β, or both IL-1α and IL-1β, in cigarette smoke-induced inflammation[86,87,222]. In addition to observing a caspase-1 independent effect in our mouse model, anti-IL-1 antibody studies in our laboratory showed IL-1α, not IL-1β, to be critical to cigarette smoke-induced inflammation[88]. In this thesis, we confirmed our previous observations that cigarette smoke-induced inflammation was IL-1α dependent using IL-1α and IL-1β gene deficient mice. The disagreement with other studies regarding the impact of IL-1β may be explained by differences in mouse models of cigarette smoke exposure. Of note, smoke exposure systems, as well as the number of cigarettes and daily duration of exposure varied between studies[86–88,222]. Our laboratory recently completed a study analyzing the gene expression profiles of different mouse models of cigarette smoke exposure showing total particular matter (TPM) to influence gene expression, with higher TPM correlating with the activation of more inflammatory genes (unpublished manuscript). It is possible that the differences in cigarette smoke

exposure protocols may have contributed to different amounts of TPM, resulting in the discrepancy between our findings and those of the other studies. These differences in experimental approach highlight the need to translate findings from animal models to human studies. A clinical trial in 2013 showed that the anti-IL-1β antibody canakinumab was not effective in improving FEV_1 in stable COPD[223,224], underscoring the need to investigate IL-1α as a clinical therapeutic target.

Our findings suggest cigarette smoke-induced inflammation to be IL-1α-, rather than IL-β- dependent even though both cytokines act through the IL-1R1. Differential roles for IL-1α and IL-1β have also been described in other mouse models of disease[225,226]. A potential explanation for their differential roles may be the differences in their localization, cellular source, and cellular compartmentalization. While IL-1β activity is tightly regulated by processing and secretion mechanisms, IL-1α is biologically active in the precursor form and localized both intracellularly and in association with the cell membrane[227–231]. In addition, IL-1α can be cleaved into the more biologically active mature form by proteases such as calpain, and secreted[232,233]. Our data indicate that while AMs isolated from cigarette smoke-exposed mice secreted IL-1α *ex vivo*, they produced little IL-1β, even following bacterial stimulation. Furthermore, only CXCL-5 expression correlated with cigarette smoke-induced neutrophilia, and CXCL-5 levels only decreased in the absence of IL-1α, suggesting CXCL-5 expression to be IL-1α-, but not IL-1β- dependent. CXCL-5 is also known as epithelial-derived neutrophil-activating peptide (ENA)-78 and is typically expressed by epithelial cells[234,235]. As AMs communicate and associate closely with the lung epithelium[236], it may be that the proximity of epithelial cells to the source of IL-1α, including AM cell membrane-

associated IL-1α, is required for CXCL-5 expression and subsequent neutrophil recruitment. IL-1 signalling-dependent communication between AMs and the epithelium is consistent with our previous observation of a requirement for IL-1R1 activation on structural cells for cigarette smoke-induced neutrophilia[88]. However, we did not pursue CXCL-5 neutralization studies and further research is needed to confirm the extent to which cigarette smoke-induced inflammation is dependent on this chemokine. The role of AM cell membrane-associated IL-1α in contact-dependent epithelial cell activation also remains to be investigated. Lastly, it is notable that anti-IL-1α antibody treated mice and IL-1α KO mice have decreased IL-1β expression[88,237]. Conversely, IL-1α expression is unaffected in IL-1β KO mice[237]. Anti-IL-1α interventions may thus further attenuate IL-1R1 signalling by reducing IL-1β expression as well.

Our data suggest the cellular source of cigarette smoke-elicited IL-1α expression is from the hematopoietic cell compartment, and likely the AM, adding support to the prevalent hypothesis that AMs are critical to COPD disease pathogenesis[238]. Macrophage depletion in mice is shown to be protective against cigarette smoke-elicited lung damage and decline in lung function[239]. However, how cigarette smoke exposure elicits the AM to produce IL-1α remain unclear. Cigarette smoke may induce lung injury, leading to an inflammatory response to dying cells as observed in sterile inflammation. Sterile inflammation is also characterized by macrophage-derived, IL-1α-dependent neutrophilia[240]. Experimentally, cigarette smoke extract induces apoptosis and necrosis of human epithelial cells *in vitro*[241,242]. There is also evidence of lung epithelial necroptosis in COPD patients[243]. Necroptosis is a regulated form of necrosis leading to plasma membrane permeabilization and the release of cellular contents[244]. Notably, cell

death produce damage-associated molecular patterns (DAMPs) that activate pattern recognition receptors (PRRs), and may elicit cigarette smoke-induced neutrophilia[245]. Indeed, a recent study in mice showed the administration of an inhibitor of necroptosis, necrostatin-1, attenuated cigarette smoke-induced BAL neutrophilia[246]. Even apoptotic cells that are considered to be non-inflammatory will release DAMPS upon secondary necrosis in COPD due to impaired macrophage phagocytosis[247–249].

Interestingly, IL-1α, as a constitutively expressed, intracellular cytokine expressed in epithelial cells, keratinocytes, and fibroblasts, is considered to be a DAMP, and it has been suggested that IL-1α released by dying cells may be sensed by other host cells to induce the release of more IL-1α[225,250,251]. A plausible explanation in our model is that cigarette smoke exposure induces epithelial cell injury, leading to the release of IL-1α. AMs respond by further amplifying IL-1α production, resulting in neutrophilia. However, neutrophilia has been shown to occur independent of IL-1α expressed by necrotic cells in the context of sterile inflammation[240]. Similarly, our chimeric data indicate that cigarette smoke-induced neutrophilia was not affected by IL-1α deficiency in the structural cell compartment, suggesting other DAMPs contribute to cigarette smoke-induced IL-1α production by AMs. In fact, numerous DAMPs, including high-mobility group box (HMGB)1, heat shock proteins (HSPs), and S100A8, have been documented to be elevated in cigarette smoke-exposed mice, as well as in the BAL and serum of COPD patients[252–255]. Of note, our laboratory also recently reported a potential role for damaged lipids, such as oxidized low-density lipoprotein (OxLDL), in IL-1α production from AMs and subsequent cigarette smoke-induced neutrophilia[256]. Some DAMPs activate TLR-4, which is known to contribute to cigarette smoke-induced

inflammation and may potentially be involved upstream of IL-1α[75,256]. Further research is needed to determine the mechanism of IL-1α induction and evaluate the potential role of lung injury and DAMPs in the context of cigarette smoke exposure, which may contribute to novel therapeutic treatment strategies.

The current study provides strong evidence of the critical requirement for IL-α in the initiation of cigarette smoke-induced neutrophilia. However, the experimental approach was prophylactic and the role of IL-1α in maintaining cigarette smoke-induced inflammation remains to be elucidated. It is plausible that once an inflammatory response is initiated, further lung damage result in the release of more DAMPs. Some DAMPs have chemotactic activity, such as the ECM degradation product Pro-Gly-Pro (PGP), and may continue to propagate the neutrophilic response independent of IL-1α[257]. Moreover, although innate immune mechanisms are sufficient to drive cigarette smoke-induced neutrophilia[72], adaptive immunity, as indicated by the formation of tertiary lymphoid tissue, is involved with chronic cigarette smoke exposure in mice, and in later stages of COPD in humans[60,258]. Further studies are needed to investigate the impact of anti-IL-1α interventions on established cigarette smoke-induced inflammation to evaluate the potential of this cytokine as a therapeutic target.

4.4. Cigarette smoke and lung bacterial infection

We observed that IL-1α expression by AMs isolated from cigarette smoke-exposed mice was further increased following NTHi stimulation. Moreover, cigarette smoke exposure exacerbated the neutrophilic response to NTHi lung infection dependent on IL-1α. Again, CXCL-5 expression correlated with the extent of neutrophilia and was reduced in cigarette smoke-exposed, NTHi-infected IL-1R1KO mice, suggesting exacerbated

neutrophilia may be a consequence of increased AM IL-1α expression in response to bacteria. It has been suggested that cigarette smoke exposure impairs the ability of AMs to respond to bacteria, leading to increased bacterial infections and COPD exacerbations. AMs isolated from smokers express attenuated levels of cytokines, including TNF-α and IL-6, following TLR-2 and TLR-4 stimulation[259]. Our findings disagree with an impairment in AM inflammatory mediator expression. Instead, we propose that cigarette smoke exposure skews the inflammatory mediator expression profile of AMs in response to bacteria. While the expression of some cytokines, such as TNF-α, were attenuated in the context of cigarette smoke exposure, IL-1α levels were increased above that observed in room air control following bacterial challenge. We speculate that cigarette smoke exposure may prime AMs towards an exacerbated IL-1α response during bacterial infection to alleviate impaired lung bacterial clearance. AMs are compromised in bacterial phagocytosis following cigarette smoke exposure[260], which in combination with the observed attenuation in pro-inflammatory cytokine expression, such as TNF-α, may contribute to decreased lung bacterial clearance. AMs may respond to the higher lung bacterial burden by increasing the existing IL-1α response to cigarette smoke in order to recruit additional effector cells, in this case neutrophils, to help clear the bacteria. Although the exacerbated neutrophilic response is associated with control of lung bacterial burden in cigarette smoke-exposed mice, lung damage is also observed and may be a consequence of excessive inflammation.

One major concern in targeting the inflammatory response during COPD exacerbations is the impact on lung bacterial clearance. Our data show cigarette smoke exposure did not impair lung bacterial clearance in wild type mice. This may be due to

the exacerbated inflammatory response to bacteria. In fact, we have previously published that cigarette smoke exposure accelerates lung NTHi clearance dependent on increased titres of NTHi-specific immunoglobulin A in the BAL[261]. In the current study, however, we observed a mouse strain-dependent difference in that BALB/c mice, but not C57BL/6 mice, had higher bacterial clearance following cigarette smoke exposure. The fact that we did not observe accelerated NTHi clearance in C57BL/6 mice, as we previously reported, may be explained by differences in the supplier of mice. We also examined the consequences on lung bacterial burden following cigarette smoke exposure in each KO mouse strain. In cigarette smoke-exposed CXCR-2 KO mice, we observed a dramatic increase in lung bacterial burden that may be attributable to the severe decrease in neutrophil recruitment below neutrophil levels elicited by NTHi in wild type room air control mice. A less severe reduction was observed in both IL-1R1 KO and IL-1α KO mice, and NTHi-elicited neutrophil levels in these KO mice were comparable to that of wild type room air control. However, while bacterial clearance was still impaired in IL-1R1 KO mice, IL-1α KO mice had similar lung NTHi levels to wild type smoke-exposed mice. The ability of IL-1α KO mice to both attenuate neutrophilia and control bacterial burden suggest a beneficial effect of preserving IL-1β function, which may have pro-inflammatory effects that target bacterial clearance independent of neutrophil recruitment. Our findings further support specific anti-IL-1α intervention strategies, rather than targeting IL-1β or IL-1R1, in the control of COPD exacerbations.

One major challenge to the development of novel therapeutic intervention strategies is the heterogeneous nature of COPD. The relative contributions of bronchiolitis and emphysema to the disease phenotype, as well as disease severity,

may differ between patients[13]. Additionally, lung biomarkers of disease, including IL-1α, may vary widely between patients[88]. These reasons may explain why a recent clinical trial using a fully human immunoglobulin G2 monoclonal IL-1R1 binding antibody, designed to inhibit receptor binding of IL-1α and IL-1β, was unsuccessful in reducing the rate of acute exacerbations of COPD and improving FEV1[211]. It is possible that our findings with IL-1α-dependent inflammation did not translate into humans from the animal model. Notably, the therapeutic potential of anti-IL-1α interventions to reduce an established exacerbated inflammatory response to bacteria has not been investigated in mice. It could be that once initiated in an IL-1α-dependent manner, other factors drive exacerbated neutrophilia upon bacterial challenge independent of IL-1α. However, we note that in the IL-1R1 antibody clinical trial, it was not investigated whether all patients expressed IL-1α, and the rate of exacerbations measurement was not specific to bacterial-associated exacerbations[211]. Indeed, different therapeutic intervention strategies may be required for specific populations of COPD patients with distinct biomarker expression characteristics[262]. Additionally, it may be more difficult to inhibit a ubiquitously expressed receptor, such as IL-1R1, than an actively secreted cytokine. In light of a potential beneficial effect of IL-1β in controlling bacterial burden observed in the current study, it is important to investigate the effect of specific anti-IL-1α intervention on patients that express IL-1α and are undergoing bacterial exacerbations.

The study in chapter 3.1 suggests that cigarette smoke exposure primes the lungs towards an IL-1α-dependent exacerbated neutrophilic response to NTHi infection, leading to lung damage and decline in lung function. In support of this hypothesis, we showed that repeated NTHi lung infection in the context of continuous cigarette smoke

exposure led to an increase in lung compliance and airspace enlargement. Clinically, smokers and COPD patients are not only at increased risk of lung exposure to pathogenic bacteria from the URT, but chronic bacterial colonization characterized by the presence of non-commensal, immunogenic bacteria such as NTHi can also occur[89,90,123]. We speculate that a decline in lung function results from chronic, repeated exposure to these pathogenic bacteria, as cigarette smoke exposure skews the lungs towards an amplified inflammatory response in an attempt to clear bacteria, at the cost of lung damage. Importantly, chronic cigarette smoke exposure and bacterial colonization may also prevent the lungs from resolving inflammation and implementing repair mechanisms. Overall, the study presented in chapter 3.1 suggests that cigarette smoke exposure induces AMs to express IL-1α that activates the epithelium to produce CXCL-5, contributing to neutrophil recruitment to the lungs. NTHi lung challenge further amplifies the AM IL-1α response, leading to exacerbated CXCR-2-dependent lung neutrophilia that correlates with augmented CXCL-5 expression (Figure 8).

4.5. Impact of cigarette smoke exposure on the URT host defence

Smokers and COPD patients may be at a higher risk of acquiring lung bacterial infections, resulting in bacterial exacerbations for COPD patients, due to a failure to control colonizing pathogens at the URT. In chapter 3.2, we investigated the impact of cigarette smoke exposure on the nasal bacterial host defence to *S. pneumoniae* and the consequences for subsequent pneumococcal infection development. Cigarette smoke exposure had profound effects on nasal pneumococcal colonization; we observed increased mortality in mice associated with pneumococcal sepsis and meningitis. This mirrors clinical observations of cigarette smoking as a risk factor for IPD[119]. To our

knowledge, this is the first animal model to describe, in the context of cigarette smoke exposure, the progression from an asymptomatic carrier state to IPD.

There is evidence to suggest that the cause of mortality in cigarette smoke-exposed mice following nasal pneumococcal colonization was meningitis and sepsis in our model. Pneumococci were cultured from brain tissue, and neutrophilic inflammation was observed at the meninges. In addition, the presence of pneumococcal bacteraemia in mice was associated with leukopenia. This observation is consistent with the lymphopenia and splenic lymphocyte apoptosis described in mouse models of sepsis and septic patients[263–265]. Moreover, all endpoint mice had detectable serum IL-6, which is considered a reliable marker of sepsis and to predict organ dysfunction and mortality[266,267]. Based on our findings, we conclude that cigarette smoke exposure predisposes mice to invasive pneumococcal infections, leading to meningitis and sepsis. We also described pneumococcal invasion into the heart as a consequence of pneumococcal bacteraemia. Inflammatory cell infiltrates in the heart tissue of endpoint mice suggest bacterial endocarditis that has been described in association with *S. pneumoniae,* with 15% of all clinical cases accounted for by pneumococcal infection in the pre-antibiotic era[268]. In addition, we found microlesions in the heart as described recently by Brown *et al* filled with gram-positive bacteria, likely pneumococci[269]. These microlesions were reported to correlate with markers of cardiac damage and collagen deposition and may lead to cardiac scarring over time[269]. Clinically, cardiac complications occur during 18% of hospitalizations with CAP[270]. In addition, cardiac scarring from these microlesions may contribute to a greater risk of sudden death in patients for up to one year following invasive disease[271]. Taken altogether, our model

presents with multiple aspects of invasive pneumococcal infections reflective of clinical causes of mortality and disease complications. These observations confirm that cigarette smoke exposure predisposed mice to mortality due to IPD and validates the use of our animal model as a tool to investigate mechanisms leading to compromised control of pneumococcal colonization at the nasal mucosa.

Cigarette smoke exposure may increase the incidence of invasive pneumococcal infection for as long as stable nasal colonization is established. Consistent nasal bacterial numbers, indicating a stable state of colonization, can be recovered from mice inoculated with various initial bacterial doses ranging from 10^5 to 10^7 CFU, and we found cigarette smoke exposure to increase mortality at several doses within this range[220]. In addition, pneumococci were detected at a late time point (day 16) during colonization in the brain homogenates of cigarette smoke-exposed mice, indicating IPD. Interestingly, room air, but not cigarette smoke-exposed mice, were beginning to clear the bacteria from the nasopharynx at this time point (day 16). This delay in nasal clearance observed in cigarette smoke-exposed mice is consistent with reports of increased incidences of pneumococcal nasal colonization in adolescents exposed to passive smoke and has been observed in another mouse model[185,272]. Therefore, it is possible that not only are smokers at increased risk for IPD as long as they remain stably colonized, delayed nasal bacterial clearance due to cigarette smoke exposure may result in a prolonged time period in which individuals are at risk of IPD.

Mechanistically, cigarette smoke exposure predisposed mice to IPD in association with attenuated nasal pro-inflammatory mediator expression at early time points, including TNF-α, CXCL-1 and CXCL-2. In naive mice, pneumococcal

colonization is reported to induce an initial influx of neutrophils, followed by a more gradual and sustained recruitment of monocytes/macrophages important in resolving colonization over the course of several weeks[159,161,273]. It is thought that although neutrophils do not directly impact bacterial numbers, they play a role in antigen priming of adaptive immunity that impacts later Th17 dependent macrophage-mediated clearance of colonizing pneumococci[159,161]. Although the baseline proportion of nasal neutrophils was high in cigarette smoke-exposed mice, we did not see a significant increase in neutrophils in response to pneumococcal colonization, as compared to room air control mice. Hence, we postulate that the impaired ability to recruit additional neutrophils in response to *S. pneumoniae* may predispose mice to IPD in cigarette smoke-exposed mice. In support of this, the effect of cigarette smoke is similar to previous observations of targeted neutrophil depletion in the context of nasal pneumococcal colonization, which had no immediate impact on nasal bacterial burden, but predisposed mice to IPD[159]. Furthermore, we show that increased survival in nasally colonized mice following smoking cessation was associated with an increase in neutrophils in the URT. Cigarette smoke may thus predispose to IPD by impairing the neutrophilic response induced by nasal pneumococcal colonization.

Mucociliary flow and epithelial barrier integrity at the nasopharynx are critical for the prevention of invasive microbial infections, and cigarette smoke exposure has been documented to impair both of these aspects of respiratory host defence[274]. Increased clearance rates of ^{99m}TC-DTPA, a marker commonly used to assess epithelial barrier integrity in the respiratory tract, have been observed in smokers following delivery to the lungs. Faster clearance through the blood to the urinary bladder is indicative of

compromised epithelial barrier function[275,276]. Contrary to these reports, we found no significant impact of cigarette smoke exposure on either the nasal clearance or bloodstream uptake of ^{99m}TC-DTPA following delivery to the upper airways. This implies that acute cigarette smoke exposure did not compromise either nasal clearance or the upper respiratory tract epithelial barrier integrity at a time point corresponding to widespread pneumococcal dissemination in our model. Along these lines, cigarette smoke-exposed mice are reported to have no significant decrease in ciliary beat frequency until after 6 months of cigarette smoke exposure[139]. However, *S. pneumoniae* has been observed to both decrease ciliary beat frequency and to cause damage at the human respiratory mucosa, in addition to down-regulating nasal tight junction protein expression in mice[277,278]. Therefore we should not rule out synergistic effects of cigarette smoke exposure and pneumococcal colonization on both nasal clearance and epithelial barrier integrity of the upper airways.

S. pneumoniae has been shown to adhere to and enter host cells through the PAFR in an IL-1α dependent manner that may facilitate bacterial invasion even if epithelial barrier function remain intact[147]. Moreover, both PAFR and IL-1α are increased in the lungs of smokers and COPD patients[88,148,213]. But we show that deficiency in PAFR or IL-1α did not rescue cigarette smoke-exposed mice from higher rates of IPD-associated mortality. This may be due to differential regulation of PAFR and IL-1α in the upper and lower respiratory tracts as expression of both factors was attenuated in the nasopharynx while we confirmed an increase in lung PAFR by cigarette smoke exposure. Thus although PAFR may potentially be involved in pneumococcal dissemination from the lungs following cigarette smoke exposure, it

played no significant role in promoting invasive disease directly from nasal colonization. It is possible that the same pathway may differentially affect the upper and lower respiratory tracts. For example, while TLR-2 was essential for controlling pneumococcal nasal colonization, it had little effect during pneumococcal lung infection in mice[279,280]. Of note, both heart microlesion formation and translocation across the blood-brain barrier by *S. pneumonia* is PAFR dependent[269,281], and may explain the small delay in mortality we observed in cigarette smoke-exposed PAFR KO mice. Ultimately however, PAFR did not contribute to the increased mortality rate in cigarette smoke-exposed mice following nasal pneumococcal colonization.

We showed accumulation of pneumococci in the spleen and brain of some cigarette smoke-exposed mice without bacterial presence in the BAL. This observation, combined with the absence of pathological features of pneumonia in endpoint mice, suggest systemic dissemination of *S. pneumoniae* from the nasopharynx in our model may not require prior lung infection. This is surprising given that smoking is associated with an increased risk of CAP[112], that mortality due to pneumococcal pneumonia is increased in smokers[282], and that *S. pneumoniae* is frequently isolated during bacterial exacerbations of COPD[108]. Since invasive infection had already progressed to the lungs, blood, and brain in the majority of cigarette smoke-exposed mice examined in our time course, we cannot rule out that we might have missed the very early phase of disease and that bacterial dissemination did occur from the lungs. On the other hand, occult pneumococcal bacteremia, the direct spread of *S. pneumoniae* from the nasopharynx into the blood is a well-known phenomenon[283]. We also observed *S. pneumoniae* invasion into the brain of cigarette smoke-exposed mice without bacterial

detection in either the BAL or spleen, consistent with a report of direct *S. pneumoniae* translocation to the brain from the nasopharynx[284]. These phenomena are particularly alarming due to the asymptomatic nature of nasal colonization and the rapidness of disease progression. Much focus has been placed on cigarette smoke's effects on pneumococcal invasiveness into the lungs, but our data suggest smokers may also be at increased risk of occult bacteraemia, which warrants further attention.

There are approximately 90 different pneumococcal serotypes and invasive potential, as well as bacterial dissemination pattern, are highly dependent on both the serotype and clonal type[285–287]. Therefore, cigarette smoke exposure may predispose to IPD in a manner dependent on the virulence potential and organ specific tropism of the *S. pneumoniae* strain acquired in the URT. The current study used a clinical blood isolate of serotype 6A that has been associated with a higher risk of acquiring meningitis[192,193,288]. This may explain the observed predisposition towards bacteraemia and meningitis, rather than pneumonia in our model. Similarly, Basilico *et al* recently reported that cigarette smoke exposure predisposed mice to ear infection following pulmonary delivery of a clinical isolate of *S. pneumoniae* isolated from a patient with otitis media[289].

Importantly, we found mortality in cigarette smoke-exposed mice was fully rescued upon smoking cessation post-nasal colonization. This observation likely explains why nasal colonization with a clinical isolate of the same serotype (6A) was not reported to cause invasive disease in a recent study by Voss *et al* [272], as mice were not exposed to cigarette smoke post-nasal pneumococcal colonization. These differences in experimental approach should be taken into consideration when investigating

mechanisms of pneumococcal colonization and IPD in the context of cigarette smoke exposure, especially given how quickly nasal CXCL-1 and CXCL-2 expression, as well as neutrophil recruitment increased following smoking cessation in colonized mice. Our data suggest that smoke's immunosuppressive effects at the nasopharynx are highly reversible upon smoking cessation. Epidemiological studies also support a reversible effect of cigarette smoke exposure on pneumococcal disease in that the odds ratio of acquiring infection is lower in former smokers compared to current smokers[112,119]. Smoking cessation may thus be the most effective intervention strategy to reduce the incidence of IPD.

We propose that cigarette smoke exposure predisposes to IPD by suppressing nasal inflammatory mediator expression. The suppressive effect of cigarette smoke exposure on nasal inflammatory processes has also been observed in humans where nasal IL-6 expression was decreased in young healthy smokers following nasal inoculation with live attenuated influenza virus[290]. The suppressive effect of cigarette smoke exposure in the URT is in contrast to our previous study in Chapter 3.1 showing cigarette smoke exposure to prime the lungs towards excessive neutrophilia in response to bacterial infection. This could be attributed to differential regulation of inflammatory processes by cigarette smoke at the upper and lower respiratory tracts, as suggested by Huvenne *et al*[291]. Cigarette smoke is a complex stimulus containing over 4500 compounds and it is yet unclear how smoke exposure may be attenuating nasal inflammatory responses to *S. pneumoniae*[292]. Innate sensing of bacterial constituents through pattern recognition receptors is critical to initiate appropriate inflammatory responses[293]. We have previously shown TLR-4 expression to be unaffected in AMs

from cigarette smoke-exposed mice[111]. Others have reported decreased AM TLR-2 expression in smokers and COPD patients[294]. Additionally, nasal TLR-4 expression was attenuated in smokers and patients with severe COPD[295]. However, the impact of cigarette smoke exposure on nasal TLR expression and function, especially that of TLR-2 for *S pneumoniae*, remains to be investigated[158]. In addition, as cigarette smoke contains bioactive LPS, some of its suppressive effects have been thought to resemble LPS tolerance, with repeated TLR-4 stimulation inducing a transient state of immune hyporesponsiveness[259,296]. Lastly, oxidative stress induced by cigarette smoke exposure causes protein carbonylation that has been associated with impaired immunity in macrophages[297]. Further research is required to elucidate mechanisms underlying suppression of nasal bacterial responses by cigarette smoke as restoring these processes may lower the risk of IPD in smokers.

We present a novel mouse model that closely resemble clinical observations of cigarette smoke-associated IPD. Our data suggest that cigarette smoke exposure may increase the risk of not only pneumonia, as reported in the literature, but also occult pneumococcal bacteraemia. Contrary to findings in the lungs, nasal expression of PAFR and IL-1α were down-regulated and contributed little to mortality associated with bacterial invasiveness from the nasopharynx. Mechanistically, we propose that cigarette smoke exposure attenuates a pro-inflammatory environment at the nasopharynx normally induced by *S. pneumoniae*, which hinders recruitment of crucial cellular effectors required for the prevention of IPD. Smoking cessation may be the most effective intervention strategy to reduce the incidence of IPD, emphasizing the need for more supportive smoking prevention and cessation programs. However, given the

addictive nature and high prevalence of cigarette smoking, future studies are also warranted to understand and restore inflammatory processes at the nasal mucosa.

4.6. Impact of cigarette smoke exposure on the nasal microbiome

Nasal microbiome dysbiosis has been described in human smokers, with increased pathogen colonization[123]. Cigarette smoke exposure may promote pathogen colonization by perturbing the nasal microbiota and decreasing colonization resistance. To our knowledge, the study in chapter 3.3 is the first to assess the effect of cigarette smoke exposure on the nasal microbiome in an experimental mouse model, where conditions such as the extent of cigarette smoke exposure and nasal pathogen acquisition can be carefully controlled. This allowed us to advance our understanding of the link between cigarette smoke exposure, pathogen colonization, and nasal microbiome dysbiosis. We observed that cigarette smoke exposure alone did not cause nasal microbiome dysbiosis. Cigarette smoke exposure also did not impact the abundance of natural *S. pneumoniae* present in mice at baseline as indicated by *lytA* measurements in the CNT of vehicle control mice. In addition, microbial composition remained similar between room air and cigarette smoke-exposed mice immediately (12h) after low dose nasal pneumococcal inoculation, suggesting cigarette smoke exposure did not compromise the ability of the microbiome to resist initial nasal pneumococcal acquisition. Our data clearly demonstrate that cigarette smoke exposure alone was not sufficient to alter the nasal microbiota. We conclude that cigarette smoke exposure increases nasal pneumococcal colonization independent of changes to nasal microbiota composition. It could be that cigarette smoke exposure impacts other aspects of bacterial-host interactions, such as increased *S. pneumoniae* adhesion to the

epithelium and an attenuated inflammatory response to *S. pneumoniae*, to promote pneumococcal colonization.

Interestingly, our findings showed significant differences in microbial composition between room air and cigarette smoke-exposed mice at day 3 following high dose nasal pneumococcal colonization reflective of clinical observations[164,182]. However, we did not observe a significant decrease in any bacterial genera in cigarette smoke-exposed mice as compared to room air-exposed mice at day 3 post-nasal pneumococcal colonization. This observation suggests that the observed decrease in commensal bacteria in smokers may be attributed to nasal pneumococcal colonization alone, rather than an effect of cigarette smoke exposure. We further investigated the impact of cigarette smoke exposure on some specific bacteria, such as *Corynebacterium* and *Lactococcus*, that may contribute to colonization resistance against *S. pneumoniae*. A decrease in *Corynebacterium* and *Lactococcus* was reported to correlate with URT pneumococcal colonization in children, and smokers had less abundant *Corynebacterium*[164,179,182]. We show that nasal pneumococcal colonization over the background of cigarette smoke exposure did not impact the levels of *Corynebacterium* and *Lactococcus* compared to nasal pneumococcal colonization alone. The decrease in commensal bacteria, such as *Corynebacterium*, found in smokers may thus be a consequence of nasal pneumococcal colonization alone, rather than cigarette smoke exposure, which should be taken into account while interpreting clinical observations.

On the other hand, we observed in cigarette smoke-exposed mice compared to room air-exposed mice at day 3 post-nasal pneumococcal colonization significant increases in the abundance of several genera, including *Fusobacterium* and *Tannerella*,

that contain bacterial species associated with periodontal disease[298,299]. Notably, smokers are at increased risk of periodontitis, and oral microbiome dysbiosis was recently reported in current smokers[117,300]. *Gemella*, *Neisseria*, and *Kingella*, which contain species with pathogenic potential, were also enriched with the combination of pneumococcal colonization and cigarette smoke exposure[301–303]. Our data suggest that the expansion of *S. pneumoniae* during cigarette smoke exposure provides an advantage for other potential pathogens present in the URT. Cigarette smoke condensate has been shown to directly increase pneumococcal biofilm formation *in vitro*[304]. It is plausible that other bacteria may benefit from increased pneumococcal biofilm formation as different bacterial species have been shown to synergize in multispecies biofilms[305]. A biofilm is a sessile microbial community consisting of cells that irreversibly attach to a substratum to form a matrix, providing a stable protective environment and a shorter bacterial replication time[306,307]. Alternatively, cigarette smoke exposure may promote other synergistic interactions between *S. pneumoniae* and *Fusobacterium*, *Gemella*, as well as *Neisseria*, to promote their growth.

We cannot rule out that changes in the nasal microbiome observed during nasal pneumococcal colonization may simply be a consequence of higher pneumococcal burden independent of cigarette smoke exposure. Although the difference was not statistically significant, we observed higher levels of CNT *lytA* in cigarette smoke-exposed mice compared to room air-exposed mice following nasal pneumococcal colonization, suggesting higher pneumococcal burden that may account for the corresponding nasal microbiome changes observed. For example, cigarette smoke-exposed mice may have increased pneumococcal biofilm formation as a result of higher

nasal pneumococcal burden, leading to the enrichment of *Fusobacterium*, *Gemella*, and *Neisseria*. Overall, our experimental model of nasal pneumococcal colonization and cigarette smoke exposure showed changes in the nasal microbiome reflective of observations in human smokers, with the enrichment of several potential pathogens. However, our findings suggest that nasal microbiome dysbiosis occur not in response to cigarette smoke exposure, but rather as a consequence following the establishment of nasal colonization by *S. pneumoniae*. Whether the microbial dysbiosis observed in smokers is simply a consequence of higher pathogenic bacterial burden, and occur independent of cigarette smoking, warrants further investigation.

We further investigated whether cigarette smoke exposure altered bacterial-bacterial interactions by assessing the abundance of specific genera, including *Haemophilus* and *Staphylococcus*, known to interact with *S. pneumoniae*. *Haemophilus influenzae* has been observed to induce nasal pneumococcal clearance, possibly by eliciting a neutrophilic response that drives *S. pneumoniae* killing[308]. However, this effect may be strain dependent as other studies have reported *H. influenza* enrichment in the presence of pneumococci without competitive interactions[214]. Nasal colonization of *Staphylococcus aureus*, on the other hand, is reported to inversely correlate with nasal pneumococcal colonization[215]. The competitive interaction between these two bacteria may be attributed to hydrogen peroxide production by *S. pneumoniae*[309]. Surprisingly, we did not detect significant differences in *Haemophilus* and *Staphylococcus* abundance between room air and cigarette-exposed mice despite significantly higher *Streptococcus* abundance at the genus level in cigarette smoke-exposed mice 3 days post-colonization. It could be that bacterial species within the

same genus are differentially impacted. Thus, changes in the abundance of individual bacterial species, such as *H. influenza* and *S. aureus*, may be masked when overall abundance is assessed as a whole on the genus level. Of note, we observed a significant increase in one *Haemophilus* OTU (data not shown), suggesting there may be changes at the species level consistent with previous studies[214,215]. Alternatively, cigarette smoke exposure may alter bacterial interactions during pneumococcal colonization. For example, cigarette smoke extract *in vitro* has been found to directly increase *S. aureus* biofilm formation and up-regulate the expression of oxidoreductase enzymes dependent on oxidative stress[310]. Cigarette smoke exposure may thus increase *S. aureus* competitiveness by inducing tolerance to pneumococcal hydrogen peroxide production. Further research is required to elucidate how cigarette smoke exposure may impact specific bacterial-bacterial interactions at the species level during nasal pneumococcal colonization.

We observed that cigarette smoke exposure increased nasal pneumococcal colonization, consistent with clinical observations[123,185–187]. Although the increase in the incidence of nasal wash pneumococcal recovery from cigarette smoke-exposed mice following very low dose pneumococcal colonization (10^3 CFU) was not significant relative to room air-exposed controls at 12 hours post-colonization, we observed a significant increase in nasal pneumococcal burden following inoculation of 10^4 CFU *S. pneumoniae*. We also assessed nasal pneumococcal burden in the same CNT samples utilized for nasal microbiome analysis. Surprisingly, we did not observe similar increases in *lytA* levels from CNT samples at 12 hours post-nasal pneumococcal colonization. Instead, when we inoculated mice with a high pneumococcal dose to

ensure maximal colonization (10^7 CFU), the amount of *lytA* was increased at day 3 post-colonization in the CNT of cigarette smoke-exposed mice, a time point when pneumococcal burden was previously observed to be similar between room air-exposed and cigarette smoke-exposed mice in the nasal wash. These differences in pneumococcal colonization levels between nasal wash and CNT samples may be explained by the presence of different subpopulations of *S. pneumoniae* during colonization. Surface and invasive subpopulations of nasally colonizing *S. pneumoniae* have been previously described. While the surface population of *S. pneumoniae* can be recovered by nasal wash, the invasive population was only recoverable following homogenization of the nasal tissue[311]. Hence we may be examining different pneumococcal populations in the CNT and the nasal wash. The variability of *lytA* assessment was also high in CNT samples, compared to culturing data that is usually presented on a log scale. This variability may explain why the difference in CNT *lytA* levels between room air and cigarette smoke-exposed mice did not reach statistical significance. Nevertheless, we confirmed the establishment of nasal pneumococcal colonization, which allowed us to evaluate corresponding nasal microbiome changes in the same CNT samples.

We took advantage of an established experimental mouse model to evaluate the effect of cigarette smoke exposure on the nasal microbiome in the absence and presence of nasal colonization by an opportunistic pathogen, in this case *S. pneumoniae*. We confirmed clinical observations that cigarette smoke exposure increases nasal pneumococcal colonization[123,185–187]. However, our findings suggest that cigarette smoke exposure alone was not sufficient to alter nasal microbiome

composition, and that clinical observations of nasal microbiome dysbiosis in smokers are likely a consequence of established pathogen colonization. We propose that cigarette smoke exposure predisposes to nasal pneumococcal colonization by impacting other aspects of bacterial-host interactions, such as the URT host defence, rather than altering the nasal microbiome to compromise pathogen colonization resistance. Observations of dysbiosis in the context of cigarette smoke exposure and confirmed pneumococcal colonization may thus be attributed to subsequent disturbance of URT microbial communities by colonizing pneumococci. Interestingly, we report here a synergy between *S. pneumoniae* and several other potential pathogens during cigarette smoke exposure post-nasal pneumococcal colonization, consistent with previous observations of increased pathogen isolation from current smokers[123]. Whether cigarette smoke directly drives synergistic interactions between pathogens during nasal pneumococcal colonization remains to be determined.

4.7. Final thoughts and future directions

The work presented in this thesis investigated the impact of cigarette smoke exposure on multiple aspects of bacterial colonization and infection, leaving some fascinating avenues for future research. Our findings suggest cigarette smoke exposure differentially impacts the inflammatory response to bacteria at the upper and lower respiratory tract. While cigarette smoke exposure primed the lungs towards an exacerbated neutrophilic response to NTHi infection, the nasal inflammatory response to *S. pneumoniae* colonization was attenuated. We hypothesize that an impaired ability to contain colonizing bacteria at the URT contributes to the increased risk of acquiring bacterial infection in smokers and COPD patients. At the same time, an established

infection in the lungs promotes excessive inflammation, leading to exacerbations of COPD and lung damage. However, we note that different bacteria were used to study the URT and lungs in this thesis. Whether *S. pneumoniae* elicits similar inflammatory responses in the lungs as NTHi following cigarette smoke exposure warrants further attention as *S. pneumoniae* is also frequently associated with COPD exacerbations[106]. Additionally, in light of the failure of the recent anti-IL-1R1 antibody clinical trial to reduce COPD exacerbation frequency[211], it is critical to evaluate whether mechanisms underlying COPD exacerbations differ dependent on the bacteria.

We show that cigarette smoke exposure predisposes to IPD in mice associated with an attenuated nasal inflammatory response to *S. pneumoniae*. However, the impact of cigarette smoke exposure on nasally colonizing microbial pathogens may also be an important contributing factor. Several *in vitro* studies have shown cigarette smoke to up-regulate bacterial virulence gene expression and increase biofilm formation in *Porphyromonas gingivalis*, *Staphylococcus aureus*, and *Pseudomonas aeruginosa*[310,312,313]. Although it has been shown that *S. pneumoniae* biofilm formation is increased in response to cigarette smoke condensate *in vitro*[304,314], how cigarette smoke directly impacts pneumococcal virulence during nasal colonization *in vivo* remains an area of future research that may lead to novel therapeutic intervention strategies.

Our study showed that microbiome dysbiosis occur as a consequence of nasal pneumococcal colonization in cigarette smoke-exposed mice, characterized by an enrichment of other potential pathogens residing in the URT. In addition to targeting aspects of the URT host defence altered by cigarette smoke exposure, future efforts to

reduce pathogen colonization in smokers can also take advantage of bacterial community interactions to restore balance to the nasal microbiome. For example, nasal re-colonization with alpha-hemolytic streptococci that competitively interact with several pathogens in patients prone to tonsillitis decreased the recurrence of infection[315]. Similarly, alpha-hemolytic streptococci re-colonization reduced the rate of recurrence of acute otitis media in susceptible children[316]. Further research is required to evaluate the potential of nasal microbiome modulation as an intervention strategy to decrease nasal pathogen colonization and reduce the risk of bacterial infection in smokers.

4.8. Overall conclusions

The work presented in this thesis has advanced our knowledge of the impact of cigarette smoke exposure on bacterial-host, as well as bacterial community interactions. The first study presented in chapter 3.1 (published in the *Journal of Immunology*) elucidated mechanisms underlying an exacerbated lung inflammatory response to bacteria in cigarette smoke-exposed mice that contributed to the decision process to pursue a clinical trial of anti-IL-1R1 antibody therapy in COPD patients. The second study presented in chapter 3.2 (published in *Infection and Immunity*) is, to our knowledge, the first to investigate the progression to IPD from an asymptomatic nasal pneumococcal carrier state in the context of cigarette smoke exposure. Importantly, we showed that the increased risk of IPD in cigarette smoke-exposed mice is associated with an attenuated nasal inflammatory response to *S. pneumoniae*, and that smokers may be at increased risk of not only pneumonia, as reported in the literature, but occult pneumococcal bacteraemia as well. The third study presented in chapter 3.3 (manuscript in preparation, planned submission to *Infection and Immunity*) tested the

prevalent hypothesis that cigarette smoke exposure increases pathogen colonization associated with perturbation of the resident nasal microbiome that may decrease colonization resistance. Our study suggests that cigarette smoke exposure alone was not sufficient to alter nasal microbiota composition and that clinical observations of microbiome dysbiosis in smokers likely occur as a consequence of nasal pathogen colonization. These findings raise the question of whether focus should be shifted towards targeting other aspects of bacterial-host interactions that contribute to increased pathogen colonization in smokers. Overall, work presented in this thesis has increased our understanding of how cigarette smoking alters bacterial-host interactions to promote bacterial infection and COPD pathogenesis.

CHAPTER 5. REFERENCES

1. U.S.DHHS. How Tobacco Smoke Causes Disease: The Biology and Behavioral Basis for Smoking-Attributable Disease: A Report of the Surgeon General. *Public Health* 792 (2010).
2. U.S. Department of Health and Human Services. *The Health Consequences of Smoking—50 Years of Progress: A Report of the Surgeon General*. *Smok. Heal.* (2014).
3. Stämpfli, M. R. & Anderson, G. P. How cigarette smoke skews immune responses to promote infection, lung disease and cancer. *Nat. Rev. Immunol.* **9,** 377–384 (2009).
4. *2004 Surgeon General's Report—The Health Consequences of Smoking*. (2004).
5. Department of Health and Human Services. The Health Consequences of Involuntary Exposure to Tobacco Smoke A Report of the Surgeon General. *Public Health* (2006).
6. Arcavi, L. & Benowitz, N. L. Cigarette smoking and infection. *Arch Intern Med* **164,** 2206–2216 (2004).
7. Jha, P. *et al.* 21st-century hazards of smoking and benefits of cessation in the United States. *N. Engl. J. Med.* **368,** 341–50 (2013).
8. Pirie, K., Peto, R., Reeves, G. K., Green, J. & Beral, V. The 21st century hazards of smoking and benefits of stopping: a prospective study of one million women in the UK. *Lancet (London, England)* **381,** 133–41 (2013).
9. Robbins, A. S. *et al.* Short term effects of cigarette smoking on hospitalisation and associated lost workdays in a young healthy population. *Tob Control* **9,** 389–396 (2000).
10. Johnson, P. B. & Richter, L. The relationship between smoking, drinking, and adolescents' self-perceived health and frequency of hospitalization: Analyses from the 1997 National Household Survey on Drug Abuse. *J. Adolesc. Health.* **30,** 175–183 (2002).
11. Wang, M. P., Ho, S. Y., Lo, W. S., Lai, M. K. & Lam, T. H. Smoking is associated with poor self-rated health among adolescents in Hong Kong. *Nicotine Tob. Res.* **14,** 682–7 (2012).
12. Weng, S. F., Ali, S. & Leonardi-Bee, J. Smoking and absence from work: Systematic review and meta-analysis of occupational studies. *Addiction* **108,** 307–319 (2013).
13. Vestbo, J. *et al.* Global strategy for the diagnosis, management, and prevention of chronic obstructive pulmonary disease: GOLD executive summary (updated 2014). *Glob. Initiat. Chronic Obstr. Lung Dis.* 21–26 (2014). doi:10.1164/ajrccm.163.5.2101039
14. Lopez, A. D. *et al.* Chronic obstructive pulmonary disease: current burden and future projections. *Eur. Respir. J.* **27,** 397–412 (2006).
15. Vos, T. *et al.* Years lived with disability (YLDs) for 1160 sequelae of 289 diseases and injuries 1990–2010: a systematic analysis for the Global Burden of Disease Study 2010. *Lancet* **380,** 2163–2196 (2012).
16. Murray, C. & Lopez, A. *The global burden of disease*. (Harvard University Press, 1996).
17. Kessler, R. *et al.* Symptom variability in patients with severe COPD: a pan-European cross-sectional study. *Eur. Respir. J.* **37,** 264–72 (2011).
18. Espinosa de los Monteros, M. J., Peña, C., Soto Hurtado, E. J., Jareño, J. & Miravitlles, M.

Variability of respiratory symptoms in severe COPD. *Arch. Bronconeumol.* **48,** 3–7 (2012).

19. Loppow, D. *et al.* In patients with chronic bronchitis a four week trial with inhaled steroids does not attenuate airway inflammation. *Respir. Med.* **95,** 115–21 (2001).

20. Hogg, J. C. *et al.* The nature of small-airway obstruction in chronic obstructive pulmonary disease. *N. Engl. J. Med.* **350,** 2645–53 (2004).

21. Cosio, M. *et al.* The relations between structural changes in small airways and pulmonary-function tests. *N. Engl. J. Med.* **298,** 1277–81 (1978).

22. Kim, W. D. *et al.* Centrilobular and panlobular emphysema in smokers. Two distinct morphologic and functional entities. *Am Rev Respir Dis* **144,** 1385–1390 (1991).

23. Gottlieb, D. J. *et al.* Urinary desmosine excretion in smokers with and without rapid decline of lung function: the Normative Aging Study. *Am. J. Respir. Crit. Care Med.* **154,** 1290–95 (1996).

24. Fletcher, C., Peto, R. & Speizer, F. *The natural history of chronic bronchitis and emphysema*. (Oxford University Press, 1976).

25. Barnes, P. J., Shapiro, S. D. & Pauwels, R. A. Chronic obstructive pulmonary disease: molecular and cellular mechanisms. *Eur Respir J* **22,** 672–688 (2003).

26. Rennard, S. I. & Vestbo, J. COPD: the dangerous underestimate of 15%. *Lancet* **367,** 1216–1219 (2006).

27. Kohansal, R. *et al.* The natural history of chronic airflow obstruction revisited: An analysis of the Framingham Offspring Cohort. *Am. J. Respir. Crit. Care Med.* **180,** 3–10 (2009).

28. Capelli, a *et al.* Increased MCP-1 and MIP-1beta in bronchoalveolar lavage fluid of chronic bronchitics. *Eur. Respir. J.* **14,** 160–5 (1999).

29. Kuschner, W. G., D'Alessandro, a., Wong, H. & Blanc, P. D. Dose-dependent cigarette smoking-related inflammatory responses in healthy adults. *Eur. Respir. J.* **9,** 1989–1994 (1996).

30. Profita, M. *et al.* Effect of cilomilast (Ariflo) on TNF-alpha, IL-8, and GM-CSF release by airway cells of patients with COPD. *Thorax* **58,** 573–9 (2003).

31. Cox, G., Gauldie, J. & Jordana, M. Bronchial epithelial cell-derived cytokines (G-CSF and GM-CSF) promote the survival of peripheral blood neutrophils in vitro. *Am. J. Respir. Cell Mol. Biol.* **7,** 507–514 (1992).

32. Vignola, a M. *et al.* Increased levels of elastase and alpha1-antitrypsin in sputum of asthmatic patients. *Am. J. Respir. Crit. Care Med.* **157,** 505–11 (1998).

33. Weitz, J. I., Crowley, K. A., Landman, S. L., Lipman, B. I. & Yu, J. Increased neutrophil elastase activity in cigarette smokers. *Ann Intern Med* **107,** 680–682 (1987).

34. Hind, C. R., Joyce, H., Tennent, G. A., Pepys, M. B. & Pride, N. B. Plasma leucocyte elastase concentrations in smokers. *J.Clin.Pathol.* **44,** 232–235 (1991).

35. Pardo, A. & Selman, M. Matrix metalloproteases in aberrant fibrotic tissue remodeling. *Proc. Am. Thorac. Soc.* **3,** 383–388 (2006).

36. Aviles, B. *et al.* Markers of Airway Remodeling in Induced Sputum From Healthy Smokers. *Arch Broncoeumol* **42,** 235–240 (2006).

37. Kinnula, V. L., Ilumets, H., Myllärniemi, M., Sovijärvi, a & Rytilä, P. 8-Isoprostane as a marker of oxidative stress in nonsymptomatic cigarette smokers and COPD. *Eur. Respir. J.* **29,** 51–5 (2007).

38. Montuschi, P. *et al.* Exhaled 8-isoprostane as an in vivo biomarker of lung oxidative stress in patients with COPD and healthy smokers. *Am J Respir Crit Care Med* **162,** 1175–1177 (2000).

39. Montuschi, P. *et al.* Increased 8-isoprostane, a marker of oxidative stress, in exhaled condensate of asthma patients. *Am. J. Respir. Crit. Care Med.* **160,** 216–220 (1999).

40. Shaykhiev, R. & Crystal, R. G. Innate immunity and chronic obstructive pulmonary disease: a mini-review. *Gerontology* **59,** 481–9 (2013).

41. Retamales, I. *et al.* Amplification of inflammation in emphysema and its association with latent adenoviral infection. *Am J Respir Crit Care Med* **164,** 469–473 (2001).

42. Di Stefano, A. *et al.* Severity of airflow limitation is associated with severity of airway inflammation in smokers. *Am. J. Respir. Crit. Care Med.* **158,** 1277–85 (1998).

43. Russell, R. E. *et al.* Alveolar macrophage-mediated elastolysis: roles of matrix metalloproteinases, cysteine, and serine proteases. *Am J Physiol Lung Cell Mol Physiol* **283,** L867–73 (2002).

44. Imai, K. *et al.* Human collagenase (matrix metalloproteinase-1) expression in the lungs of patients with emphysema. *Am. J. Respir. Crit. Care Med.* **163,** 786–791 (2001).

45. Ohnishi, K., Takagi, M., Kurokawa, Y., Satomi, S. & Konttinen, Y. T. Matrix metalloproteinase-mediated extracellular matrix protein degradation in human pulmonary emphysema. *Lab Invest* **78,** 1077–1087 (1998).

46. Molet, S. *et al.* Increase in macrophage elastase (MMP-12) in lungs from patients with chronic obstructive pulmonary disease. *Inflamm. Res.* **54,** 31–36 (2005).

47. Quint, J. K. & Wedzicha, J. A. The neutrophil in chronic obstructive pulmonary disease. *J. Allergy Clin. Immunol.* **119,** 1065–71 (2007).

48. Traves, S. L., Culpitt, S. V, Russell, R. E., Barnes, P. J. & Donnelly, L. E. Increased levels of the chemokines GROalpha and MCP-1 in sputum samples from patients with COPD. *Thorax* **57,** 590–595 (2002).

49. Tanino, M. *et al.* Increased levels of interleukin-8 in BAL fluid from smokers susceptible to pulmonary emphysema. *Thorax* **57,** 405–411 (2002).

50. Borregaard, N. & Cowland, J. B. Granules of the human neutrophilic polymorphonuclear leukocyte. *Blood* **89,** 3503–3521 (1997).

51. Yamamoto, C. *et al.* Airway inflammation in COPD assessed by sputum levels of interleukin-8. *Chest* **112,** 505–10 (1997).

52. Stănescu, D. *et al.* Airways obstruction, chronic expectoration, and rapid decline of FEV1 in smokers are associated with increased levels of sputum neutrophils. *Thorax* **51,** 267–271 (1996).

53. Keatings, V. M. & Barnes, P. J. Granulocyte activation markers in induced sputum: Comparison between chronic obstructive pulmonary disease, asthma, and normal subjects. *Am. J. Respir. Crit. Care Med.* **155,** 449–453 (1997).

54. Eiserich, J. P. *et al.* Formation of nitric oxide-derived inflammatory oxidants by myeloperoxidase in neutrophils. *Nature* **391,** 393–7 (1998).

55. Gaut, J. P. *et al.* Myeloperoxidase produces nitrating oxidants in vivo. *J. Clin. Invest.* **109,** 1311–9 (2002).

56. Dhami, R. *et al.* Acute cigarette smoke-induced connective tissue breakdown is mediated by neutrophils and prevented by alpha1-antitrypsin. *Am. J. Respir. Cell Mol. Biol.* **22,** 244–252 (2000).

57. MacNee, W. Oxidative stress and lung inflammation in airways disease. *Eur. J. Pharmacol.* **429,** 195–207 (2001).

58. Dekhuijzen, P. N. *et al.* Increased exhalation of hydrogen peroxide in patients with stable and unstable chronic obstructive pulmonary disease. *Am J Respir Crit Care Med* **154,** 813–816 (1996).

59. Adcock, I. M., Brown, C. R., Kwon, O. & Barnes, P. J. Oxidative stress induces NF kappa B DNA binding and inducible NOS mRNA in human epithelial cells. *Biochem. Biophys. Res. Commun.* **199,** 1518–24 (1994).

60. Hogg, J. C. *et al.* The nature of small-airway obstruction in chronic obstructive pulmonary disease. *N Engl J Med* **350,** 2645–2653 (2004).

61. Saetta, M. *et al.* CD8+ T-lymphocytes in peripheral airways of smokers with chronic obstructive pulmonary disease. *Am. J. Respir. Crit. Care Med.* **157,** 822–826 (1998).

62. Majo, J., Ghezzo, H. & Cosio, M. G. Lymphocyte population and apoptosis in the lungs of smokers and their relation to emphysema. *Eur. Respir. J.* **17,** 946–953 (2001).

63. Saetta, M. *et al.* Increased expression of the chemokine receptor CXCR3 and its ligand CXCL10 in peripheral airways of smokers with chronic obstructive pulmonary disease. *Am. J. Respir. Crit. Care Med.* **165,** 1404–1409 (2002).

64. Hashimoto, S. *et al.* Upregulation of two death pathways of perforin/granzyme and FasL/Fas in septic acute respiratory distress syndrome. *Am. J. Respir. Crit. Care Med.* **161,** 237–243 (2000).

65. Eppert, B. L., Wortham, B. W., Flury, J. L. & Borchers, M. T. Functional characterization of T cell populations in a mouse model of chronic obstructive pulmonary disease. *J. Immunol.* **190,** 1331–40 (2013).

66. van der Strate, B. W. A. *et al.* Cigarette smoke-induced emphysema: A role for the B cell? *Am. J. Respir. Crit. Care Med.* **173,** 751–758 (2006).

67. Patel, I. S. *et al.* Relationship between bacterial colonisation and the frequency, character, and severity of COPD exacerbations. *Thorax* **57,** 759–764 (2002).

68. Becker, C. G. & Dubin, T. Activation of factor XII by tobacco glycoprotein. *J Exp Med* **146,** 457–467 (1977).

69. Lee, S.-H. *et al.* Antielastin autoimmunity in tobacco smoking-induced emphysema. *Nat. Med.* **13,** 567–9 (2007).

70. Takahashi, S. & Betsuyaku, T. The chronic obstructive pulmonary disease comorbidity spectrum in Japan differs from that in western countries. *Respir. Investig.* **53**, 259-270 (2015).

71. Vlahos, R. & Bozinovski, S. Recent advances in pre-clinical mouse models of COPD. *Clin. Sci.* **126,** 253–65 (2014).

72. Botelho, F. M. *et al.* Innate immune processes are sufficient for driving cigarette smoke-induced

inflammation in mice. *Am J Respir Cell Mol Biol* **42,** 394–403

73. Hoenderdos, K. & Condliffe, A. The neutrophil in chronic obstructive pulmonary disease. *Am. J. Respir. Cell Mol. Biol.* **48,** 531–9 (2013).

74. Rouhani, F. *et al.* Lung neutrophil burden correlates with increased pro-inflammatory cytokines and decreased lung function in individuals with alpha1-antitrypsin deficiency. in *Chest* **117,** 250S-251S (2000).

75. Doz, E. *et al.* Cigarette smoke-induced pulmonary inflammation is TLR4/MyD88 and IL-1R1/MyD88 signaling dependent. *J Immunol* **180,** 1169–1178 (2008).

76. Kang, M. J. *et al.* IL-18 is induced and IL-18 receptor alpha plays a critical role in the pathogenesis of cigarette smoke-induced pulmonary emphysema and inflammation. *J Immunol* **178,** 1948–1959 (2007).

77. Roos, A. B. *et al.* IL-17A and the promotion of neutrophilia in acute exacerbation of chronic obstructive pulmonary disease. *Am. J. Respir. Crit. Care Med.* **192,** 428–437 (2015).

78. Dinarello, C. A. Immunological and inflammatory functions of the interleukin-1 family. *Annu Rev Immunol* **27,** 519–550 (2009).

79. Rock, K. L., Latz, E., Ontiveros, F. & Kono, H. The sterile inflammatory response. *Annu Rev Immunol* **28,** 321–342 (2009).

80. Mosley, B. *et al.* The interleukin-1 receptor binds the human interleukin-1 alpha precursor but not the interleukin-1 beta precursor. *J Biol Chem* **262,** 2941–2944 (1987).

81. Thornberry, N. A. *et al.* A novel heterodimeric cysteine protease is required for interleukin-1 beta processing in monocytes. *Nature* **356,** 768–774 (1992).

82. Masumoto, J. *et al.* ASC, a novel 22-kDa protein, aggregates during apoptosis of human promyelocytic leukemia HL-60 cells. *J Biol Chem* **274,** 33835–33838 (1999).

83. Kuida, K. *et al.* Altered cytokine export and apoptosis in mice deficient in interleukin-1 beta converting enzyme. *Science* **267,** 2000–2003 (1995).

84. Martinon, F., Mayor, A. & Tschopp, J. The inflammasomes: guardians of the body. *Annu Rev Immunol* **27,** 229–265 (2009).

85. Castro, P. *et al.* Inhibition of interleukin-1beta reduces mouse lung inflammation induced by exposure to cigarette smoke. *Eur. J. Pharmacol.* **498,** 279–86 (2004).

86. Churg, A., Zhou, S., Wang, X., Wang, R. & Wright, J. L. The role of interleukin-1beta in murine cigarette smoke-induced emphysema and small airway remodeling. *Am. J. Respir. Cell Mol. Biol.* **40,** 482–490 (2009).

87. Pauwels, N. S. *et al.* Role of IL-1{alpha} and the Nlrp3/caspase-1/IL-1{beta} axis in cigarette smoke-induced pulmonary inflammation and COPD. *Eur Respir J* **38**, 1019-1028 (2011).

88. Botelho, F. M. *et al.* IL-1alpha/IL-1R1 expression in chronic obstructive pulmonary disease and mechanistic relevance to smoke-induced neutrophilia in mice. *PLoS One* **6,** e28457

89. Soler, N. *et al.* Airway inflammation and bronchial microbial patterns in patients with stable chronic obstructive pulmonary disease. *Eur. Respir. J.* **14,** 1015–22 (1999).

90. Zalacain, R. *et al.* Predisposing factors to bacterial colonization in chronic obstructive pulmonary disease. *Eur. Respir. J.* **13,** 343–8 (1999).

91. Morris, A. *et al.* Comparison of the respiratory microbiome in healthy nonsmokers and smokers. *Am. J. Respir. Crit. Care Med.* **187,** 1067–1075 (2013).

92. Sze, M. A. *et al.* The lung tissue microbiome in chronic obstructive pulmonary disease. *Am. J. Respir. Crit. Care Med.* **185,** 1073–1080 (2012).

93. Hilty, M. *et al.* Disordered microbial communities in asthmatic airways. *PLoS One* **5,** e8578 (2010).

94. Huang, Y. J. *et al.* A persistent and diverse airway microbiota present during chronic obstructive pulmonary disease exacerbations. *OMICS* **14,** 9–59 (2010).

95. Sze, M. A., Hogg, J. C. & Sin, D. D. Bacterial microbiome of lungs in COPD. *Int. J. Chron. Obstruct. Pulmon. Dis.* **9,** 229–38 (2014).

96. Berenson, C. S. *et al.* Impaired alveolar macrophage response to Haemophilus antigens in chronic obstructive lung disease. *Am J Respir Crit Care Med* **174,** 31–40 (2006).

97. Berenson, C. S., Garlipp, M. A., Grove, L. J., Maloney, J. & Sethi, S. Impaired phagocytosis of nontypeable Haemophilus influenzae by human alveolar macrophages in chronic obstructive pulmonary disease. *J. Infect. Dis.* **194,** 1375–1384 (2006).

98. Larsen, J. M. *et al.* Divergent pro-inflammatory profile of human dendritic cells in response to commensal and pathogenic bacteria associated with the airway microbiota. *PLoS One* **7,** e31976 (2012).

99. Sethi, S., Maloney, J., Grove, L., Wrona, C. & Berenson, C. S. Airway inflammation and bronchial bacterial colonization in chronic obstructive pulmonary disease. *Am. J. Respir. Crit. Care Med.* **173,** 991–8 (2006).

100. Singh, R. *et al.* Inflammatory thresholds and the species-specific effects of colonising bacteria in stable chronic obstructive pulmonary disease. *Respir. Res.* **15,** 114 (2014).

101. Donaldson, G. C., Seemungal, T. A. R., Bhowmik, A. & Wedzicha, J. A. Relationship between exacerbation frequency and lung function decline in chronic obstructive pulmonary disease. *Thorax* **57,** 847–52 (2002).

102. Donaldson, G. C. & Wedzicha, J. A. COPD exacerbations .1: Epidemiology. *Thorax* **61,** 164–8 (2006).

103. Crooks, S. W., Bayley, D. L., Hill, S. L. & Stockley, R. A. Bronchial inflammation in acute bacterial exacerbations of chronic bronchitis: The role of leukotriene B4. *Eur. Respir. J.* **15,** 274–280 (2000).

104. Aaron, S. D. *et al.* Granulocyte inflammatory markers and airway infection during acute exacerbation of chronic obstructive pulmonary disease. *Am. J. Respir. Crit. Care Med.* **163,** 349–55 (2001).

105. Vestbo, J. *et al.* Global strategy for the diagnosis, management, and prevention of chronic obstructive pulmonary disease GOLD executive summary. *Am. J. Respir. Crit. Care Med.* **187,** 347–365 (2013).

106. Sethi, S. & Murphy, T. F. Infection in the pathogenesis and course of chronic obstructive pulmonary disease. *N Engl J Med* **359,** 2355–2365 (2008).

107. Tunney, M. M. *et al.* Lung microbiota and bacterial abundance in patients with bronchiectasis when clinically stable and during exacerbation. *Am. J. Respir. Crit. Care Med.* **187,** 1118–26 (2013).

108. Sethi, S., Evans, N., Grant, B. J. & Murphy, T. F. New strains of bacteria and exacerbations of chronic obstructive pulmonary disease. *N Engl J Med* **347,** 465–471 (2002).

109. Sethi, S. *et al.* Inflammatory profile of new bacterial strain exacerbations of chronic obstructive pulmonary disease. *Am. J. Respir. Crit. Care Med.* **177,** 491–497 (2008).

110. Gaschler, G. J. *et al.* Bacteria challenge in smoke-exposed mice exacerbates inflammation and skews the inflammatory profile. *Am J Respir Crit Care Med* **179,** 666–675 (2009).

111. Gaschler, G. J. *et al.* Cigarette smoke exposure attenuates cytokine production by mouse alveolar macrophages. *Am J Respir Cell Mol Biol* **38,** 218–226 (2008).

112. Almirall, J., González, C. A., Balanzó, X. & Bolíbar, I. Proportion of community-acquired pneumonia cases attributable to tobacco smoking. *Chest* **116,** 375–379 (1999).

113. Kolappan, C. & Gopi, P. G. Tobacco smoking and pulmonary tuberculosis. *Thorax* **57,** 964–966 (2002).

114. Straus, W. L. *et al.* Risk factors for domestic acquisition of legionnaires disease. Ohio legionnaires Disease Group. *Arch. Intern. Med.* **156,** 1685–1692 (1996).

115. Fischer, M. *et al.* Tobacco smoke as a risk factor for meningococcal disease. *Pediatr. Infect. Dis. J.* **16,** 979–83 (1997).

116. Murphy, T. F. Otitis media, bacterial colonization, and the smoking parent. *Clin. Infect. Dis.* **42,** 904–906 (2006).

117. Arbes, S. J., Agústsdóttir, H. & Slade, G. D. Environmental tobacco smoke and periodontal disease in the United States. *Am. J. Public Health* **91,** 253–257 (2001).

118. Larsson, P.-G., Fåhraeus, L., Carlsson, B., Jakobsson, T. & Forsum, U. Predisposing factors for bacterial vaginosis, treatment efficacy and pregnancy outcome among term deliveries; results from a preterm delivery study. *BMC Women's Health* **7,** 20 (2007).

119. Nuorti, J. P. *et al.* Cigarette smoking and invasive pneumococcal disease. Active Bacterial Core Surveillance Team. *N Engl J Med* **342,** 681–689 (2000).

120. Charlson, E. S. *et al.* Topographical continuity of bacterial populations in the healthy human respiratory tract. *Am. J. Respir. Crit. Care Med.* **184,** 957–963 (2011).

121. Human Microbiome Project Consortium. Structure, function and diversity of the healthy human microbiome. *Nature* **486,** 207–214 (2012).

122. Gillespie, J. J. *et al.* PATRIC: the comprehensive bacterial bioinformatics resource with a focus on human pathogenic species. *Infect. Immun.* **79,** 4286–98 (2011).

123. Brook, I. & Gober, A. E. Recovery of potential pathogens and interfering bacteria in the nasopharynx of smokers and nonsmokers. *Chest* **127,** 2072–2075 (2005).

124. Bogaert, D., De Groot, R. & Hermans, P. W. Streptococcus pneumoniae colonisation: the key to pneumococcal disease. *Lancet Infect Dis* **4,** 144–154 (2004).

125. Zhang, N., van Crombruggen, K., Gevaert, E. & Bachert, C. Barrier function of the nasal mucosa in health and type-2 biased airway diseases. *Allergy* **71**, 295-307 (2016).

126. Sleigh, M. A., Blake, J. R. & Llron, N. The Propulsion of Mucus by Cilia. *Am. Rev. Respir. Dis.* **137,** 726–741 (1988).

127. Schneeberger, E. E. & Lynch, R. D. The tight junction: a multifunctional complex. *Am. J. Physiol. Cell Physiol.* **286,** C1213–C1228 (2004).

128. Shaykhiev, R. *et al.* Cigarette smoking reprograms apical junctional complex molecular architecture in the human airway epithelium in vivo. *Cell. Mol. Life Sci.* **68,** 877–92 (2011).

129. Heijink, I. H., Brandenburg, S. M., Postma, D. S. & van Oosterhout, A. J. M. Cigarette smoke impairs airway epithelial barrier function and cell-cell contact recovery. *Eur. Respir. J.* **39,** 419–28 (2012).

130. Coles, S. J., Bhaskar, K. R., O'Sullivan, D. D., Neill, K. H. & Reid, L. M. Airway mucus: composition and regulation of its secretion by neuropeptides in vitro. *Ciba Found. Symp.* **109,** 40–60 (1984).

131. Marttin, E., Schipper, N. G. ., Verhoef, J. C. & Merkus, F. W. H. . Nasal mucociliary clearance as a factor in nasal drug delivery. *Adv. Drug Deliv. Rev.* **29,** 13–38 (1998).

132. Schipper, N. G., Verhoef, J. C. & Merkus, F. W. The nasal mucociliary clearance: relevance to nasal drug delivery. *Pharm. Res.* **8,** 807–14 (1991).

133. Saetta, M. *et al.* Goblet cell hyperplasia and epithelial inflammation in peripheral airways of smokers with both symptoms of chronic bronchitis and chronic airflow limitation. *Am. J. Respir. Crit. Care Med.* **161,** 1016–1021 (2000).

134. Allinson, J. P. *et al.* The Presence of Chronic Mucus Hypersecretion Across Adult Life in Relation to COPD Development. *Am J Respir Crit Care Med* **Epub ahead,** 1–60 (2015).

135. Clunes, L. a. *et al.* Cigarette smoke exposure induces CFTR internalization and insolubility, leading to airway surface liquid dehydration. *FASEB J.* **26,** 533–545 (2012).

136. Hill, D. B. *et al.* A biophysical basis for mucus solids concentration as a candidate biomarker for airways disease. *PLoS One* **9,** 1–11 (2014).

137. Baraniuk, J. N. *et al.* Protein networks in induced sputum from smokers and COPD patients. *Int J Chron Obs. Pulmon Dis* **10,** 1957–1975 (2015).

138. Tamashiro, E. *et al.* Cigarette smoke exposure impairs respiratory epithelial ciliogenesis. *Am. J. Rhinol. Allergy* **23,** 117–122 (2009).

139. Simet, S. M. *et al.* Long-term cigarette smoke exposure in a mouse model of ciliated epithelial cell function. *Am. J. Respir. Cell Mol. Biol.* **43,** 635–640 (2010).

140. Agius, A. M., Smallman, L. A. & Pahor, A. L. Age, smoking and nasal ciliary beat frequency. *Clin. Otolaryngol. Allied Sci.* **23,** 227–30 (1998).

141. Pagliuca, G. *et al.* Cytologic and Functional Alterations of Nasal Mucosa in Smokers: Temporary or Permanent Damage? *Otolaryngol. -- Head Neck Surg.* **152,** 740–745 (2015).

142. Livraghi-Butrico, A. *et al.* Mucus clearance, MyD88-dependent and MyD88-independent immunity modulate lung susceptibility to spontaneous bacterial infection and inflammation. *Mucosal Immunol.* **5,** 397–408 (2012).

143. Piatti, G., Gazzola, T. & Allegra, L. Bacterial adherence in smokers and non-smokers. *Pharmacol Res* **36,** 481–484 (1997).

144. Raman, A. S., Swinburne, A. J. & Fedullo, A. J. Pneumococcal adherence to the buccal epithelial cells of cigarette smokers. *Chest* **83,** 23–27 (1983).

145. Zhang, J. R. *et al.* The polymeric immunoglobulin receptor translocates pneumococci across human nasopharyngeal epithelial cells. *Cell* **102,** 827–837 (2000).

146. Orihuela, C. J. *et al.* Laminin receptor initiates bacterial contact with the blood brain barrier in experimental meningitis models. *J. Clin. Invest.* **119,** 1638–1646 (2009).

147. Cundell, D. R., Gerard, N. P., Gerard, C., Idanpaan-Heikkila, I. & Tuomanen, E. I. Streptococcus pneumoniae anchor to activated human cells by the receptor for platelet-activating factor. *Nature* **377,** 435–438 (1995).

148. Grigg, J. *et al.* Cigarette smoke and platelet-activating factor receptor dependent adhesion of Streptococcus pneumoniae to lower airway cells. *Thorax* **67,** 908–913

149. Grigg, J. The platelet activating factor receptor: a new anti-infective target in respiratory disease? *Thorax* **67,** 840–841

150. Barbier, M. *et al.* Novel phosphorylcholine-containing protein of Pseudomonas aeruginosa chronic infection isolates interacts with airway epithelial cells. *JID* **197,** 465–73 (2008).

151. Pneumococcal conjugate vaccine for childhood immunization--WHO position paper. *Wkly Epidemiol Rec* **82,** 93–104 (2007).

152. Levine, O. S. *et al.* Pneumococcal vaccination in developing countries. *Lancet* **367,** 1880–1882 (2006).

153. Mandell, L. A. *et al.* Infectious Diseases Society of America/American Thoracic Society consensus guidelines on the management of community-acquired pneumonia in adults. *Clin Infect Dis* **44 Suppl 2,** S27–72 (2007).

154. Hendley, J. O., Sande, M. A., Stewart, P. M. & Gwaltney, J. M. Spread of Streptococcus pneumoniae in families. I. Carriage rates and distribution of types. *J. Infect. Dis.* **132,** 55–61 (1975).

155. Ekdahl, K. *et al.* Duration of nasopharyngeal carriage of penicillin-resistant *Streptococcus pneumoniae*: experiences from the South Swedish Pneumococcal Intervention Project. *Clin Infect Dis* **25,** 1113–7 (1997).

156. Garcia-Vidal, C. *et al.* Pneumococcal pneumonia presenting with septic shock: host- and pathogen-related factors and outcomes. *Thorax* **65,** 77–81

157. Grau, I. *et al.* Smoking and alcohol abuse are the most preventable risk factors for invasive pneumonia and other pneumococcal infections. *Int. J. Infect. Dis.* **25,** 59–64 (2014).

158. Beisswenger, C., Lysenko, E. S. & Weiser, J. N. Early bacterial colonization induces toll-like receptor-dependent transforming growth factor beta signaling in the epithelium. *Infect Immun* **77,** 2212–2220 (2009).

159. Matthias, K. A., Roche, A. M., Standish, A. J., Shchepetov, M. & Weiser, J. N. Neutrophil-toxin interactions promote antigen delivery and mucosal clearance of Streptococcus pneumoniae. *J.*

Immunol. **180,** 6246–6254 (2008).

160. Weiser, J. N. The pneumococcus: why a commensal misbehaves. *J Mol Med* **88,** 97–102

161. Zhang, Z., Clarke, T. B. & Weiser, J. N. Cellular effectors mediating Th17-dependent clearance of pneumococcal colonization in mice. *J Clin Invest* **119,** 1899–1909 (2009).

162. Grice, E. A. & Segre, J. A. The skin microbiome. *Nat. Rev. Microbiol.* **9,** 244–53 (2011).

163. Ding, T. & Schloss, P. D. Dynamics and associations of microbial community types across the human body. *Nature* **509,** 357–60 (2014).

164. Ramakrishnan, V. R. *et al.* The microbiome of the middle meatus in healthy adults. *PLoS One* **8,** (2013).

165. Marsland, B. J. & Gollwitzer, E. S. Host–microorganism interactions in lung diseases. *Nat. Rev. Immunol.* **14,** 827–835 (2014).

166. Konopka, A. What is microbial community ecology? *ISME J.* **3,** 1223–1230 (2009).

167. Faust, K. *et al.* Microbial co-occurrence relationships in the human microbiome. *PLoS Comput. Biol.* **8,** e1002606 (2012).

168. Smith, K., McCoy, K. D. & Macpherson, A. J. Use of axenic animals in studying the adaptation of mammals to their commensal intestinal microbiota. *Semin. Immunol.* **19,** 59–69 (2007).

169. Crowe, C. C., Sanders, W. E. & Longley, S. Bacterial interference. II. Role of the normal throat flora in prevention of colonization by group A Streptococcus. *J. Infect. Dis.* **128,** 527–532 (1973).

170. Berger, G., Bitterman, R. & Azzam, Z. S. The Human Microbiota: The Rise of an 'Empire'. *Rambam Maimonides Med. J.* **6,** e0018 (2015).

171. Zhou, Y. *et al.* Exploration of bacterial community classes in major human habitats. *Genome Biol.* **15,** R66 (2014).

172. Swords, W. E. *et al.* Non-typeable Haemophilus influenzae adhere to and invade human bronchial epithelial cells via an interaction of lipooligosaccharide with the PAF receptor. *Mol. Microbiol.* **37,** 13–27 (2000).

173. Yan, M. *et al.* Nasal microenvironments and interspecific interactions influence nasal microbiota complexity and S. aureus carriage. *Cell Host Microbe* **14,** 631–640 (2013).

174. Brüggemann, H. *et al.* The complete genome sequence of Propionibacterium acnes, a commensal of human skin. *Science* **305,** 671–673 (2004).

175. de Steenhuijsen Piters, W. A. A., Sanders, E. A. M. & Bogaert, D. The role of the local microbial ecosystem in respiratory health and disease. *Philos. Trans. R. Soc. B Biol. Sci.* **370,** 20140294 (2015).

176. Dobson, A., Cotter, P. D., Paul Ross, R. & Hill, C. Bacteriocin production: A probiotic trait? *Appl. Environ. Microbiol.* **78,** 1–6 (2012).

177. Cursino, L. *et al.* Exoproducts of the Escherichia coli strain H22 inhibiting some enteric pathogens both in vitro and in vivo. *J. Appl. Microbiol.* **100,** 821–829 (2006).

178. Tilman, D., Reich, P. B. & Knops, J. M. H. Biodiversity and ecosystem stability in a decade-long grassland experiment. *Nature* **441,** 629–632 (2006).

179. Pettigrew, M. M. *et al.* Upper respiratory tract microbial communities, acute otitis media pathogens, and antibiotic use in healthy and sick children. *Appl. Environ. Microbiol.* **78,** 6262–6270 (2012).

180. Hilty, M. *et al.* Nasopharyngeal microbiota in infants with acute otitis media. *J. Infect. Dis.* **205,** 1048–1055 (2012).

181. Abreu, N. A. *et al.* Sinus Microbiome Diversity Depletion and Corynebacterium tuberculostearicum Enrichment Mediates Rhinosinusitis. *Sci. Transl. Med.* **4,** 151ra124–151ra124 (2012).

182. Charlson, E. S. *et al.* Disordered microbial communities in the upper respiratory tract of cigarette smokers. *PLoS One* **5,** e15216 (2010).

183. Laufer, A. S. *et al.* Microbial communities of the upper respiratory tract and otitis media in children. *MBio* **2,** e00245–10 (2011).

184. Brook, I. & Gober, A. E. Effect of smoking cessation on the microbial flora. *Arch. Otolaryngol. Head. Neck Surg.* **133,** 135–8 (2007).

185. Cardozo, D. M. *et al.* Prevalence and risk factors for nasopharyngeal carriage of Streptococcus pneumoniae among adolescents. *J. Med. Microbiol.* **57,** 185–189 (2008).

186. Greenberg, D. *et al.* The contribution of smoking and exposure to tobacco smoke to Streptococcus pneumoniae and Haemophilus influenzae carriage in children and their mothers. *Clin. Infect. Dis.* **42,** 897–903 (2006).

187. Lee, C., Middaugh, N., Howie, S. & Ezzati, M. Association of secondhand smoke exposure with pediatric invasive bacterial disease and bacterial carriage: A systematic review and meta-analysis. *PLoS Med.* **7,** 1–14 (2010).

188. Cremers, A. J. *et al.* The adult nasopharyngeal microbiome as a determinant of pneumococcal acquisition. *Microbiome* **2,** 44 (2014).

189. Krone, C. L., Biesbroek, G., Trzciński, K., Sanders, E. A. M. & Bogaert, D. Respiratory microbiota dynamics following Streptococcus pneumoniae acquisition in young and elderly mice. *Infect. Immun.* **82,** 1725–1731 (2014).

190. Radin, J. N. *et al.* β-arrestin 1 participates in platelet-activating factor receptor-mediated endocytosis of Streptococcus pneumoniae. *Infect. Immun.* **73,** 7827–7835 (2005).

191. Horai, R. *et al.* Production of mice deficient in genes for interleukin (IL)-1alpha, IL-1beta, IL-1alpha/beta, and IL-1 receptor antagonist shows that IL-1beta is crucial in turpentine-induced fever development and glucocorticoid secretion. *J Exp Med* **187,** 1463–1475 (1998).

192. Nakamura, S., Davis, K. M. & Weiser, J. N. Synergistic stimulation of type I interferons during influenza virus coinfection promotes Streptococcus pneumoniae colonization in mice. *J Clin Invest* **121,** 3657–3665

193. Kim, J. O. & Weiser, J. N. Association of intrastrain phase variation in quantity of capsular polysaccharide and teichoic acid with the virulence of Streptococcus pneumoniae. *J Infect Dis* **177,** 368–377 (1998).

194. Dorrington, M. G. *et al.* MARCO Is Required for TLR2- and Nod2-Mediated Responses to Streptococcus pneumoniae and Clearance of Pneumococcal Colonization in the Murine

Nasopharynx. *J Immunol* **190,** 250–258

195. Roche, A. M. & Weiser, J. N. Identification of the targets of cross-reactive antibodies induced by Streptococcus pneumoniae colonization. *Infect. Immun.* **78,** 2231–2239 (2010).

196. Drannik, A. G. *et al.* Impact of cigarette smoke on clearance and inflammation after Pseudomonas aeruginosa infection. *Am. J. Respir. Crit. Care Med.* **170,** 1164–71 (2004).

197. Jobse, B. N. *et al.* Detection of lung dysfunction using ventilation and perfusion SPECT in a mouse model of chronic cigarette smoke exposure. *J. Nucl. Med.* **54,** 616–23 (2013).

198. Bartram, A. K., Lynch, M. D. J., Stearns, J. C., Moreno-Hagelsieb, G. & Neufeld, J. D. Generation of multimillion-sequence 16S rRNA gene libraries from complex microbial communities by assembling paired-end Illumina reads. *Appl. Environ. Microbiol.* **77,** 3846–3852 (2011).

199. Whelan, F. J. *et al.* The loss of topography in the microbial communities of the upper respiratory tract in the elderly. *Ann. Am. Thorac. Soc.* **11,** 513–521 (2014).

200. Gohir, W., Whelan, F. J., Surette, M. G., Moore, C. & Jonathan, D. Pregnancy-related changes in the maternal gut microbiota are dependent upon the mother's periconceptional diet. *Gut Microbes* **6,** 310–320 (2015).

201. Martin, M. Cutadapt removes adapter sequences from high-throughput sequencing reads. *EMBnet.journal* **17,** 10 (2011).

202. Masella, A. P., Bartram, A. K., Truszkowski, J. M., Brown, D. G. & Neufeld, J. D. PANDAseq: paired-end assembler for illumina sequences. *BMC Bioinformatics* **13,** 1–7 (2012).

203. Ye, Y. Identification and quantification of abundant species from pyrosequences of 16S rRNA by consensus alignment. in *Proc. - 2010 IEEE Int. Conf. Bioinforma. Biomed. BIBM 2010* 153–157 (2010). doi:10.1109/BIBM.2010.5706555

204. Wang, Q., Garrity, G. M., Tiedje, J. M. & Cole, J. R. Na??ve Bayesian classifier for rapid assignment of rRNA sequences into the new bacterial taxonomy. *Appl. Environ. Microbiol.* **73,** 5261–5267 (2007).

205. DeSantis, T. Z. *et al.* Greengenes, a chimera-checked 16S rRNA gene database and workbench compatible with ARB. *Appl. Environ. Microbiol.* **72,** 5069–5072 (2006).

206. Caporaso, J. G. *et al.* QIIME allows analysis of high-throughput community sequencing data. *Nat. Methods* **7,** 335–6 (2010).

207. McMurdie, P. J. & Holmes, S. Phyloseq: An R Package for Reproducible Interactive Analysis and Graphics of Microbiome Census Data. *PLoS One* **8,** (2013).

208. Oksanen, A. J. *et al.* Community Ecology Package. 263 (2012). doi:10.4135/9781412971874.n145

209. Love, M. I., Huber, W. & Anders, S. Moderated estimation of fold change and dispersion for RNA-seq data with DESeq2. *Genome Biol.* **15,** 1–34 (2014).

210. Thevaranjan, N. *et al. Streptococcus pneumoniae* colonization disrupts the microbial community within the upper respiratory tract of aging mice. *Infect. Immun.* IAI.01275–15 (2016). doi:10.1128/IAI.01275-15

211. Calverley, P. *et al.* A Phase 2 Study Of MEDI8968, An Anti-Interleukin-1 Receptor I (IL-1RI) Monoclonal Antibody, In Adults With Moderate-to-Very Severe Chronic Obstructive Pulmonary

Disease (COPD). American Thoracic Conference Scientific Abstract. (2015). doi:http://www.atsjournals.org/doi/abs/10.1164/ajrccm-conference.2015.191.1_MeetingAbstracts.A3964

212. Thatcher, T. H. *et al.* Role of CXCR2 in cigarette smoke-induced lung inflammation. *Am J Physiol Lung Cell Mol Physiol* **289,** L322–8 (2005).

213. Shukla, S. D. *et al.* Airway epithelial platelet-activating factor receptor expression is markedly upregulated in chronic obstructive pulmonary disease. *Int. J. Chron. Obstruct. Pulmon. Dis.* **9,** 853–61 (2014).

214. Margolis, E., Yates, A. & Levin, B. R. The ecology of nasal colonization of Streptococcus pneumoniae, Haemophilus influenzae and Staphylococcus aureus: the role of competition and interactions with host's immune response. *BMC Microbiol.* **10,** 59 (2010).

215. Bae, S. *et al.* Nasal colonization by four potential respiratory bacteria in healthy children attending kindergarten or elementary school in Seoul, Korea. *J. Med. Microbiol.* **61,** 678–685 (2012).

216. Domino, E. F., Kadoya, C., Matsuoka, S., Ni, L. & Fedewa, K. S. Comparative American and Japanese tobacco smoke uptake parameters after overnight tobacco deprivation. *Prog. Neuro-Psychopharmacology Biol. Psychiatry* **27,** 973–984 (2003).

217. McCool, T. L. & Weiser, J. N. Limited role of antibody in clearance of Streptococcus pneumoniae in a murine model of colonization. *Infect Immun* **72,** 5807–5813 (2004).

218. Southam, D. S., Dolovich, M., O'Byrne, P. M. & Inman, M. D. Distribution of intranasal instillations in mice: effects of volume, time, body position, and anesthesia. *Am. J. Physiol. Lung Cell. Mol. Physiol.* **282,** L833–L839 (2002).

219. Miller, M. A. *et al.* Visualization of murine intranasal dosing efficiency using luminescent Francisella tularensis: effect of instillation volume and form of anesthesia. *PLoS One* **7,** e31359 (2012).

220. Wu, H. Y. *et al.* Establishment of a Streptococcus pneumoniae nasopharyngeal colonization model in adult mice. *Microb. Pathog.* **23,** 127–137 (1997).

221. Lemon, K. P. *et al.* Comparative analyses of the Bacterial microbiota of the human nostril and oropharynx. *MBio* **1,** (2010).

222. Eltom, S. *et al.* Role of the inflammasome-caspase1/11-IL-1/18 axis in cigarette smoke driven airway inflammation: an insight into the pathogenesis of COPD. *PLoS One* **9,** e112829 (2014).

223. Rogliani, P., Calzetta, L., Ora, J. & Matera, M. G. Canakinumab for the treatment of chronic obstructive pulmonary disease. *Pulm. Pharmacol. Ther.* **31,** 15–27 (2015).

224. Barnes, P. J. New anti-inflammatory targets for chronic obstructive pulmonary disease. *Nat Rev Drug Discov* **12,** 543–559 (2013).

225. Rider, P. *et al.* IL-1α and IL-1β recruit different myeloid cells and promote different stages of sterile inflammation. *J. Immunol.* **187,** 4835–4843 (2011).

226. Bersudsky, M. *et al.* Non-redundant properties of IL-1α and IL-1β during acute colon inflammation in mice. *Gut* **63,** 598–609 (2014).

227. Dinarello, C. A. The IL-1 family and inflammatory diseases. *Clin. Exp. Rheumatol.* **20,** (2002).

228. Schroder, K. & Tschopp, J. The inflammasomes. *Cell* **140,** 821–832(2010).

229. Apte, R. N. & Voronov, E. Is interleukin-1 a good or bad 'guy' in tumor immunobiology and immunotherapy? *Immunol. Rev.* **222,** 222–241 (2008).

230. Brody, D. T. & Durum, S. K. Membrane IL-1: IL-1 alpha precursor binds to the plasma membrane via a lectin-like interaction. *J. Immunol.* **143,** 1183–7 (1989).

231. Dvorkin, T. *et al.* Immune phenomena involved in the in vivo regression of fibrosarcoma cells expressing cell-associated IL-1alpha. *J. Leukoc. Biol.* **80,** 96–106 (2006).

232. Kavita, U. & Mizel, S. B. Differential sensitivity of interleukin-1 alpha and -beta precursor proteins to cleavage by calpain, a calcium-dependent protease. *J Biol Chem* **270,** 27758–27765 (1995).

233. Brough, D. *et al.* Ca2+ stores and Ca2+ entry differentially contribute to the release of IL-1 beta and IL-1 alpha from murine macrophages. *J. Immunol.* **170,** 3029–3036 (2003).

234. Schmouder, R. L., Streiter, R. M., Walz, A. & Kunkel, S. L. Epithelial-derived neutrophil-activating factor-78 production in human renal tubule epithelial cells and in renal allograft rejection. *Transplantation* **59,** 118–124 (1995).

235. Corbett, M. S., Schmitt, I., Riess, O. & Walz, A. Characterization of the gene for human neutrophil-activating peptide 78 (ENA-78). *Biochem. Biophys. Res. Commun.* **205,** 612 (1994).

236. Westphalen, K. *et al.* Sessile alveolar macrophages communicate with alveolar epithelium to modulate immunity. *Nature* **506,** 503–506 (2014).

237. Groß, O. *et al.* Inflammasome Activators Induce Interleukin-1α Secretion via Distinct Pathways with Differential Requirement for the Protease Function of Caspase-1. *Immunity* **36,** 388–400 (2012).

238. Barnes, P. J. Alveolar macrophages as orchestrators of COPD. *COPD* **1,** 59–70 (2004).

239. Beckett, E. L. *et al.* A new short-term mouse model of chronic obstructive pulmonary disease identifies a role for mast cell tryptase in pathogenesis. *J. Allergy Clin. Immunol.* **131,** (2013).

240. Kono, H., Karmarkar, D., Iwakura, Y. & Rock, K. L. Identification of the cellular sensor that stimulates the inflammatory response to sterile cell death. *J. Immunol.* **184,** 4470–8 (2010).

241. Kosmider, B., Messier, E. M., Chu, H. W. & Mason, R. J. Human alveolar epithelial cell injury induced by cigarette smoke. *PLoS One* **6,** (2011).

242. van der Toorn, M. *et al.* Cigarette smoke-induced blockade of the mitochondrial respiratory chain switches lung epithelial cell apoptosis into necrosis. *Am. J. Physiol. Lung Cell. Mol. Physiol.* **292,** L1211–8 (2007).

243. Mizumura, K. *et al.* Mitophagy-dependent necroptosis contributes to the pathogenesis of COPD. *J. Clin. Invest.* **124,** 3987–4003 (2014).

244. Kaczmarek, A., Vandenabeele, P. & Krysko, D. V. Necroptosis: The Release of Damage-Associated Molecular Patterns and Its Physiological Relevance. *Immunity* **38,** 209–223 (2013).

245. Pouwels, S. D. *et al.* DAMPs activating innate and adaptive immune responses in COPD. *Mucosal Immunol.* **7,** 215–26 (2014).

246. Pouwels, S. D. *et al.* Cigarette smoke-induced necroptosis and DAMP release trigger neutrophilic airway inflammation in mice. *Am. J. Physiol. Lung Cell. Mol. Physiol.* ajplung.00174.2015 (2015). doi:10.1152/ajplung.00174.2015

247. Zitvogel, L., Kepp, O. & Kroemer, G. Decoding Cell Death Signals in Inflammation and Immunity. *Cell* **140,** 798–804 (2010).

248. Kono, H. & Rock, K. L. How dying cells alert the immune system to danger. *Nat. Rev. Immunol.* **8,** 279–89 (2008).

249. Krysko, O., Vandenabeele, P., Krysko, D. V & Bachert, C. Impairment of phagocytosis of apoptotic cells and its role in chronic airway diseases. *Apoptosis* **15,** 1137–46 (2010).

250. Hirsiger, S., Simmen, H. P., Werner, C. M. L., Wanner, G. A. & Rittirsch, D. Danger signals activating the immune response after trauma. *Mediators Inflamm.* **2012,** (2012).

251. Dinarello, C. A. *et al.* Interleukin 1 induces interleukin 1. I. Induction of circulating interleukin 1 in rabbits in vivo and in human mononuclear cells in vitro. *J. Immunol.* **139,** 1902–1910 (1987).

252. Pouwels, S. D., Heijink, I. H., van Oosterhout, A. J. & Nawijn, M. C. A specific profile of DAMPs identifies susceptibility towards smoke induced neutrophilic airway inflammation in mice. *Eur. Respir. J.* **43,** 1183–1186 (2014).

253. Hacker, S. *et al.* Elevated HSP27, HSP70 and HSP90?? in chronic obstructive pulmonary disease: Markers for immune activation and tissue destruction. *Clin. Lab.* **55,** 31–40 (2009).

254. Merkel, D., Rist, W., Seither, P., Weith, A. & Lenter, M. C. Proteomic study of human bronchoalveolar lavage fluids from smokers with chronic obstructive pulmonary disease by combining surface-enhanced laser desorption/ionization-mass spectrometry profiling with mass spectrometric protein identification. *Proteomics* **5,** 2972–2980 (2005).

255. Ferhani, N. *et al.* Expression of high-mobility group box 1 and of receptor for advanced glycation end products in chronic obstructive pulmonary disease. *Am J Respir Crit Care Med* **181,** 917–927 (2010).

256. Morissette, M. C., Shen, P., Thayaparan, D. & Stämpfli, M. R. Disruption of pulmonary lipid homeostasis drives cigarette smoke-induced lung inflammation in mice. *Eur. Respir. J.* **46,** 1451–1460 (2015).

257. Weathington, N. M. *et al.* A novel peptide CXCR ligand derived from extracellular matrix degradation during airway inflammation. *Nat. Med.* **12,** 317–323 (2006).

258. Morissette, M. C. *et al.* Persistence of pulmonary tertiary lymphoid tissues and anti-nuclear antibodies following cessation of cigarette smoke exposure. *Respir. Res.* **15,** 49 (2014).

259. Chen, H., Cowan, M. J., Hasday, J. D., Vogel, S. N. & Medvedev, A. E. Tobacco smoking inhibits expression of proinflammatory cytokines and activation of IL-1R-associated kinase, p38, and NF-kappaB in alveolar macrophages stimulated with TLR2 and TLR4 agonists. *J Immunol* **179,** 6097–6106 (2007).

260. Morissette, M. C., Shen, P., Thayaparan, D. & Stampfli, M. R. Impacts of peroxisome proliferatoractivated receptor-?? activation on cigarette smoke-induced exacerbated response to bacteria. *Eur. Respir. J.* **45,** 191–200 (2015).

261. Gaschler, G. J., Zavitz, C. C. J., Bauer, C. M. T. & Stampfli, M. R. Mechanisms of clearance of

nontypeable Haemophilus influenzae from cigarette smoke-exposed mouse lungs. *Eur. Respir. J.* **36,** 1131–1142 (2010).

262. Hurst, J. R. Precision Medicine in Chronic Obstructive Pulmonary Disease. *Am. J. Respir. Crit. Care Med.* **193,** 593–4 (2016).

263. Sarkar, A. *et al.* Caspase-1 regulates Escherichia coli sepsis and splenic B cell apoptosis independently of interleukin-1beta and interleukin-18. *Am. J. Respir. Crit. Care Med.* **174,** 1003–10 (2006).

264. Felmet, K. a., Hall, M. W., Clark, R. S. B., Jaffe, R. & Carcillo, J. a. Prolonged Lymphopenia, Lymphoid Depletion, and Hypoprolactinemia in Children with Nosocomial Sepsis and Multiple Organ Failure. *J. Immunol.* **174,** 3765–3772 (2005).

265. Inoue, S. *et al.* Reduction of immunocompetent T cells followed by prolonged lymphopenia in severe sepsis in the elderly. *Crit. Care Med.* **41,** 810–9 (2013).

266. Bozza, F. a *et al.* Cytokine profiles as markers of disease severity in sepsis: a multiplex analysis. *Crit. Care* **11,** R49 (2007).

267. Gentile, L. F. *et al.* Is there value in plasma cytokine measurements in patients with severe trauma and sepsis? *Methods* **61,** 3–9 (2013).

268. Thayer WS. Bacterial or infective endocarditis; Gibson lectures for 1930. *Edinb. Med. J.* **38,** 237–65, 307–34 (1931).

269. Brown, A. O. *et al.* Streptococcus pneumoniae Translocates into the Myocardium and Forms Unique Microlesions That Disrupt Cardiac Function. (2014). doi:10.1371/journal.ppat.1004383

270. Corrales-Medina, V. F. *et al.* Cardiac complications in patients with community-acquired pneumonia: A systematic review and meta-analysis of observational studies. *PLoS Med.* **8,** (2011).

271. Brown, A. O., Millett, E. R. C., Quint, J. K. & Orihuela, C. J. Cardiotoxicity During Invasive Pneumococcal Disease. *Am. J. Respir. Crit. Care Med.* 150128140317009 (2015). doi:10.1164/rccm.201411-1951PP

272. Voss, M. *et al.* Cigarette smoke-promoted acquisition of bacterial pathogens in the upper respiratory tract leads to enhanced inflammation in mice. *Respir. Res.* **16,** (2015).

273. van Rossum, A. M. C., Lysenko, E. S. & Weiser, J. N. Host and Bacterial Factors Contributing to the Clearance of Colonization by Streptococcus pneumoniae in a Murine Model Host and Bacterial Factors Contributing to the Clearance of Colonization by Streptococcus pneumoniae in a Murine Model. *Infect. Immun.* **73,** 7718–7726 (2005).

274. Sherman, C. B. The health consequences of cigarette smoking. Pulmonary diseases. *Med Clin North Am* **76,** 355–375 (1992).

275. Greiff, L., Wollmer, P., Erjefält, I., Pipkorn, U. & Persson, C. G. Clearance of 99mTc DTPA from guinea pig nasal, tracheobronchial, and bronchoalveolar airways. *Thorax* **45,** 841–845 (1990).

276. Effros, R. M., Mason, G. R. & Mena, I. 99mTc-DTPA aerosol deposition and clearance in COPD, interstitial disease, and smokers. *J. Thorac. Imaging* **1,** 54–60 (1986).

277. Rayner, C. F. J. *et al.* Interaction of pneumolysin-sufficient and -deficient isogenic variants of Streptococcus pneumoniae with human respiratory mucosa. *Infect. Immun.* **63,** 442–447 (1995).

278. Clarke, T. B., Francella, N., Huegel, A. & Weiser, J. N. Invasive bacterial pathogens exploit TLR-mediated downregulation of tight junction components to facilitate translocation across the epithelium. *Cell Host Microbe* **9,** 404–414 (2011).

279. Beisswenger, C., Lysenko, E. S. & Weiser, J. N. Early bacterial colonization induces toll-like receptor-dependent transforming growth factor ?? signaling in the epithelium. *Infect. Immun.* **77,** 2212–2220 (2009).

280. Knapp, S. *et al.* Toll-like receptor 2 plays a role in the early inflammatory response to murine pneumococcal pneumonia but does not contribute to antibacterial defense. *J Immunol* **172,** 3132–3138 (2004).

281. Ring, A., Weiser, J. N. & Tuomanen, E. I. Pneumococcal trafficking across the blood-brain barrier molecular analysis of a novel bidirectional pathway. *J. Clin. Invest.* **102,** 347–360 (1998).

282. Bello, S. *et al.* Tobacco Smoking Increases the Risk for Death From Pneumococcal Pneumonia. *CHEST.* **146,** 1029 (2014).

283. Joffe, M. D. & Alpern, E. R. Occult pneumococcal bacteremia: a review. *Pediatr. Emerg. Care* **26,** 448–454; quiz 455–457 (2010).

284. van Ginkel, F. W. *et al.* Pneumococcal carriage results in ganglioside-mediated olfactory tissue infection. *Proc Natl Acad Sci U S A* **100,** 14363–14367 (2003).

285. Bentley, S. D. *et al.* Genetic analysis of the capsular biosynthetic locus from all 90 pneumococcal serotypes. *PLoS Genet* **2,** e31 (2006).

286. Sandgren, A. *et al.* Effect of clonal and serotype-specific properties on the invasive capacity of Streptococcus pneumoniae. *J. Infect. Dis.* **189,** 785–796 (2004).

287. Orihuela, C. J. *et al.* Organ-specific models of Streptococcus pneumoniae disease. *Scand. J. Infect. Dis.* **35,** 647–652 (2003).

288. van Hoek, A. J., Andrews, N., Waight, P. A., George, R. & Miller, E. Effect of serotype on focus and mortality of invasive pneumococcal disease: Coverage of different vaccines and insight into non-vaccine serotypes. *PLoS One* **7,** e39150 (2012).

289. Basilico, P., Cremona, T., Oevermann, A., Piersigilli, A. & Benarafa, C. Increased myeloid cell production and lung bacterial clearance in mice exposed to cigarette smoke. *Am J Respir Cell Mol Biol* **54,** 424–35 (2016).

290. Noah, T. L. *et al.* Tobacco smoke exposure and altered nasal responses to live attenuated influenza virus. *Environ. Health Perspect.* **119,** 78–83 (2011).

291. Huvenne, W. *et al.* Different regulation of cigarette smoke induced inflammation in upper versus lower airways. *Respir. Res.* **11,** 100 (2010).

292. Sopori, M. Effects of cigarette smoke on the immune system. *Nat Rev Immunol* **2,** 372–377 (2002).

293. Kawai, T. & Akira, S. The role of pattern-recognition receptors in innate immunity: update on Toll-like receptors. *Nat Immunol* **11,** 373–384

294. Droemann, D. *et al.* Toll-like receptor 2 expression is decreased on alveolar macrophages in cigarette smokers and COPD patients. *Respir Res* **6,** 68 (2005).

295. MacRedmond, R. E., Greene, C. M., Dorscheid, D. R., McElvaney, N. G. & O'Neill, S. J. Epithelial expression of TLR4 is modulated in COPD and by steroids, salmeterol and cigarette smoke. *Respir. Res.* **8,** 84 (2007).

296. Medvedev, A. E., Sabroe, I., Hasday, J. D. & Vogel, S. N. Tolerance to microbial TLR ligands: molecular mechanisms and relevance to disease. *J Endotoxin Res* **12,** 133–150 (2006).

297. Bozinovski, S. *et al.* Carbonylation caused by cigarette smoke extract is associated with defective macrophage immunity. *Am J Respir Cell Mol Biol* **45,** 229–236

298. Signat, B., Roques, C., Poulet, P. & Duffaut, D. Fusobacterium nucleatum in periodontal health and disease. *Curr. Issues Mol. Biol.* **13,** 25–36 (2011).

299. Cecil, J. D. *et al.* Differential Responses of Pattern Recognition Receptors to Outer Membrane Vesicles of Three Periodontal Pathogens. *PLoS One* **11,** e0151967 (2016).

300. Wu, J. *et al.* Cigarette smoking and the oral microbiome in a large study of American adults. *Isme J* 1–12 (2016). doi:10.1038/ismej.2016.37

301. Takayanagi, N., Kagiyama, N., Ishiguro, T., Tokunaga, D. & Sugita, Y. Etiology and outcome of community-acquired lung abscess. *Respiration* **80,** 98–105 (2010).

302. Stephens, D. S., Greenwood, B. & Brandtzaeg, P. Epidemic meningitis, meningococcaemia, and Neisseria meningitidis. *Lancet* **369,** 2196–2210 (2007).

303. El Houmami, N. *et al.* Patterns of Kingella kingae Disease Outbreaks. *Pediatr. Infect. Dis. J.* **35,** 340–346 (2016).

304. Mutepe, N. D. *et al.* Effects of cigarette smoke condensate on pneumococcal biofilm formation and pneumolysin. *Eur Respir J* **41,** 392–395

305. Burmolle, M. *et al.* Enhanced biofilm formation and increased resistance to antimicrobial agents and bacterial invasion are caused by synergistic interactions in multispecies biofilms. *Appl. Environ. Microbiol.* **72,** 3916–3923 (2006).

306. Costerton, J. W., Stewart, P. S. & Greenberg, E. P. Bacterial biofilms: a common cause of persistent infections. *Science* **284,** 1318–1322 (1999).

307. Moscoso, M., Garcia, E. & Lopez, R. Pneumococcal biofilms. *Int Microbiol* **12,** 77–85 (2009).

308. Lysenko, E. S., Ratner, A. J., Nelson, A. L. & Weiser, J. N. The role of innate immune responses in the outcome of interspecies competition for colonization of mucosal surfaces. *PLoS Pathog.* **1,** 0003–0011 (2005).

309. Uehara, Y. *et al.* H2O2 Produced by Viridans Group Streptococci May Contribute to Inhibition of Methicillin-Resistant Staphylococcus aureus Colonization of Oral Cavities in Newborns. *Clin. Infect. Dis.* **32,** 1408–1413 (2001).

310. Kulkarni, R. *et al.* Cigarette smoke increases Staphylococcus aureus biofilm formation via oxidative stress. *Infect Immun* **80,** 3804–3811

311. Briles, D. E., Novak, L., Hotomi, M., Van Ginkel, F. W. & King, J. Nasal colonization with Streptococcus pneumoniae includes subpopulations of surface and invasive pneumococci. *Infect. Immun.* **73,** 6945–6951 (2005).

312. Bagaitkar, J. *et al.* Tobacco-induced alterations to Porphyromonas gingivalis-host interactions.

Env. Microbiol **11,** 1242–1253 (2009).

313. Antunes, M. B. *et al.* Molecular basis of tobacco-induced bacterial biofilms: an in vitro study. *Otolaryngol Head Neck Surg* **147,** 876–884

314. Cockeran, R. *et al.* Exposure of a 23F Serotype Strain of Streptococcus pneumoniae to Cigarette Smoke Condensate Is Associated with Selective Upregulation of Genes Encoding the Two-Component Regulatory System 11 (TCS11). *Biomed Res Int* Article ID 976347 (2014).

315. Roos, K., Holm, S., Grahn, E. & Lagergren, L. Recolonization with selected alpha-streptococci for prophylaxis of recurrent streptococcal pharyngotonsillitis: a randomized placebo-controlled multicentre study. *Scand J Infect Dis* **28,** 459–462 (1996).

316. Roos, K., Håkansson, E. G. & Holm, S. Effect of recolonisation with 'interfering' alpha streptococci on recurrences of acute and secretory otitis media in children: randomised placebo controlled trial. *BMJ* **322,** 210–212 (2001).

CHAPTER 6. FIGURE LEGENDS, FIGURES, AND TABLES

Figure 1: Cigarette smoke-induced neutrophilia is dependent on IL-1α produced by the hematopoietic cell compartment. C57BL/6, IL-1α KO and IL-1β KO mice were cigarette smoke-exposed for 4 days and sacrificed 18 h following the final cigarette smoke exposure. IL-1α and IL-1β protein levels were determined in lung homogenates. CXCL-1 and CXCL-2 protein levels were assessed in the BAL fluid. Neutrophils (NEU) were counted in the BAL fluid. Room air (open bars), smoke (solid bars). (A) IL-1α expression in C57BL/6 mice following cigarette smoke exposure. Neutrophil cell number, and chemokine levels in the BAL fluid of IL-1α KO mice. (B) IL-1β expression in C57BL/6 mice following cigarette smoke exposure. Neutrophil cell number, and chemokine levels in the BAL fluid of IL-1β KO mice. (C) IL-1α chimeric mice were generated as shown and cigarette smoke-exposed for 4 days to assess neutrophil levels in the BAL fluid. Data are shown as mean ± SEM. n=4-10 mice per group. Statistical analysis was performed using General Linear Model, followed by individual t-test.*$p<0.05$. NS, not significant.

Figure 2: Cigarette smoke exposure primes alveolar macrophages to produce IL-1α in response to bacteria. (A) Mononuclear cells (MNC) were quantified in the BAL fluid of 4 day and 8 week cigarette smoke-exposed C57BL/6 mice. Room air (open bars), smoke (solid bars) (B) Alveolar macrophages on cytospins generated from 8 week cigarette smoke-exposed mice and stained with H&E. (C, E, and F) Alveolar macrophages were isolated by adherence from 8 week cigarette smoke-exposed C57BL/6 mice, cultured in media (RPMI 1640), and stimulated with Pam_3CSK_4, LPS, or NTHi for 24 h. TNF-α, IL-1α, and IL-1β levels in culture supernatants were determined by ELISA. (D) IL-1α mRNA expression was determined by RT-qPCR in alveolar macrophages isolated from 8 week cigarette smoke-exposed C57BL/6 mice after 4 h stimulation with LPS. Gene expression was normalized to that of the room air un-stimulated control group. Room air (open bars), smoke (solid bars). Data are shown as mean ± SEM. n=5 mice per group. Statistical analysis was performed using General Linear Model, followed by individual t-test.*$p<0.05$.

Figure 3: Cigarette smoke exposure exacerbates NTHi-elicited neutrophilia and CXCL-5 expression. BALB/c or CXCR2 KO mice were cigarette smoke-exposed for 8 weeks and challenged intranasally with 10^6 CFU NTHi. Mice were sacrificed 12 h post-infection. (A) Total cell number (TCN), mononuclear cells (MNC), and neutrophils (NEU) in the BAL fluid of BALB/c mice. Room air (open bars), smoke (solid bars). (B) Neutrophil levels in the BAL fluid of smoke-exposed CXCR2 KO mice on a BALB/c background (gray shaded background). (C) CXCL-1 and CXCL-5 levels in the BAL fluid of BALB/c mice were assessed by ELISA. (D) Immunohistochemistry was carried out to assess CXCL-5 expression in lung tissue. Scale bar, 50μm. (E) Precision cut lung slices were generated from 8 week cigarette smoke-exposed C57BL/6 mice and stimulated with NTHi for 6 h. CXCL-5 mRNA expression was assessed by RT-qPCR. Gene expression was normalized to that of the room air un-stimulated control group. Data are shown as mean ± SEM. n=5-10 mice per group (n=3 for lung slice experiments). Statistical analysis was performed using General Linear Model, followed by individual t-test.*$p<0.05$.

Figure 4: Exacerbated neutrophilia induced by NTHi in cigarette smoke-exposed mice is dependent on IL-1R1. C57BL/6 and IL-1R1 KO mice were cigarette smoke-exposed for 8 weeks and challenged intranasally with 10^6 CFU NTHi. Mice were sacrificed 12 h post-infection for the assessment of (A) cellular inflammation in the BAL fluid. Total cell number (TCN),

mononuclear cells (MNC), neutrophils (NEU). (B) BAL fluid CXCL-1 and CXCL-5 protein levels by ELISA. Room air (open bars), smoke (solid bars). Data are shown as mean ± SEM. n=5-10 mice per group. Statistical analysis was performed using General Linear Model, followed by individual t-test.*p<0.05.

Figure 5: Exacerbated neutrophilia induced by NTHi in cigarette smoke-exposed mice is dependent on IL-1α, but not IL-1-β. C57BL/6, IL-1α KO, and IL-1β KO mice were cigarette smoke-exposed for 8 weeks and challenged intranasally with 10^6 CFU NTHi. Mice were sacrificed 12 h post-infection. (A) IL-1α and IL-1β levels in lung homogenates of C57BL/6 mice were assessed by ELISA. Room air (open bars), smoke (solid bars). (B) Immunohistochemistry was carried out to assess IL-1α expression in lung tissue from C57BL/6 mice. Scale bar, 25μm. (C) Cellular inflammation in the BAL fluid of IL-1α KO mice. (D) Cellular inflammation in the BAL fluid of IL-1β KO mice. Total cell number (TCN), mononuclear cells (MNC), neutrophils (NEU). Room air (open bars), smoke (solid bars). Data are shown as mean ± SEM. n=5-10 mice per group. Statistical analysis was performed using General Linear Model, followed by individual t-test.*p<0.05.

Figure 6: Targeting exacerbated neutrophilia may compromise bacterial clearance in cigarette smoke-exposed mice. IL-1R1 KO, CXCR2 KO, and IL-1α KO mice were cigarette smoke-exposed for 8 weeks and challenged intranasally with 10^6 CFU NTHi. Mice were sacrificed 12 h post-infection and lung bacterial burden was determined by plating lung homogenates onto chocolate agar plates. Room air (open bars), smoke (solid bars). Data are shown as mean ± SEM. n=5-10 mice per group. Statistical analysis was performed using General Linear Model, followed by individual t-test.*p<0.05.

Figure 7: Repeated NTHi infection increases lung compliance in cigarette smoke-exposed mice. (A) C57BL/6 mice were cigarette smoke-exposed for 10 weeks and administered 10^6 CFU NTHi intranasally every 2 weeks for a total of 4 administrations. (B) Pressure volume curves. (C) Compliance data. (D) Airspace size was quantified by pneumometric software in H&E-stained lung sections. Data are shown as mean ± SEM. n=5-10 mice per group. Statistical analysis was performed using General Linear Model, followed by individual t-test.*p<0.05.

Figure 8: Cigarette smoke induces IL-1α-dependent inflammatory responses. Cigarette smoke induces alveolar macrophages to produce IL-1α, which recruits neutrophils to the lungs associated with increased CXCR2 chemokines. Cigarette smoke exposure alters alveolar macrophage phenotype and primes them for an exacerbated IL-1α response to bacterial infection, leading to increased neutrophilia associated with higher CXCL-5 expression.

Figure 9: Cigarette smoke exposure compromises the nasal host response following nasal *S. pneumoniae* colonization. Room air control or 1 week cigarette smoke-exposed mice were nasally colonized with approximately 10^6 CFU *S. pneumoniae*. Mice continued to be cigarette smoke-exposed and were euthanized on day 2 post-colonization. (A) Nasal wash bacterial burden. n=4-5 mice per group. Data are representative of 3 independent experiments. (B) mRNA was isolated from lysis Buffer RLT nasal washes. Gene expression was determined by RT-qPCR and normalized to that of the room air vehicle control group. n=3-5 mice per group. *Tnfa*, *Cxcl1*, *Cxcl2* data: representative of 3 independent experiments, *Ccl2* data: representative of 2 independent experiments (C) Neutrophil and macrophage proportions in the nasal wash were determined using flow cytometry. Room air (open bars), smoke (solid bars), *S.p.* (*S.*

pneumoniae). Data are shown as mean ± SEM. n=4-5 mice per group.*p<0.05 when compared to corresponding control as assessed by independent t-test.

Figure 10: Cigarette smoke exposure predisposes mice to IPD and mortality following nasal pneumococcal colonization. Room air control or 1 week cigarette smoke-exposed mice were nasally colonized with approximately 10^6 CFU *S. pneumoniae*. Mice continued to be cigarette smoke-exposed for 16 days post-nasal colonization and were euthanized as they reached endpoint. (A) Survival curve showing room air control mice (solid line), and smoke-exposed mice (dotted line). Individual weights of surviving and endpoint mice are shown as percentages of initial weights on day of bacterial colonization (day 0). Control (open circles), smoke (closed circles). (B) Bacterial burden in various tissues of mice at endpoint. (C) Bacterial burden in various tissues of mice surviving to day 16. Control (open circles), smoke (closed circles). n=10 per group of control or cigarette smoke-exposed mice. Survival curves were compared by log-rank test; p<0.05 was considered significant. *p<0.05 when compared to corresponding control as assessed by independent t-test.

Figure 11: Cigarette smoke exposure predisposes to mortality in mice following nasal pneumococcal colonization over a range of initial bacterial inoculation doses. Room air control or 1 week cigarette smoke-exposed mice were nasally colonized with the indicated dose of *S. pneumoniae*. Mice continued to be cigarette smoke-exposed for 25 days post-nasal colonization and were euthanized as they reached endpoint. Survival curves are shown. Control (solid line), smoke (dotted line), n=5 mice per group. Survival curves were compared by log-rank test, p<0.05 was considered significant.

Figure 12: Endpoint mice show features of sepsis and meningitis. Room air control or 1 week cigarette smoke-exposed mice were nasally colonized with approximately 10^6 CFU *S. pneumoniae*. Mice continued to be cigarette smoke-exposed post-nasal colonization and were euthanized as they reached endpoint. (A) Blood leukocyte cell counts were determined in mice surviving to day 16, in endpoint mice, and in vehicle control mice. (B) IL-6 was measured by ELISA in the serum of surviving and endpoint mice. Room air (open circles), smoke (closed circles). (C-H) Mice reaching endpoint were perfused with 10% formalin. Tissues were fixed in formalin, sectioned, and stained with H&E. Representative images are shown: (C) inflammatory cell infiltrate at the meninges (arrow), (F) higher magnification of (C), (D) endomyocarditis (arrow), (G) higher magnification of (D), (E) cardiac microlesion (arrow), (H) Gram-positive stain of cardiac microlesion (arrow). n=5-10 per group of control or smoke-exposed mice.

Figure 13: Cigarette smoke-exposed mice at endpoint have no increased lung inflammation. Room air control or 1 week cigarette smoke-exposed mice were nasally colonized with approximately 10^6 CFU *S. pneumoniae*. Mice continued to be cigarette smoke-exposed for 16 days post-nasal colonization and were euthanized as they reached endpoint. The single lung lobe of (A) cigarette smoke-exposed mouse at endpoint and (B) cigarette smoke-exposed mouse surviving to day 16, were fixed with formalin, sectioned, and stained with H&E. Representative images are shown. (C) Differential cell counts of the BAL fluid from surviving and endpoint mice are shown with that of vehicle control. n=5-10 per group of room air or cigarette smoke-exposed mice.

Figure 14: Invasive infection occurs rapidly into the blood and brain of cigarette smoke-exposed mice. Room air control or 1 week cigarette smoke-exposed mice were nasally colonized with approximately 10^6 CFU *S. pneumoniae*. Mice continued to be cigarette smoke-exposed and bacterial burden was assessed daily for 4 days in the indicated tissue samples. (A) Percentage of cigarette smoke-exposed mice with detectable *S. pneumoniae* in each tissue

sample over 4 days. Health status of mice was also assessed prior to euthanization each day. (B) Breakdown of bacterial dissemination patterns in cigarette smoke-exposed mice by day. (C) Breakdown of bacterial dissemination patterns in room air-exposed mice by day. n=8 mice per time point.

Figure 15: Cigarette smoke-exposed mice show no changes in BAL inflammation or nasal bacterial burden over the course of 4 days despite widespread bacterial dissemination. 1 week cigarette smoke-exposed mice were nasally colonized with approximately 10^6 CFU *S. pneumoniae*. Mice continued to be cigarette smoke-exposed and were sacrificed daily for 4 days for the determination of (A) BAL cellular inflammation and (B) nasal wash bacterial burden. Gray circles in (A) indicate cigarette smoke-exposed mice with bacterial burden detected in the BAL, while black circles represent mice with no BAL bacteria. Data are shown as mean ± SEM. n=8 cigarette smoke-exposed mice per time point.

Figure 16: Cigarette smoke exposure does not compromise nasal clearance of ^{99m}Tc-DTPA. Room air control or 1 week cigarette smoke-exposed mice were anesthetised and nasally inoculated with ^{99m}Tc-DTPA at a time point corresponding to day 3 post-nasal colonization. Dynamic images were acquired every 30 seconds using SPECT to observe distribution of the radioligand. A standard region of interest was positioned at the nasal region and the activity of ^{99m}Tc-DTPA every 30 seconds was measured and expressed as percent maximal activity (obtained in the first frame). Control (open circles), smoke (closed circles). n=5-6 mice per group. (B) Representative images of ^{99m}TC-DTPA activity in the nasal region immediately after inoculation and 20 minutes later. (C-D) A whole body scan was performed at 30 minutes post-^{99m}TC-DTPA administration, followed by a whole body CT scan. (C) CT scan of mouse outlining the regions of interest in the upper airways and whole body. (D) Observed radioactive signal in the whole body 30 minutes following nasal delivery of ^{99m}TC-DTPA. Mouse is in the same orientation as shown in (C).

Figure 17: PAFR or IL-1α deficiency does not rescue cigarette smoke-exposed mice from mortality following nasal pneumococcal colonization. Room air control or 1 week cigarette smoke-exposed mice were nasally colonized with approximately 10^6 CFU *S. pneumoniae*. Mice continued to be cigarette smoke-exposed post-nasal colonization. (A) Lung mRNA expression of PAFR (*Ptafr*) and IL-1α at day 3 post-nasal colonization. Lung PAFR mRNA expression was also assessed in IL-1α KO mice following 4 days of cigarette smoke exposure. Gene expression was determined by RT-qPCR and normalized to that of the room air vehicle control group of the appropriate mouse strain. n=5 mice per group. (B) Lysis Buffer RLT nasal wash mRNA expression of PAFR and IL-1α at day 2 post-nasal colonization. Gene expression was determined by RT-qPCR and normalized to that of the room air vehicle control group. Room air (open bars), smoke (solid bars). Data are shown as mean ± SEM. n=3-5 mice per group. Data are representative of 2 independent experiments.*$p<0.05$ when compared to corresponding control as assessed by independent t-test. (C) Survival curves of cigarette smoke-exposed IL-1α KO and PAFR KO mice post-nasal pneumococcal colonization. Wild type mice (solid line), KO mice (dotted line). n=9-10 mice per group. Data are representative of 2 independent experiments. Survival curves were compared by log-rank test, $p<0.05$ was considered significant.

Figure 18: Smoking cessation fully protects mice from mortality following nasal pneumococcal colonization. 1 week cigarette smoke-exposed mice were nasally colonized with approximately 10^6 CFU *S. pneumoniae* and either continued or stopped cigarette smoke exposure following colonization. (A) Survival curve of mice that continued to be cigarette smoke-exposed (solid line) or underwent smoking cessation (dotted line). n=10 mice per group.

Survival curves were compared by log-rank test, $p<0.05$ was considered significant. (B) Neutrophil proportions in the nasal wash from the smoking and cessation groups were determined at day 2 post-nasal colonization using flow cytometry. n=5 mice per group. (C) mRNA was isolated from lysis Buffer RLT nasal washes from the smoke-exposed and cessation groups at day 2 post-nasal colonization. Gene expression was determined by RT-qPCR and normalized to that of the cigarette smoke-exposed group. Smoke (black bars), cessation (gray bars). Data are shown as mean ± SEM. n=8-10 mice per group. *$p<0.05$ when compared to corresponding control as assessed by independent t-test.

Figure 19: Cigarette smoke exposure increases nasal pneumococcal colonization in mice. Room air control or 1 week cigarette smoke-exposed mice were nasally colonized with the indicated dose of *S. pneumoniae* strain TIGR4 and sacrificed at the specified time points. Mice continued to be cigarette smoke-exposed post-nasal colonization. (A) Survival following nasal pneumococcal colonization (10^7 CFU). Room air control mice (solid line), cigarette smoke-exposed mice (dotted line). n=10 mice per group. Survival curves were compared by log-rank test; $p<0.05$ was considered significant. (B) *S. pneumoniae* presence as determined by culturing on blood agar in the nasal wash at 12 h following low dose nasal pneumococcal colonization (10^3 CFU). n=7 mice per group. Fisher's exact test was utilized to assess whether increased association between cigarette smoke exposure and pneumococcal presence was significant. $p<0.05$ was considered significant. (C) Nasal pneumococcal burden was determined in the nasal wash by plating on blood agar at the indicated time points post-nasal pneumococcal colonization (10^4 CFU). n=5-6 mice per group. *$p<0.05$ when compared to corresponding control as assessed by independent t-test. (D-E) Complete nasal turbinates were isolated at the indicated *S. pneumoniae* nasal inoculation doses and time points post-nasal pneumococcal colonization. DNA was extracted and levels of the *S. pneumoniae* specific gene *lytA* relative to host *Gapdh* were determined by RT-qPCR. n=5 mice per group. Room air (open circles), smoke (closed circles). Differences between groups were assessed by independent t-test. $p<0.05$ was considered significant.

Figure 20: Cigarette smoke exposure alone does not alter the nasal microbiome. Room air or 1 week cigarette smoke-exposed mice were administered PBS (vehicle control) and smoke-exposed for an additional (A) 1 day and (B) 3 days. 16S rRNA sequencing was carried out on complete nasal turbinates. Principal coordinate analyses (PCoA) of the Bray-Curtis distance indicate that bacterial communities do not cluster together dependent on cigarette smoke exposure. Plots indicate β-diversity between samples, with each point representing one mouse. Distances between points represent how similar bacterial communities are between mice; the closer the samples, the more similar their microbiomes. n=5 mice per group. Statistical analyses were carried out with PERMANOVA.

Figure 21: Relative abundances of major bacterial phyla and taxonomic summaries are similar between room air and cigarette smoke-exposed mice. Room air or 1 week cigarette smoke-exposed mice were administered PBS (vehicle control) and smoke-exposed for an additional day. 16S rRNA sequencing was carried out on complete nasal turbinates. (A) Relative abundances of the major bacterial phyla present are shown. Room air (open circles), smoke (closed circles). (B) Taxonomic summary plots are shown for individual mice. The relative abundance of each taxon is represented by the height of the bar. P: phylum, F: family, G: genus. n=5 mice per group.

Figure 22: Pneumococcal acquisition does not perturb the nasal microbiome in cigarette smoke-exposed mice as compared to room air control. Room air or 1 week cigarette smoke-exposed mice were nasally inoculated with 10^4 CFU *S. pneumoniae* and sacrificed 12 h

post-nasal pneumococcal colonization. 16S rRNA sequencing was carried out on complete nasal turbinates. (A) Principal coordinate analysis (PCoA) of the Bray-Curtis distance indicate that bacterial communities do not cluster together dependent on cigarette smoke exposure. Plots indicate β-diversity between samples, with each point representing one mouse. Distances between points represent how similar bacterial communities are between mice; the closer the samples, the more similar their microbiomes. Statistical analyses were carried out with PERMANOVA. (B) Relative abundances of the major bacterial phyla present are shown. Room air (open circles), smoke (closed circles). (C) Taxonomic summary plots are shown for individual mice. The relative abundance of each taxon is represented by the height of the bar. P: phylum, F: family, G: genus. n=5 mice per group.

Figure 23: Established nasal pneumococcal colonization is associated with significant differences in nasal microbiome composition between room air and cigarette smoke-exposed mice. Room air or 1 week cigarette smoke-exposed mice were nasally inoculated with 10^7 CFU *S. pneumoniae* and sacrificed 3 days post-nasal pneumococcal colonization. 16S rRNA sequencing was carried out on complete nasal turbinates. (A) Principal coordinate analysis (PCoA) of the Bray-Curtis distance indicate that bacterial communities cluster together dependent on cigarette smoke exposure. Plots indicate β-diversity between samples, with each point representing one mouse. Distances between points represent how similar bacterial communities are between mice; the closer the samples, the more similar their microbiomes. Differences between room air and cigarette smoke-exposed mice were determined to be statistically significant by PERMANOVA. Cigarette smoke-exposed mice with high nasal pneumococcal burden as determined by *lytA* measurement are indicated. (B) Relative abundances of the major bacterial phyla present are shown. Room air (open circles), smoke (closed circles). (C) Taxonomic summary plots are shown for individual mice. The relative abundance of each taxon is represented by the height of the bar. P: phylum, F: family, G: genus. n=5 mice per group. *Samples with *lytA* levels greater than a fold change of 0.5 relative to host *Gapdh*.

Figure 24: Most abundant bacterial genera which are significantly increased in cigarette smoke-exposed mice at day 3 following established nasal pneumococcal colonization. Room air or 1 week cigarette smoke-exposed mice were either nasally inoculated with 10^4 CFU *S. pneumoniae* and sacrificed 12h post-nasal pneumococcal colonization or nasally inoculated with 10^7 CFU *S. pneumoniae* and sacrificed 3 days post-nasal pneumococcal colonization. 16S rRNA sequencing was carried out on complete nasal turbinates. Relative abundances of (A) *Fusobacterium* (B) *Gemella* and (C) *Neisseria*. Room air (open circles), smoke (closed circles). n=5 mice per group. Statistical analysis was carried out using DESeq2. *p<0.01 as compared to *S. pneumoniae* colonized room air control. All bacterial genera found to be significantly different are listed in Table 1.

Figure 25: *Corynebacterium* and *Lactococcus* abundances are not impacted by cigarette smoke exposure in the presence of nasal pneumococcal colonization. Room air or 1 week cigarette smoke-exposed mice were nasally inoculated with 10^7 CFU *S. pneumoniae* and sacrificed 3 days post-nasal pneumococcal colonization. 16S rRNA sequencing was carried out on complete nasal turbinates. Relative abundances of (A) *Corynebacterium* and (B) *Lactococcus*. Room air (open circles), smoke (closed circles). n=5 mice per group. Statistical analysis was carried out using DESeq2. p<0.01 was considered significant.

Figure 26: *Haemophilus* and *Staphylococcus* abundances are not impacted by cigarette smoke exposure in the presence of nasal pneumococcal colonization. Room air or 1 week cigarette smoke-exposed mice were either nasally inoculated with 10^4 CFU *S. pneumoniae* and

sacrificed 12h post-nasal pneumococcal colonization or nasally inoculated with 10^7 CFU *S. pneumoniae* and sacrificed 3 days post-nasal pneumococcal colonization. 16S rRNA sequencing was carried out on complete nasal turbinates. Relative abundances of (A) *Streptococcus* (B) *Haemophilus* and (C) *Staphylococcus*. Room air (open circles), smoke (closed circles). n=5 mice per group. Statistical analysis was carried out using DESeq2. $p<0.01$ was considered significant.

Figure 1

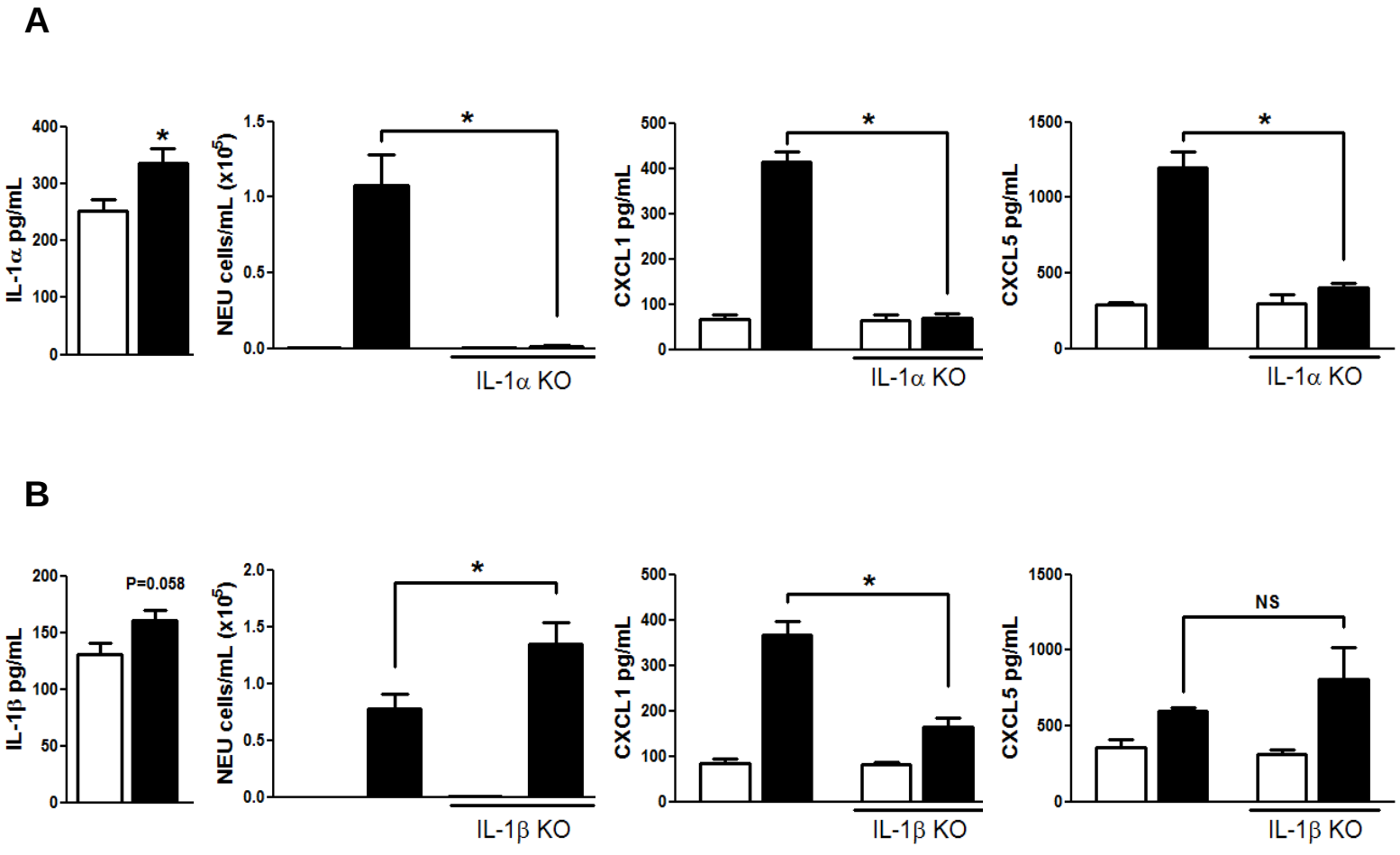
A
IL-1α pg/mL
NEU cells/mL (x10^5)
CXCL1 pg/mL
CXCL5 pg/mL
IL-1α KO
B
IL-1β pg/mL
P=0.058
NEU cells/mL (x10^5)
CXCL1 pg/mL
CXCL5 pg/mL
NS
IL-1β KO
C
Day 0
Whole body irradiation (11 Gy)
Day 0
Injection of bone marrow cells of wild-type (WT) or IL-1 α -/- (KO) donor genotype
Wild-type (WT) or IL-1α-/- (KO) recipient
Week 8
Groups generated
WT into WT
WT into KO
KO into WT
KO into KO
NEU cells/mL (x10^5)
NS
Room Air
Smoke
WT to WT
WT to KO
KO to WT
KO to KO

Figure 2

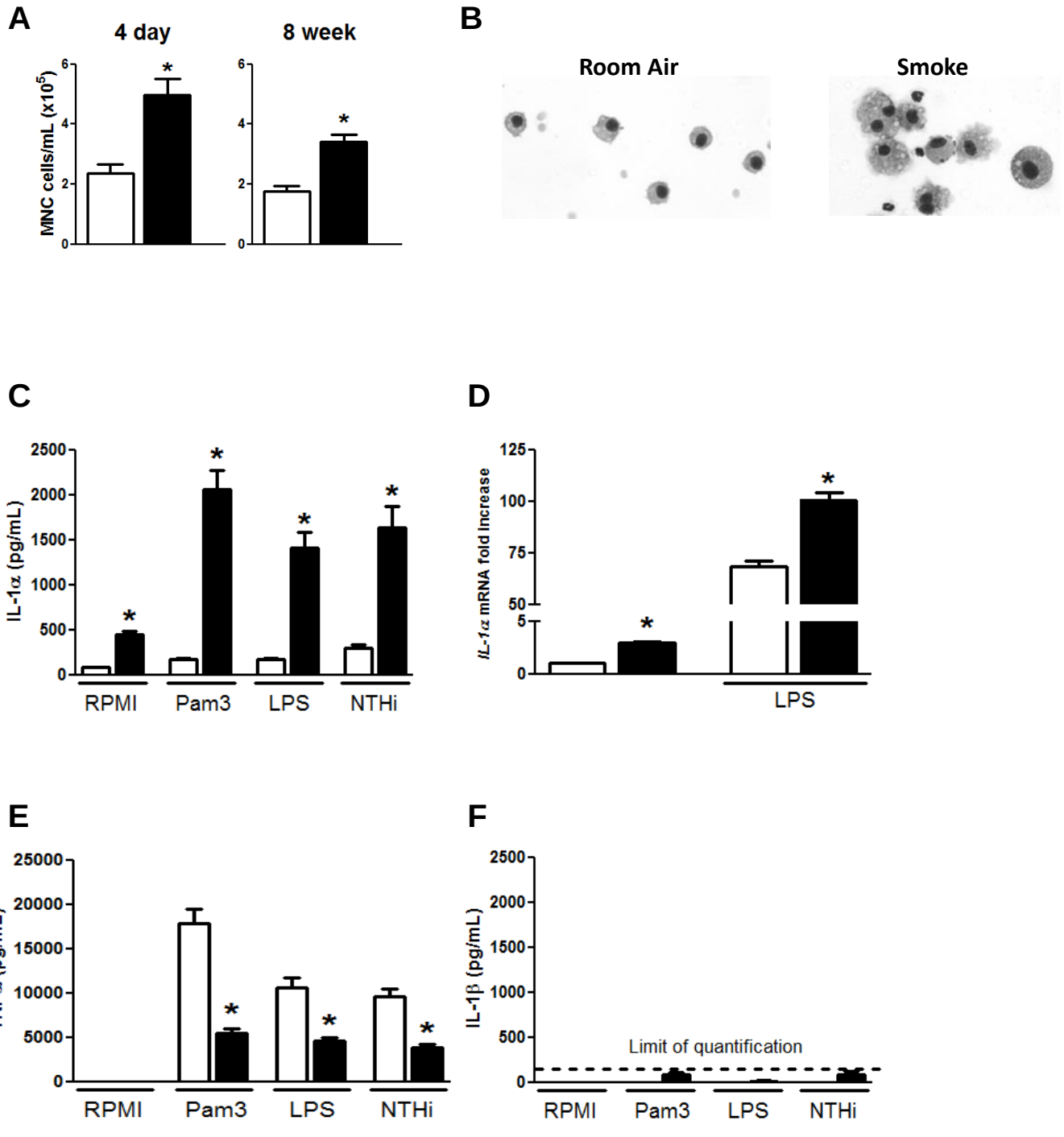
A
4 day
8 week
MNC cells/mL (x10^5)
B
Room Air
Smoke
C
IL-1α (pg/mL)
RPMI
Pam3
LPS
NTHi
D
IL-1α mRNA fold Increase
LPS
E
TNFα (pg/mL)
RPMI
Pam3
LPS
NTHi
F
IL-1β (pg/mL)
Limit of quantification
RPMI
Pam3
LPS
NTHi

Figure 3

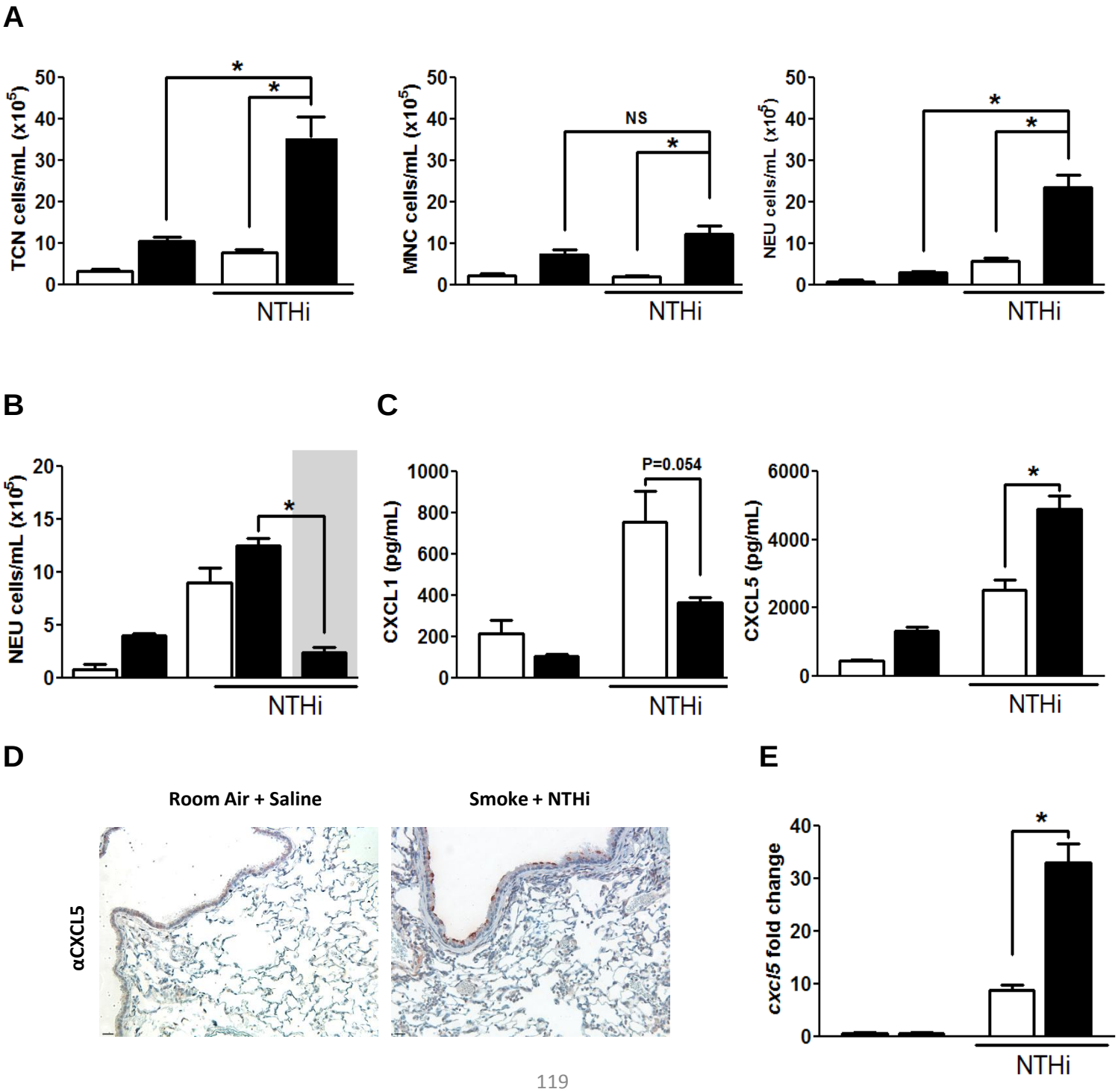
A
TCN cells/mL (x10^5)
MNC cells/mL (x10^5)
NEU cells/mL (x10^5)
NS
NTHi
B
NEU cells/mL (x10^5)
NTHi
C
CXCL1 (pg/mL)
P=0.054
CXCL5 (pg/mL)
NTHi
D
Room Air + Saline
Smoke + NTHi
αCXCL5
E
cxcl5 fold change
NTHi

Figure 4

A

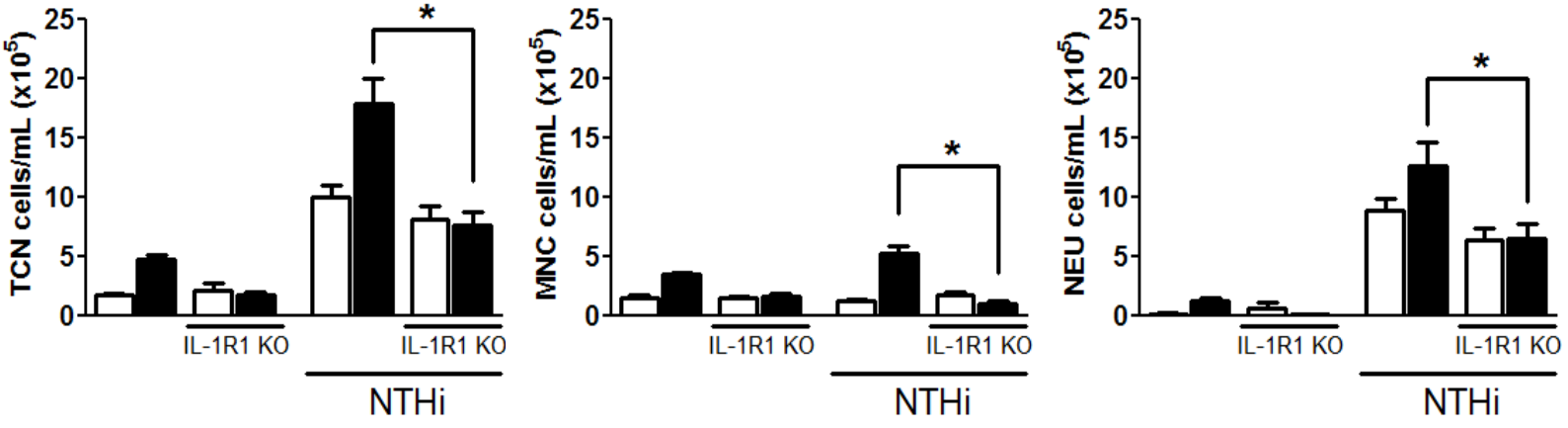
TCN cells/mL (x10^5)
MNC cells/mL (x10^5)
NEU cells/mL (x10^5)
25
20
15
10
5
0
*
IL-1R1 KO
IL-1R1 KO
NTHi

B

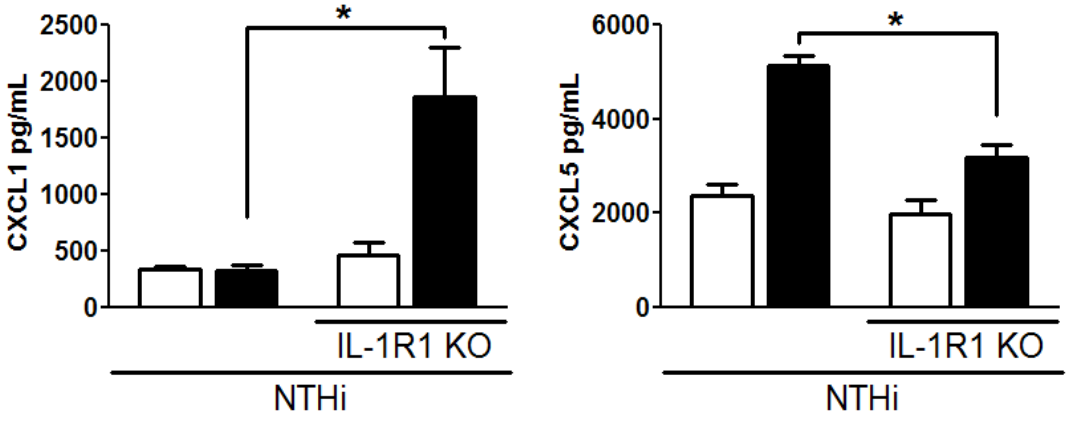
CXCL1 pg/mL
2500
2000
1500
1000
500
0
CXCL5 pg/mL
6000
4000
2000
0
*
IL-1R1 KO
NTHi

Figure 5

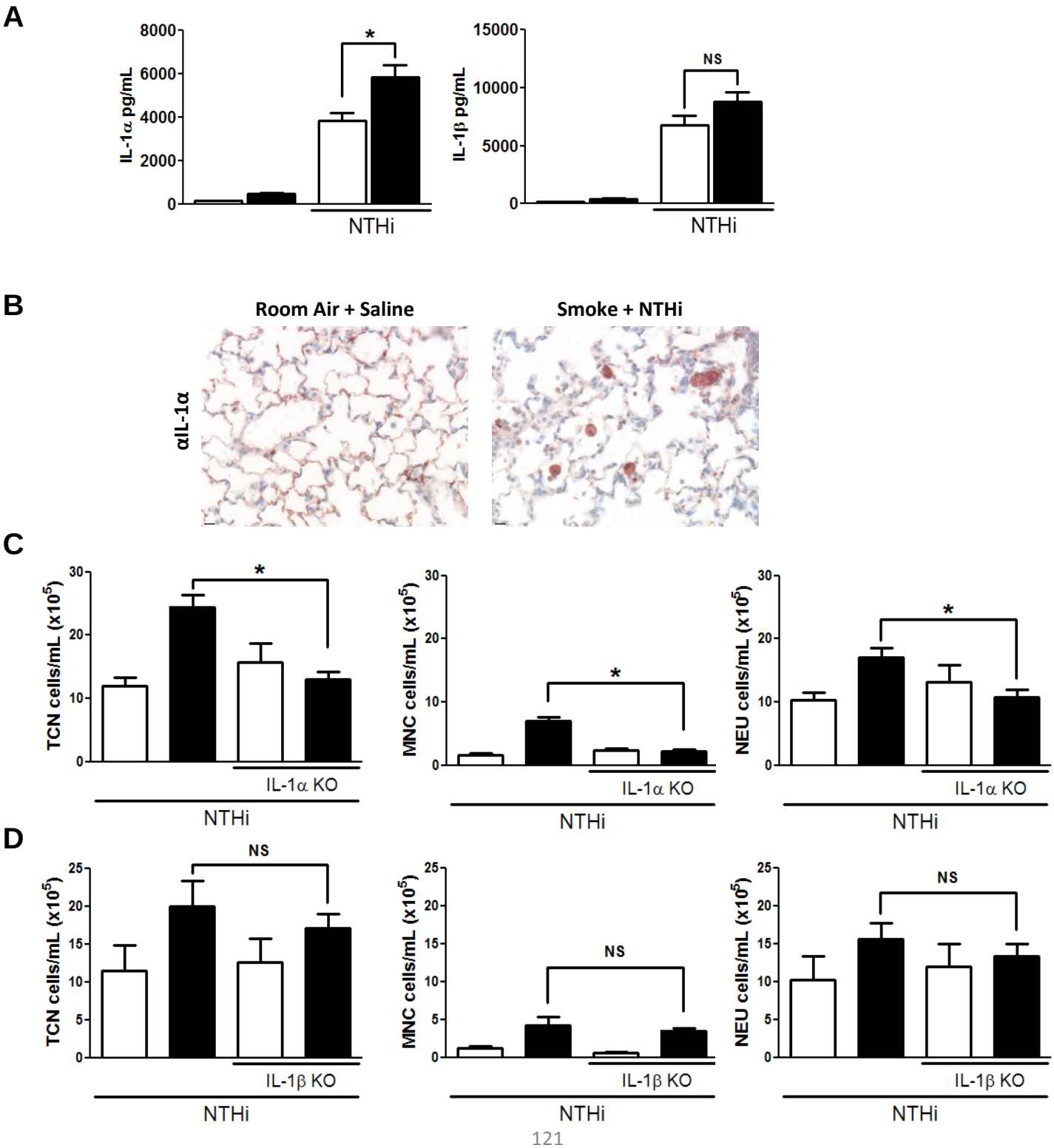
A
IL-1α pg/mL
8000
6000
4000
2000
0
*
NTHi
IL-1β pg/mL
15000
10000
5000
0
NS
NTHi
B
Room Air + Saline
Smoke + NTHi
αIL-1α
C
TCN cells/mL (x10^5)
30
20
10
0
*
IL-1α KO
NTHi
MNC cells/mL (x10^5)
30
20
10
0
*
IL-1α KO
NTHi
NEU cells/mL (x10^5)
30
20
10
0
*
IL-1α KO
NTHi
D
TCN cells/mL (x10^5)
25
20
15
10
5
0
NS
IL-1β KO
NTHi
MNC cells/mL (x10^5)
25
20
15
10
5
0
NS
IL-1β KO
NTHi
NEU cells/mL (x10^5)
25
20
15
10
5
0
NS
IL-1β KO
NTHi

Figure 6

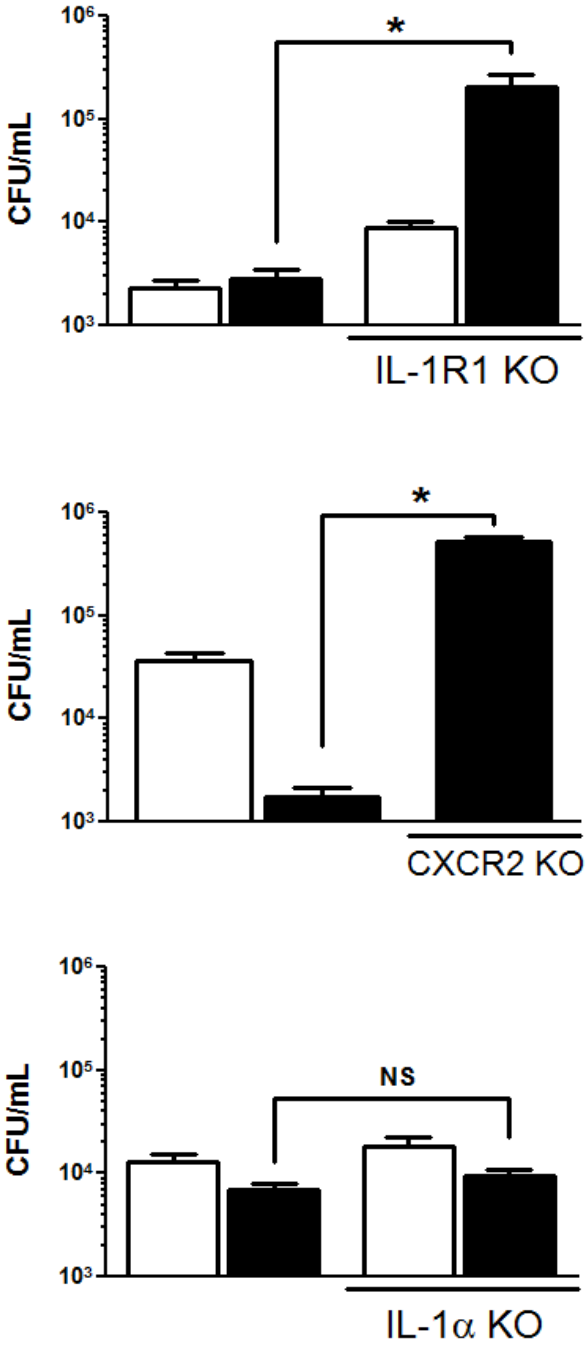
CFU/mL
10^6
10^5
10^4
10^3
*
IL-1R1 KO
CFU/mL
10^6
10^5
10^4
10^3
*
CXCR2 KO
CFU/mL
10^6
10^5
10^4
10^3
NS
IL-1α KO

Figure 7

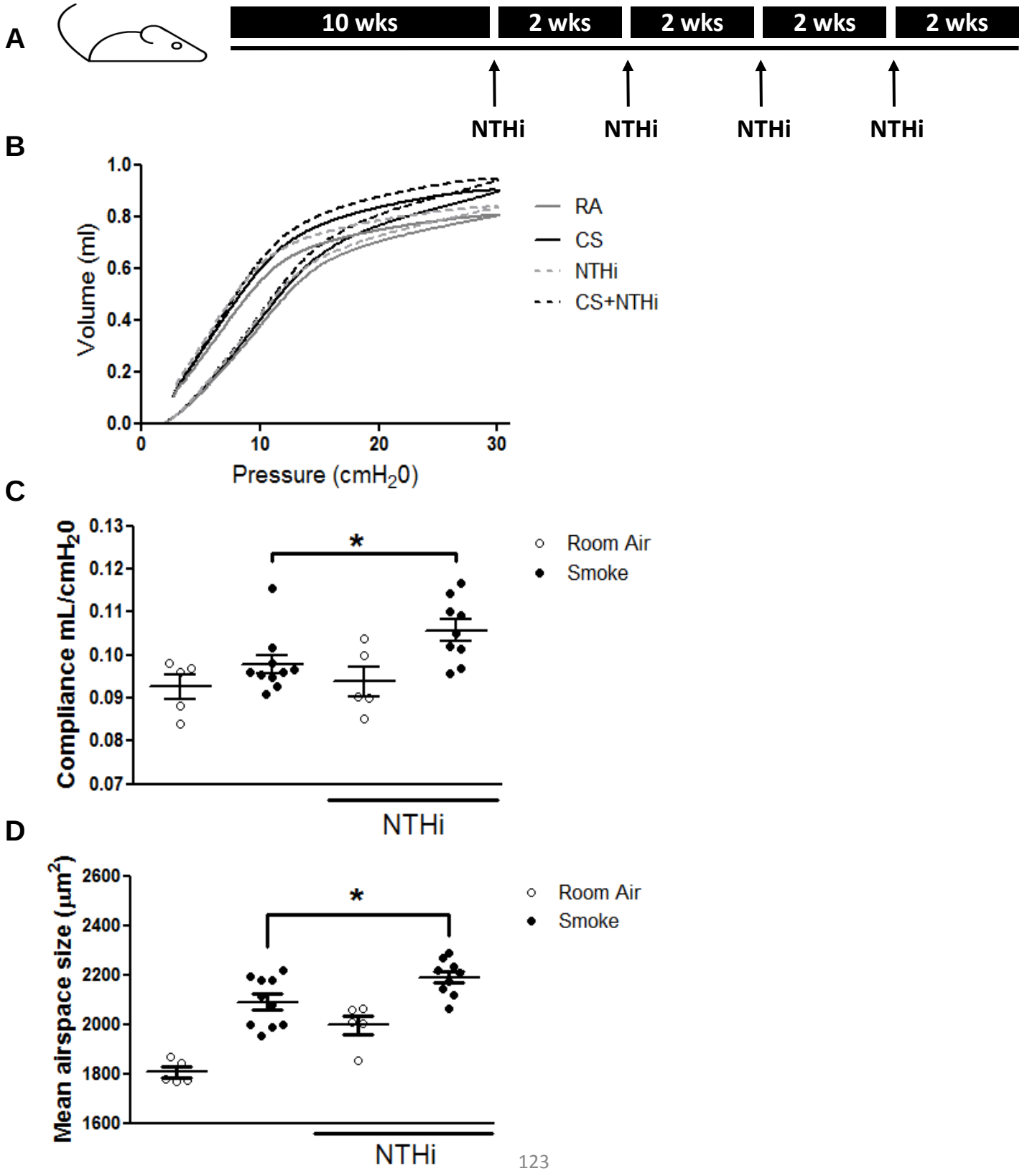
A
10 wks
2 wks
2 wks
2 wks
2 wks
NTHi
NTHi
NTHi
NTHi
B
Volume (ml)
1.0
0.8
0.6
0.4
0.2
0.0
0
10
20
30
Pressure (cmH20)
RA
CS
NTHi
CS+NTHi
C
Compliance mL/cmH20
0.13
0.12
0.11
0.10
0.09
0.08
0.07
*
Room Air
Smoke
NTHi
D
Mean airspace size (µm2)
2600
2400
2200
2000
1800
1600
*
Room Air
Smoke
NTHi

Figure 8

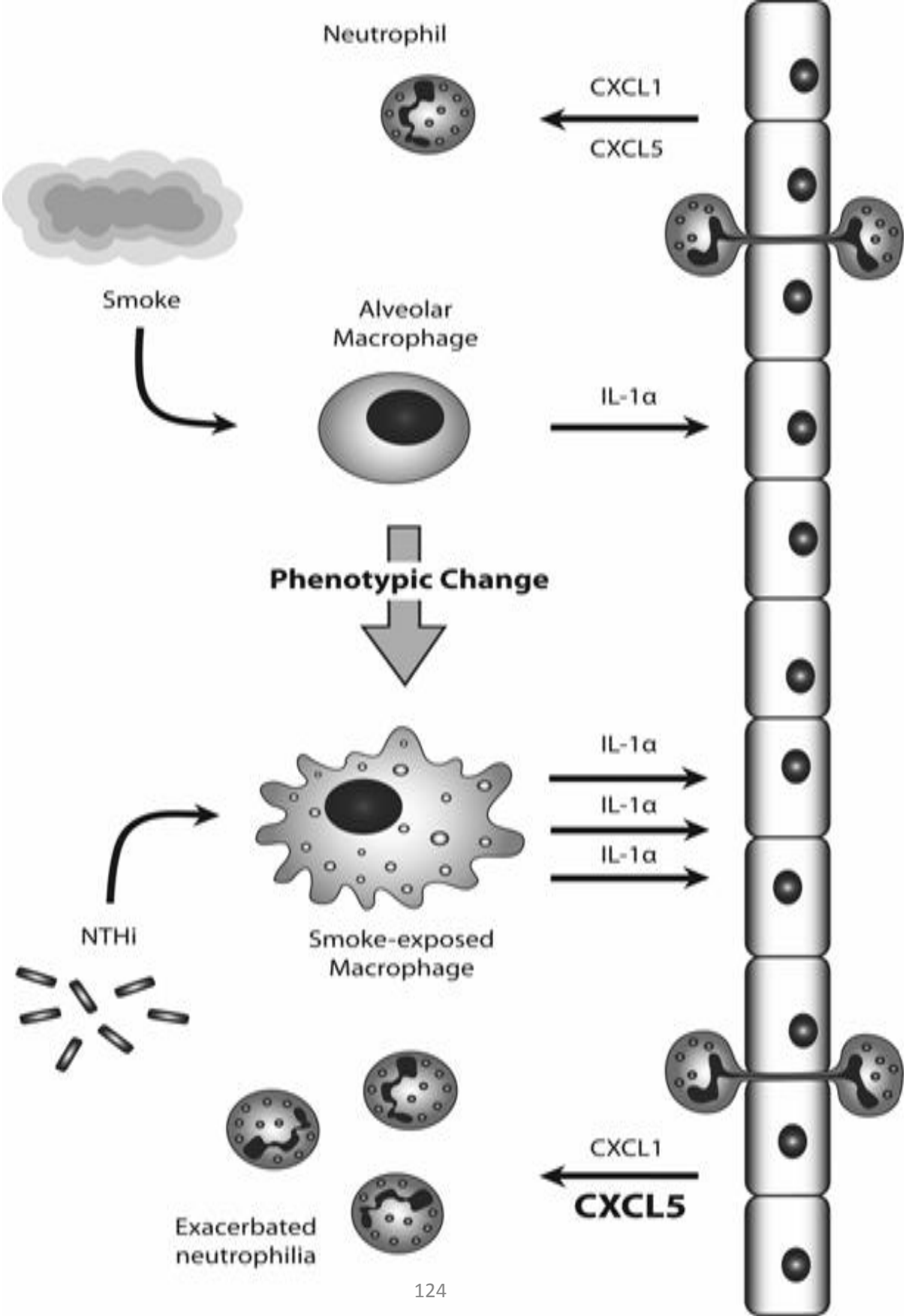
Neutrophil
CXCL1
CXCL5
Smoke
Alveolar Macrophage
IL-1α
Phenotypic Change
IL-1α
IL-1α
IL-1α
NTHi
Smoke-exposed Macrophage
CXCL1
CXCL5
Exacerbated neutrophilia

Figure 9

A

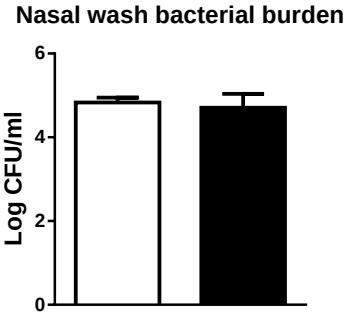
Nasal wash bacterial burden
Log CFU/ml
6
4
2
0

B

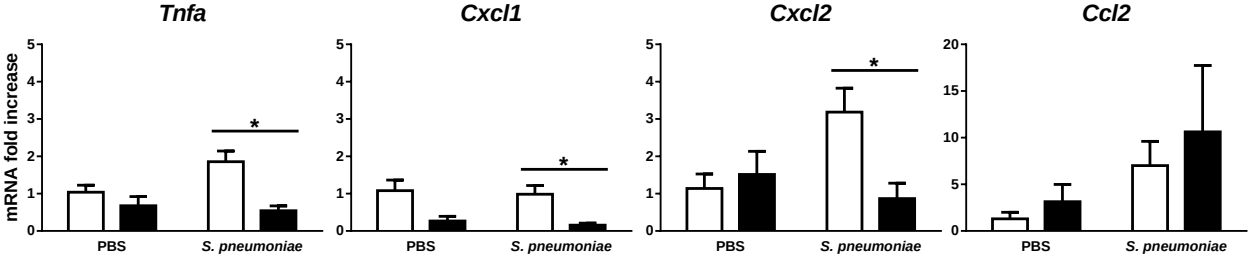
Tnfa
Cxcl1
Cxcl2
Ccl2
mRNA fold increase
*
PBS
S. pneumoniae

C

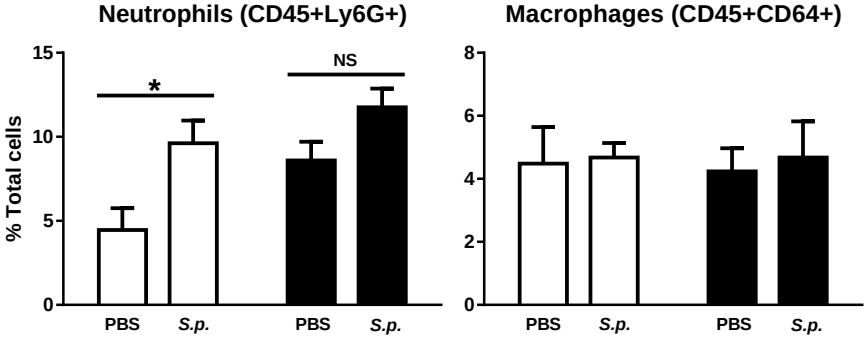
Neutrophils (CD45+Ly6G+)
Macrophages (CD45+CD64+)
% Total cells
*
NS
PBS
S.p.

Figure 10

A

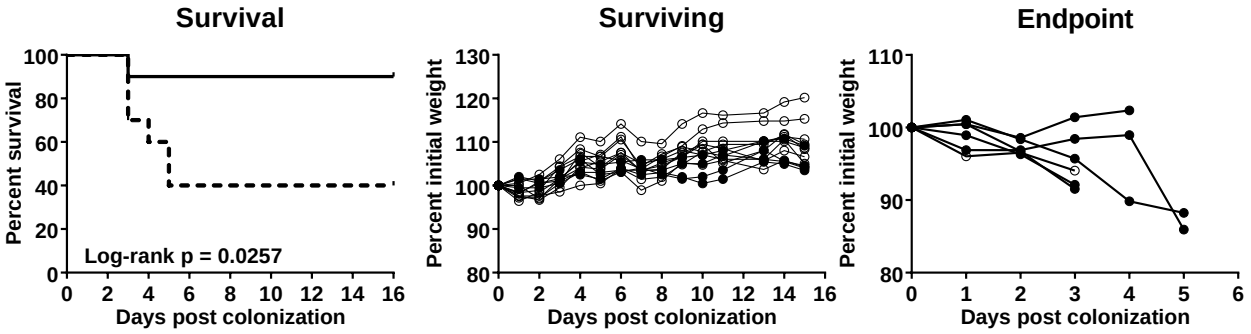

B Endpoint

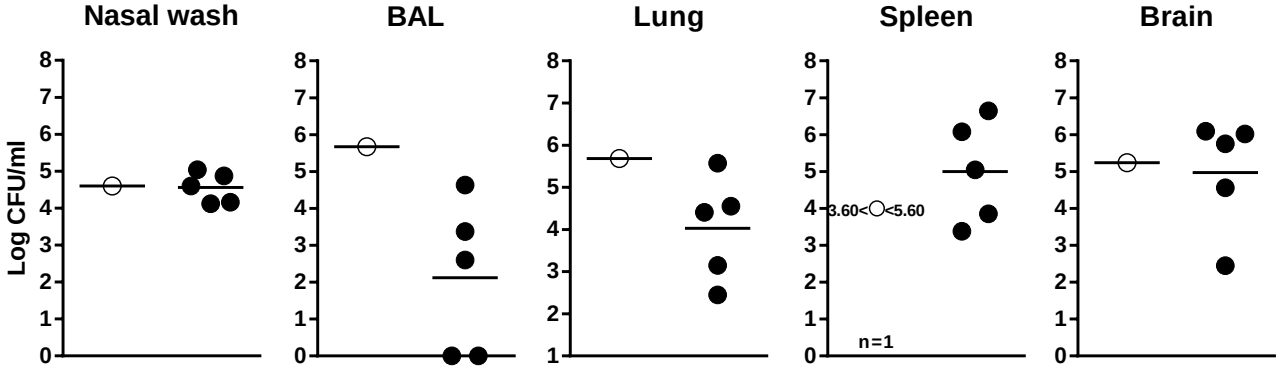

C Surviving

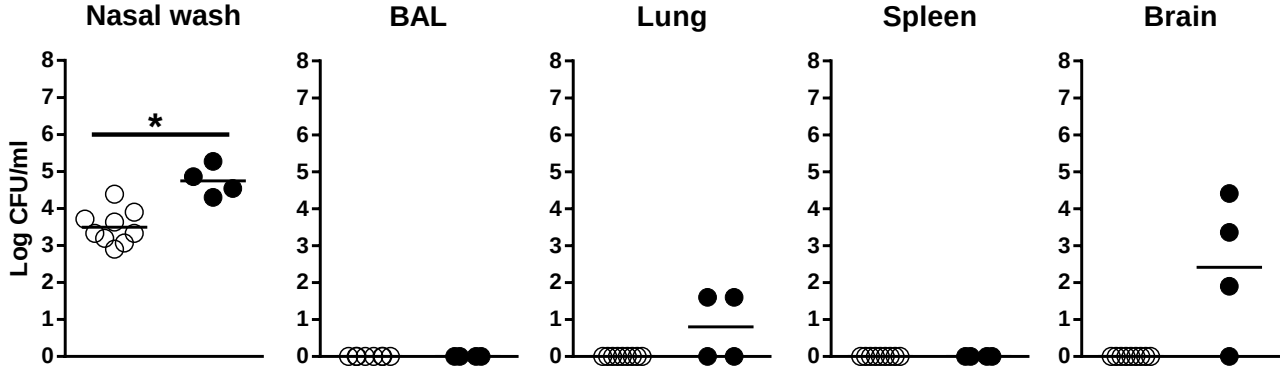

Figure 11

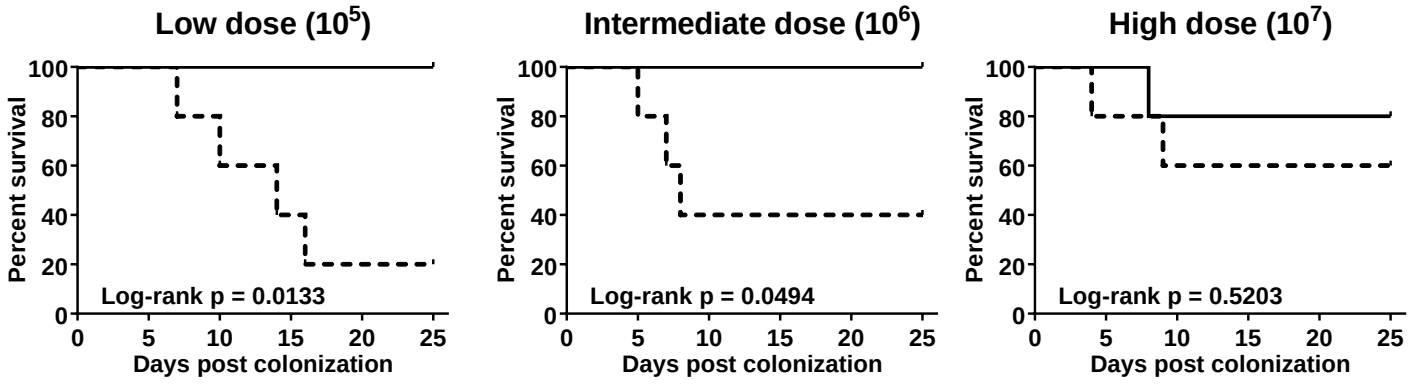
Low dose (10^5)
Intermediate dose (10^6)
High dose (10^7)
Percent survival
Days post colonization
Log-rank p = 0.0133
Log-rank p = 0.0494
Log-rank p = 0.5203
0
20
40
60
80
100
0
5
10
15
20
25

Figure 12

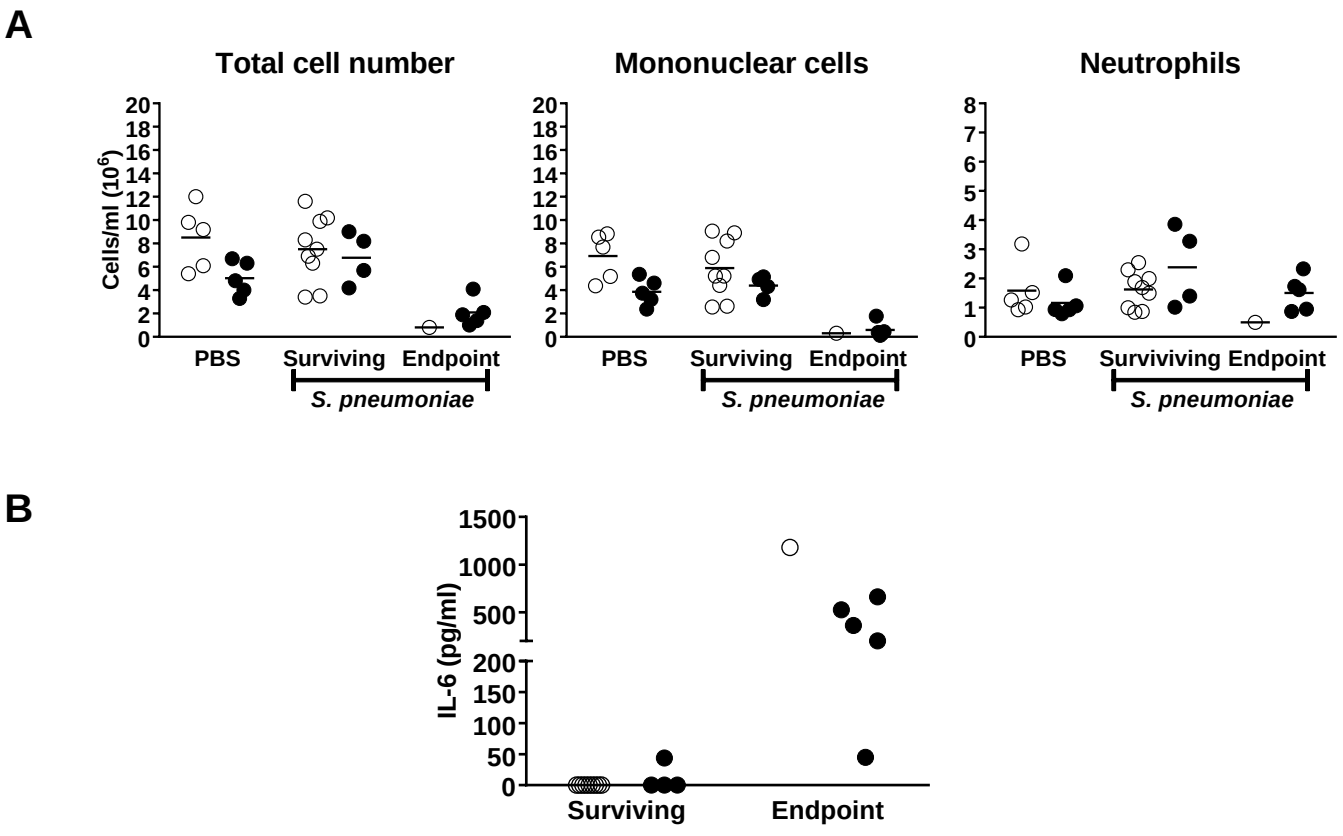
A
Total cell number
Mononuclear cells
Neutrophils
Cells/ml (10^6)
PBS
Surviving
Endpoint
Surviviving
S. pneumoniae
B
IL-6 (pg/ml)
1500
1000
500
200
150
100
50
0
Surviving
Endpoint
C
D
E
F
G
H

Figure 13

A

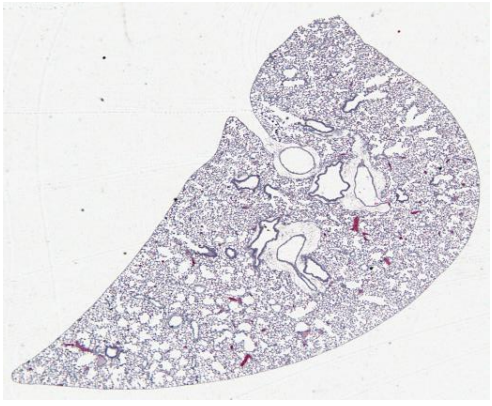

B

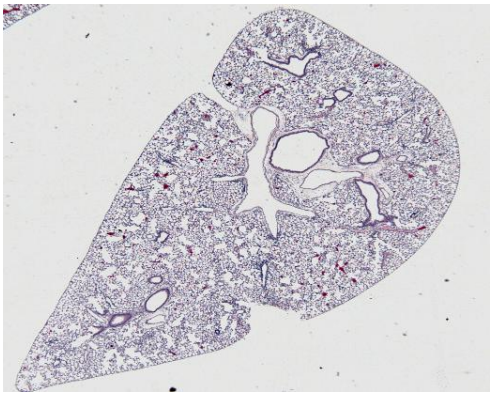

C

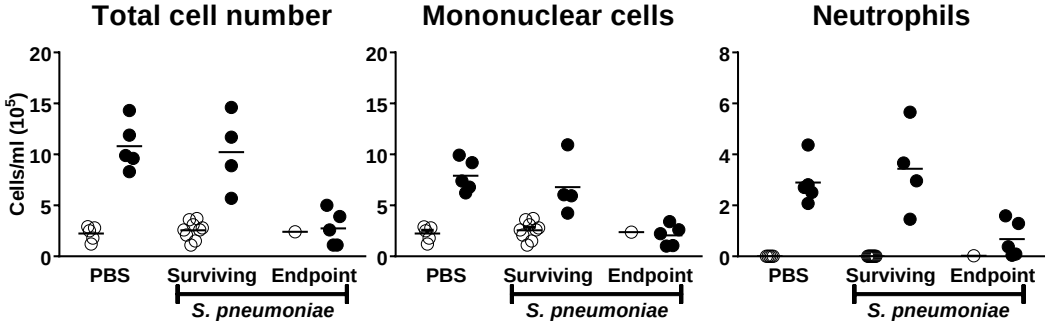

Figure 14

A

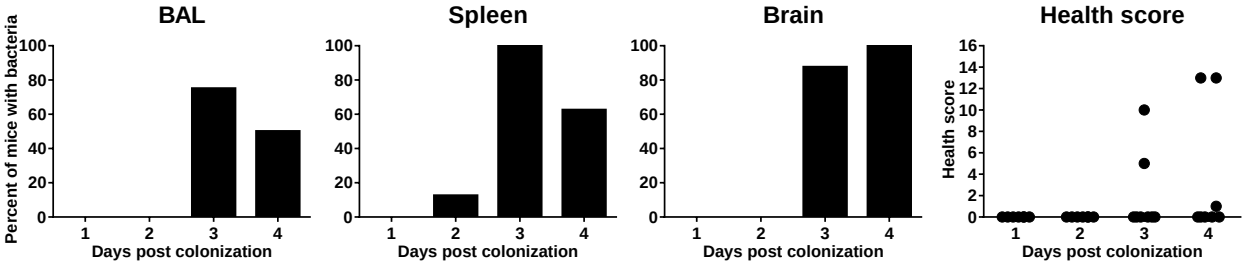

B Cigarette smoke-exposed

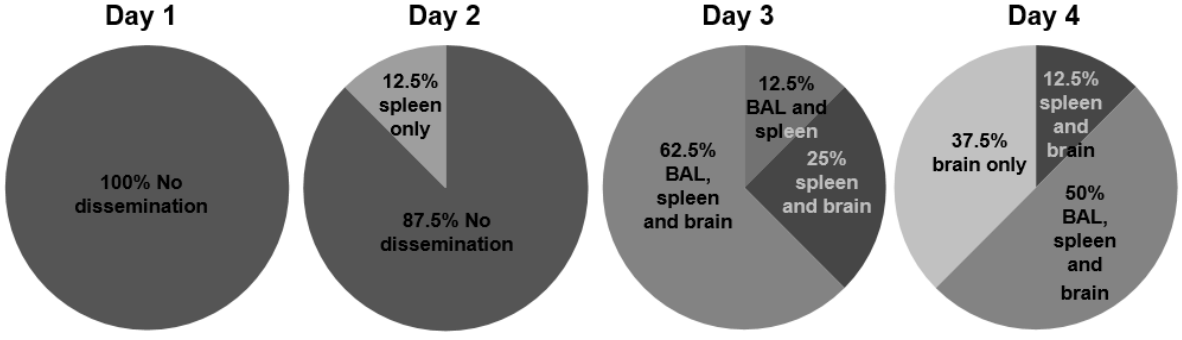

C Room air control

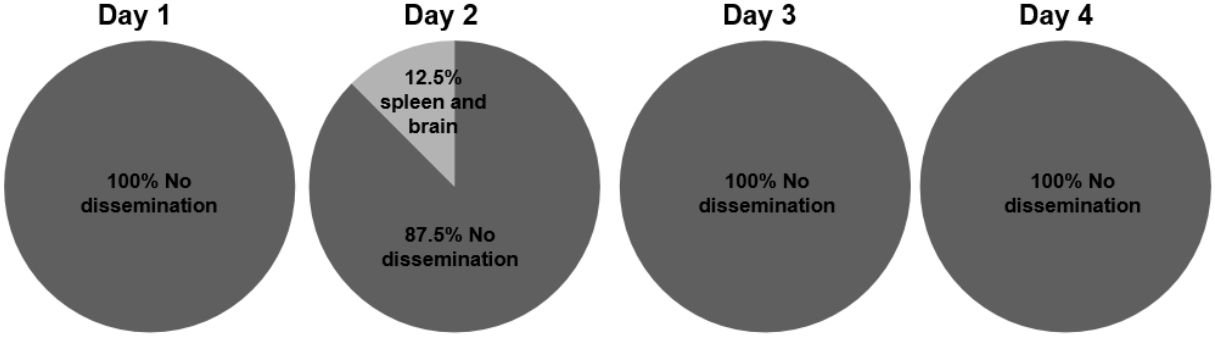

Figure 15

A

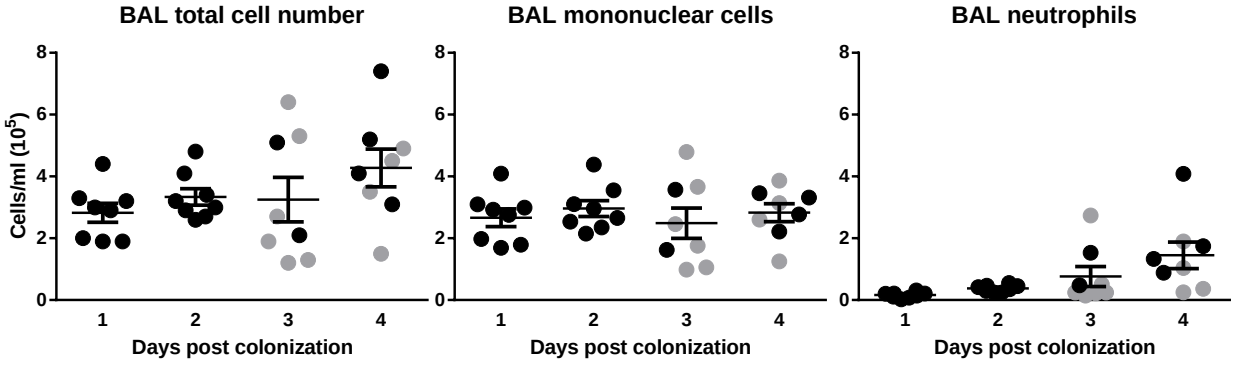
BAL total cell number
BAL mononuclear cells
BAL neutrophils
Cells/ml (10^5)
0
2
4
6
8
1
2
3
4
Days post colonization

B

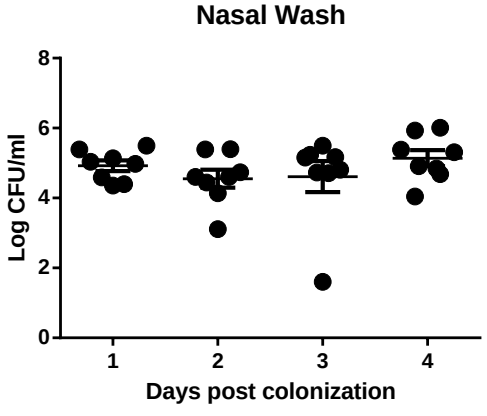
Nasal Wash
Log CFU/ml
0
2
4
6
8
1
2
3
4
Days post colonization

Figure 16

A

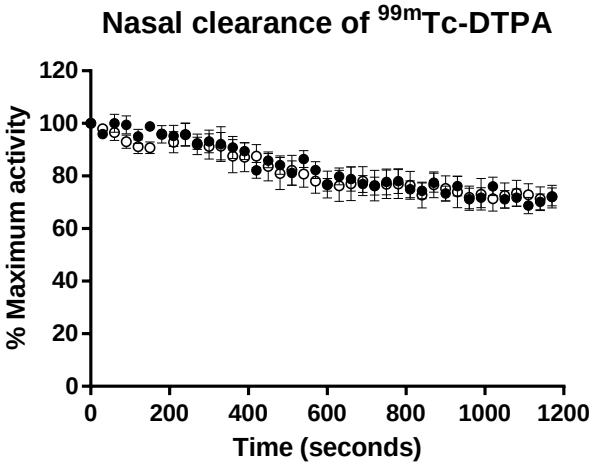

B

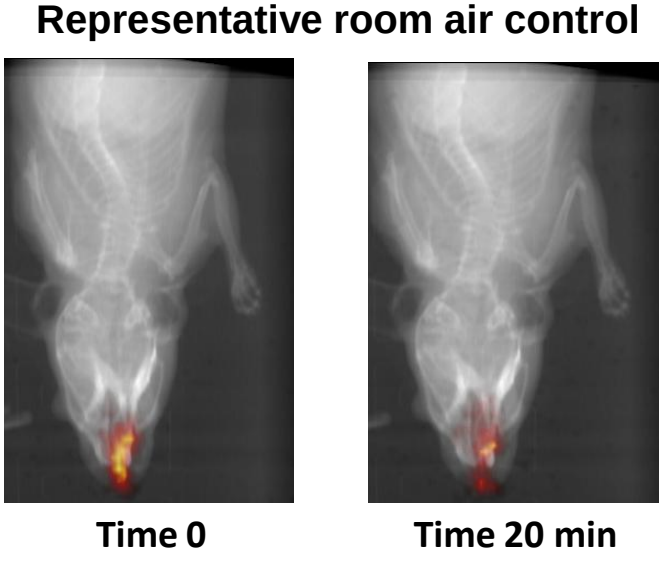

C

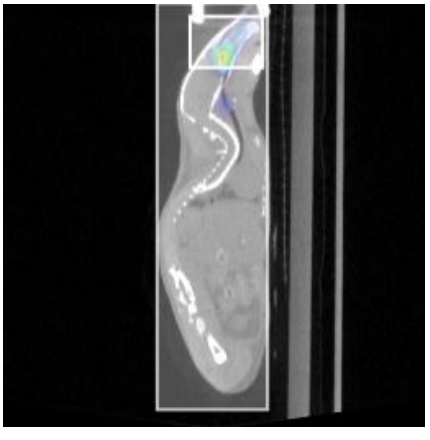

D

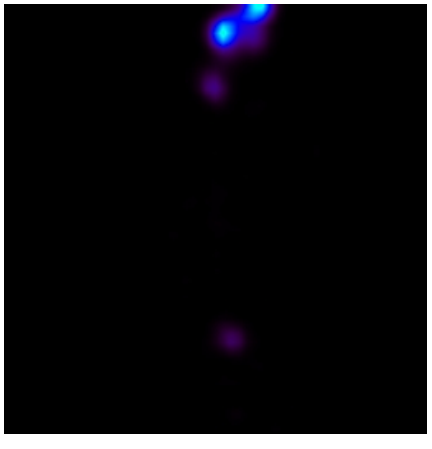

Figure 17

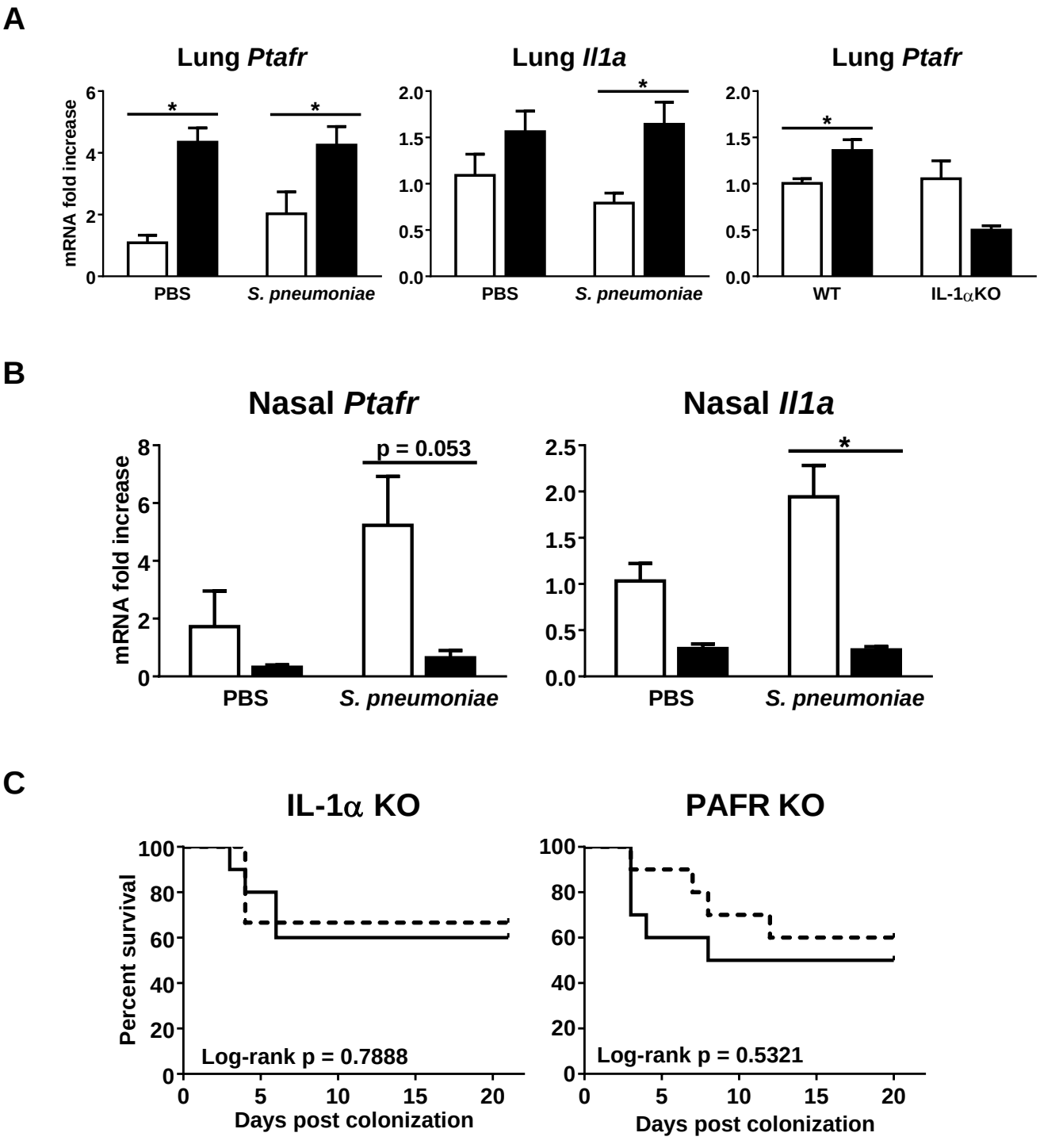
A
Lung Ptafr
Lung Il1a
Lung Ptafr
mRNA fold increase
PBS
S. pneumoniae
PBS
S. pneumoniae
WT
IL-1αKO
B
Nasal Ptafr
Nasal Il1a
p = 0.053
mRNA fold increase
PBS
S. pneumoniae
PBS
S. pneumoniae
C
IL-1α KO
PAFR KO
Percent survival
Log-rank p = 0.7888
Log-rank p = 0.5321
Days post colonization
Days post colonization

Figure 18

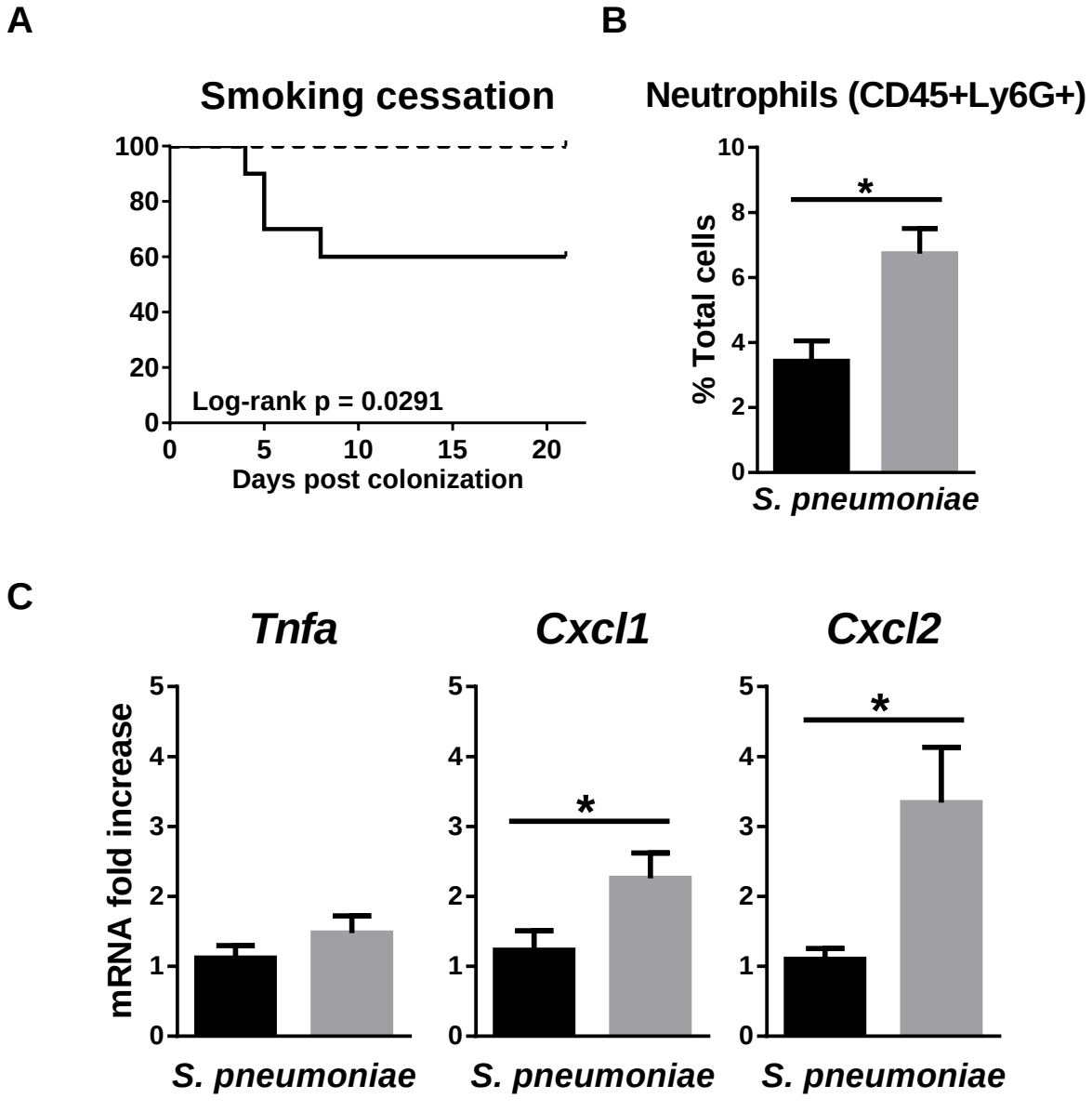
A
Smoking cessation
100
80
60
40
20
0
Log-rank p = 0.0291
0
5
10
15
20
Days post colonization
B
Neutrophils (CD45+Ly6G+)
% Total cells
10
8
6
4
2
0
*
S. pneumoniae
C
Tnfa
Cxcl1
Cxcl2
mRNA fold increase
5
4
3
2
1
0
*
*
*
S. pneumoniae
S. pneumoniae
S. pneumoniae

Figure 19

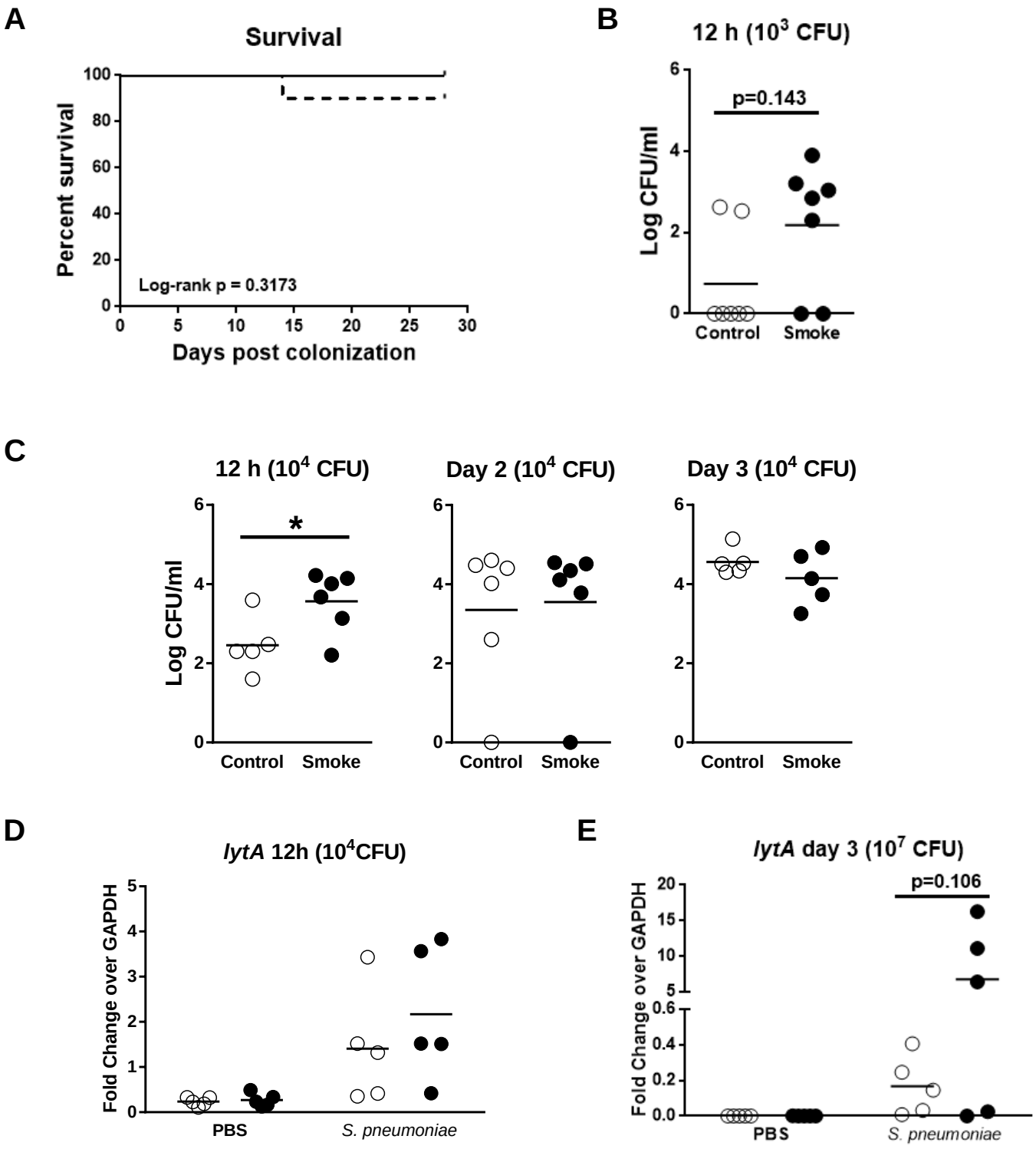
A
Survival
Percent survival
Log-rank p = 0.3173
Days post colonization
B
12 h (10^3 CFU)
p=0.143
Log CFU/ml
Control
Smoke
C
12 h (10^4 CFU)
Day 2 (10^4 CFU)
Day 3 (10^4 CFU)
*
Log CFU/ml
Control
Smoke
D
lytA 12h (10^4CFU)
Fold Change over GAPDH
PBS
S. pneumoniae
E
lytA day 3 (10^7 CFU)
p=0.106
Fold Change over GAPDH
PBS
S. pneumoniae

Figure 20

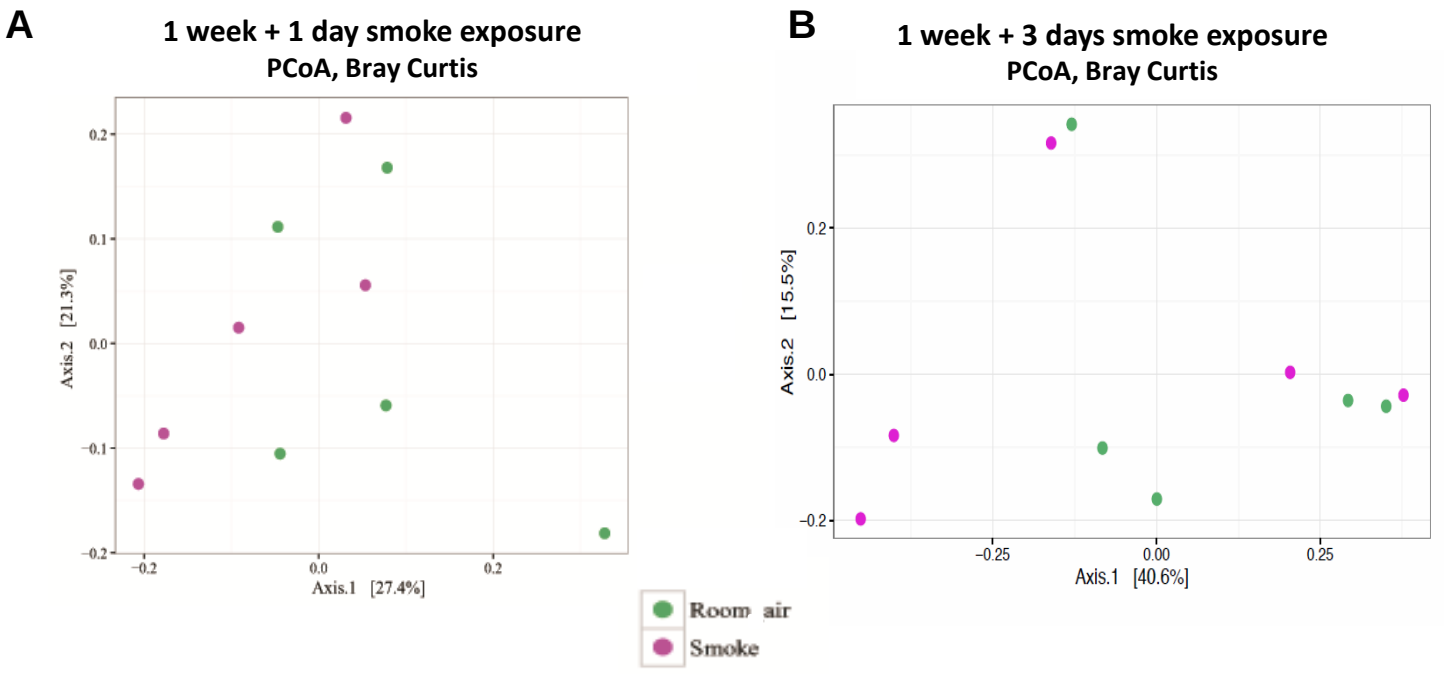
A
1 week + 1 day smoke exposure
PCoA, Bray Curtis
Axis.2 [21.3%]
Axis.1 [27.4%]
B
1 week + 3 days smoke exposure
PCoA, Bray Curtis
Axis.2 [15.5%]
Axis.1 [40.6%]
Room air
Smoke

Figure 21

A

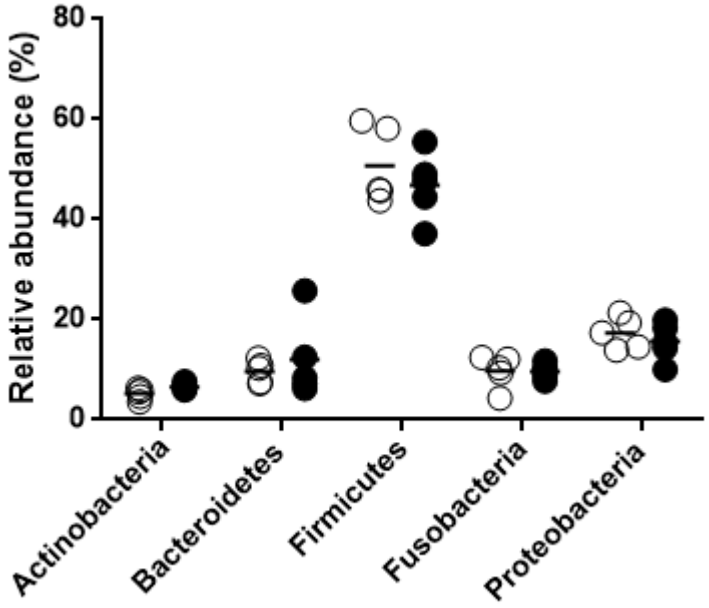
Relative abundance (%)
80
60
40
20
0
Actinobacteria
Bacteroidetes
Firmicutes
Fusobacteria
Proteobacteria

B

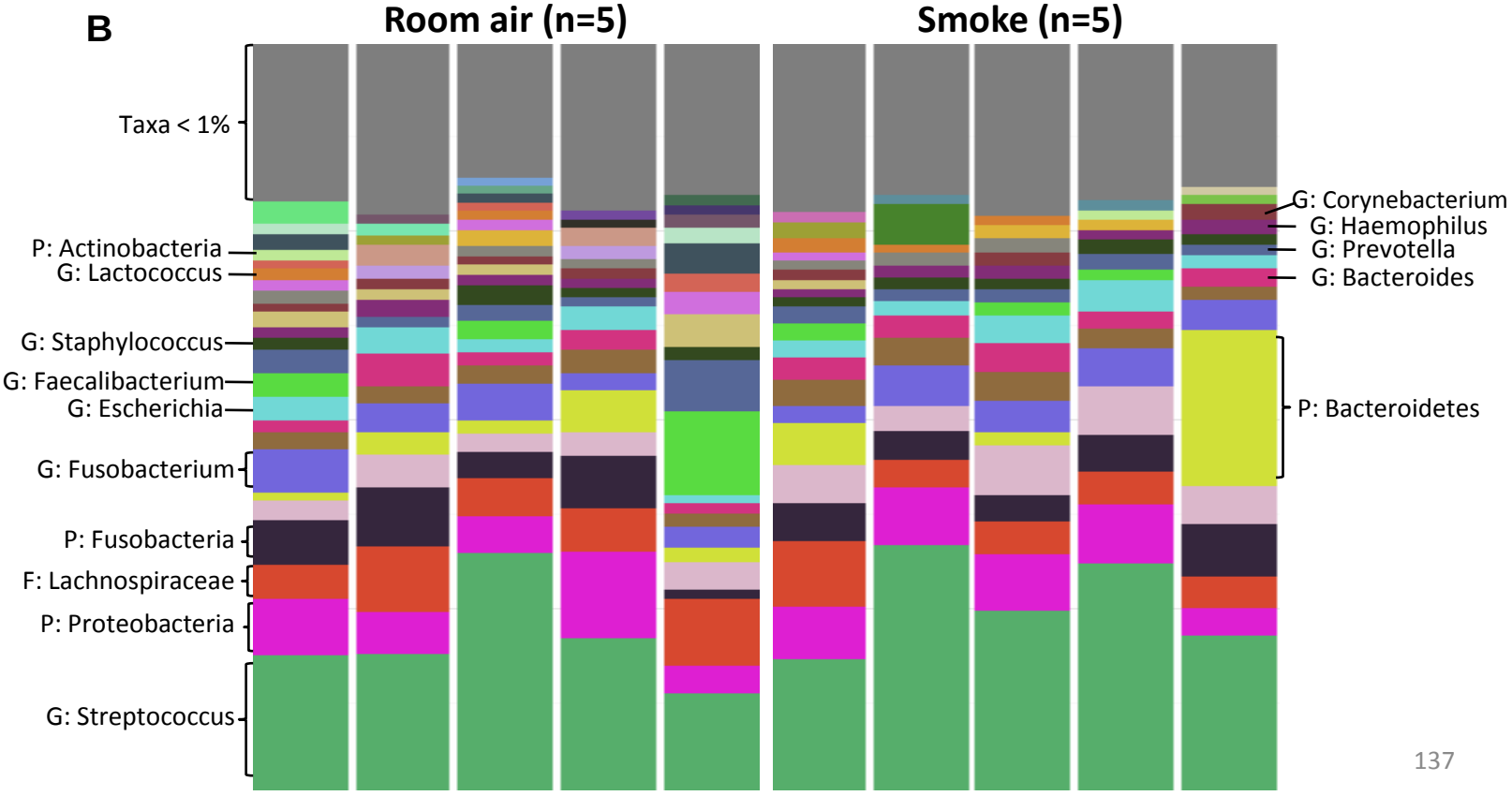
Room air (n=5)
Smoke (n=5)
Taxa < 1%
P: Actinobacteria
G: Lactococcus
G: Staphylococcus
G: Faecalibacterium
G: Escherichia
G: Fusobacterium
P: Fusobacteria
F: Lachnospiraceae
P: Proteobacteria
G: Streptococcus
G: Corynebacterium
G: Haemophilus
G: Prevotella
G: Bacteroides
P: Bacteroidetes

Figure 22

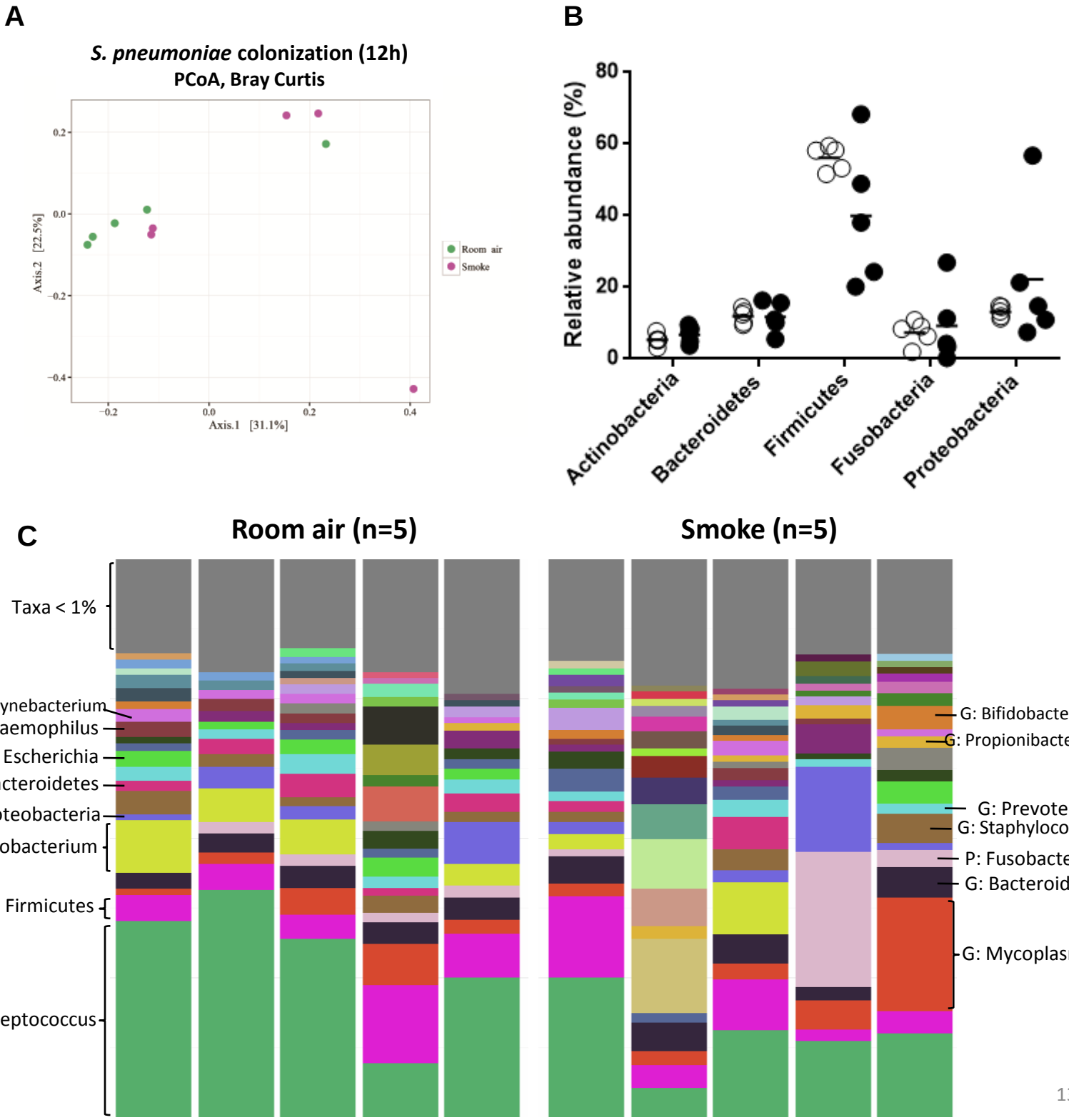
A
S. pneumoniae colonization (12h)
PCoA, Bray Curtis
Axis.2 [22.5%]
Axis.1 [31.1%]
Room air
Smoke
B
Relative abundance (%)
Actinobacteria
Bacteroidetes
Firmicutes
Fusobacteria
Proteobacteria
C
Room air (n=5)
Smoke (n=5)
Taxa < 1%
G: Corynebacterium
G: Haemophilus
G: Escherichia
P: Bacteroidetes
P: Proteobacteria
G: Fusobacterium
P: Firmicutes
G: Streptococcus
G: Bifidobacterium
G: Propionibacterium
G: Prevotella
G: Staphylococcus
P: Fusobacteria
G: Bacteroides
G: Mycoplasma

Figure 23

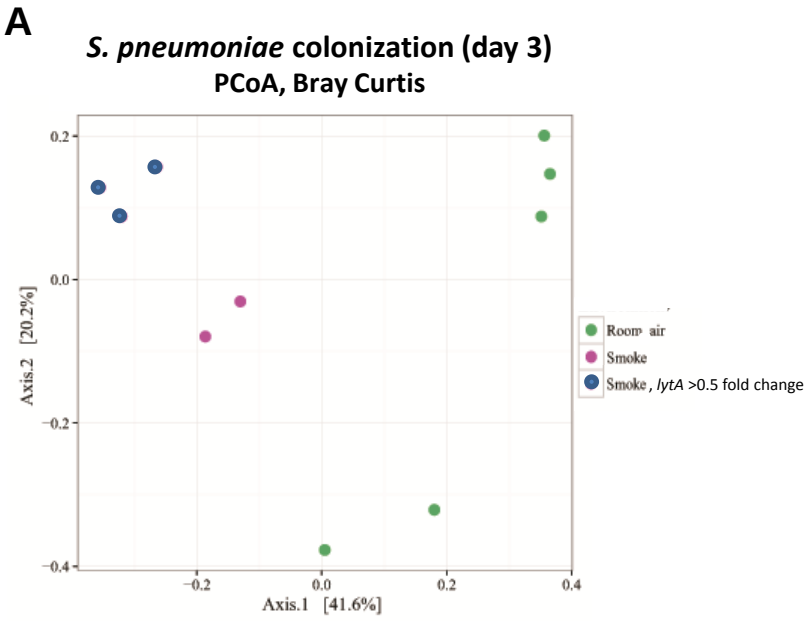
A
S. pneumoniae colonization (day 3)
PCoA, Bray Curtis
Axis.2 [20.2%]
Axis.1 [41.6%]
Room air
Smoke
Smoke, lytA >0.5 fold change

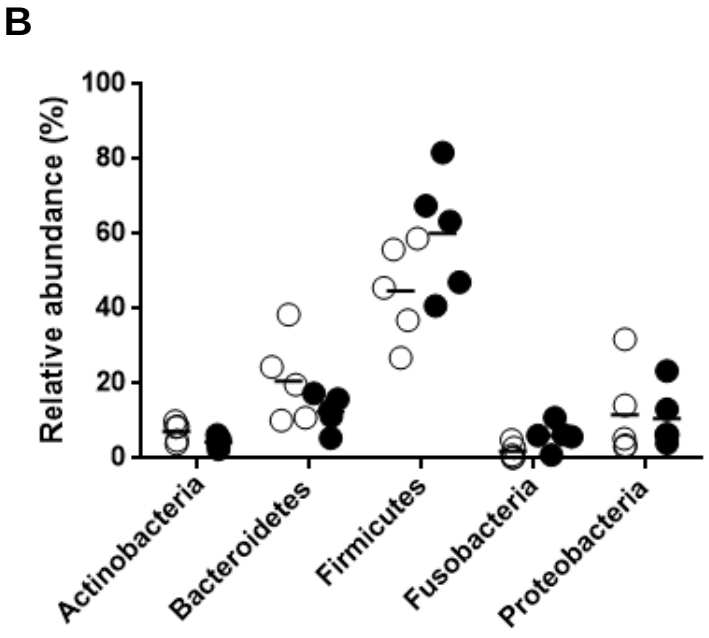
B
Relative abundance (%)
Actinobacteria
Bacteroidetes
Firmicutes
Fusobacteria
Proteobacteria

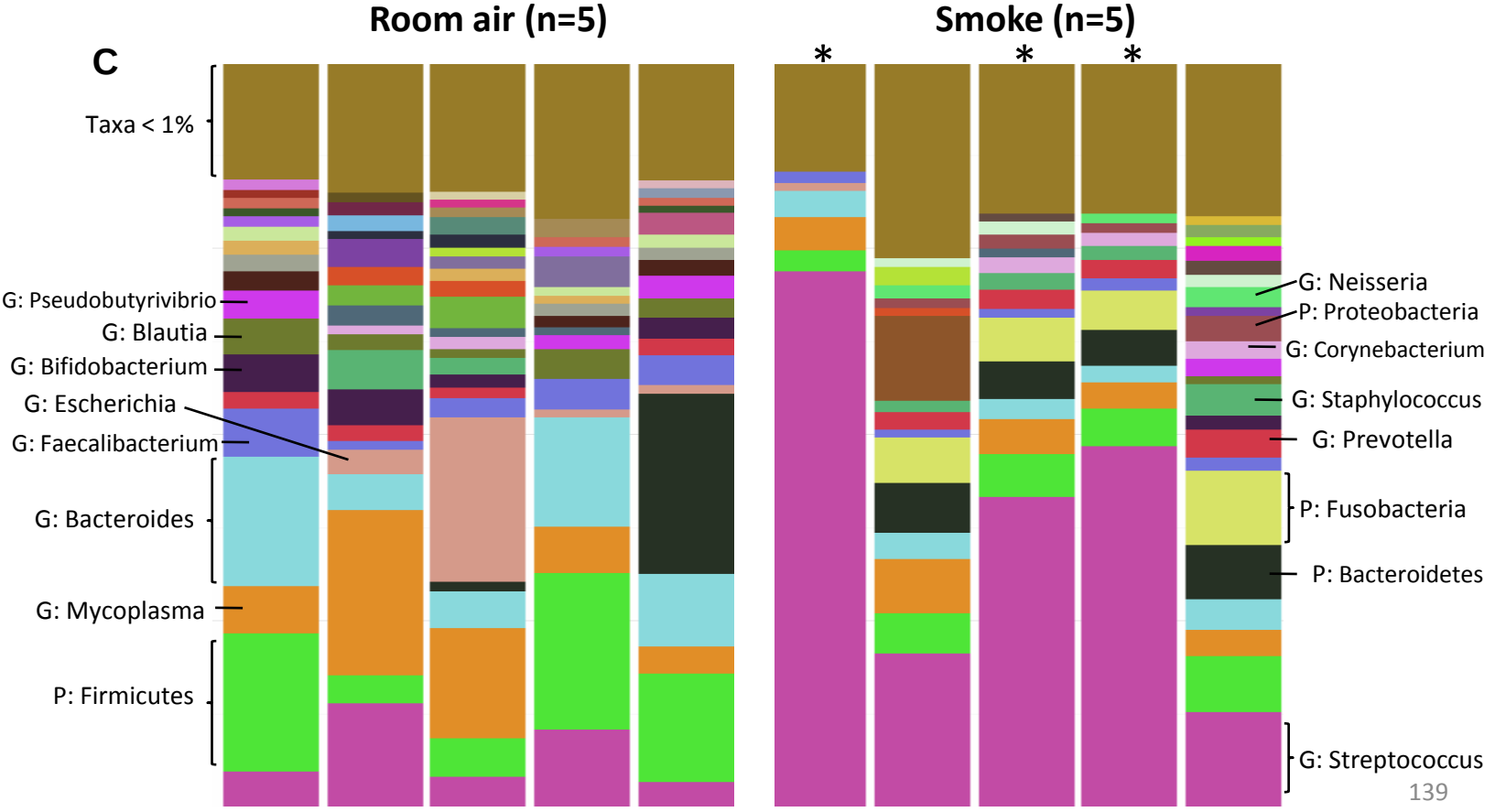
C
Room air (n=5)
Smoke (n=5)
Taxa < 1%
G: Pseudobutyrivibrio
G: Blautia
G: Bifidobacterium
G: Escherichia
G: Faecalibacterium
G: Bacteroides
G: Mycoplasma
P: Firmicutes
G: Neisseria
P: Proteobacteria
G: Corynebacterium
G: Staphylococcus
G: Prevotella
P: Fusobacteria
P: Bacteroidetes
G: Streptococcus

Figure 24

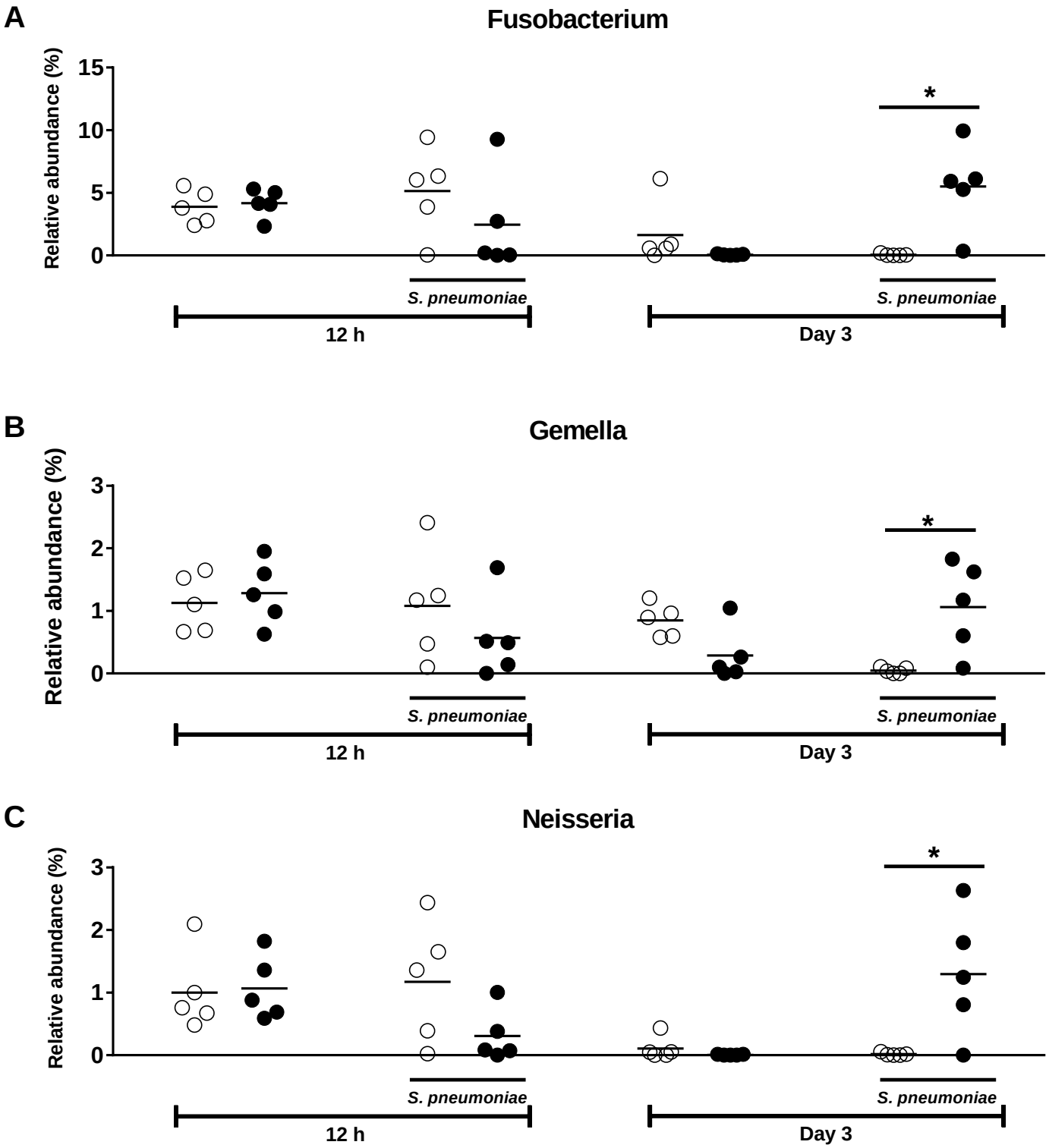
A
Fusobacterium
Relative abundance (%)
15
10
5
0
*
S. pneumoniae
S. pneumoniae
12 h
Day 3
B
Gemella
Relative abundance (%)
3
2
1
0
*
S. pneumoniae
S. pneumoniae
12 h
Day 3
C
Neisseria
Relative abundance (%)
3
2
1
0
*
S. pneumoniae
S. pneumoniae
12 h
Day 3

Figure 25

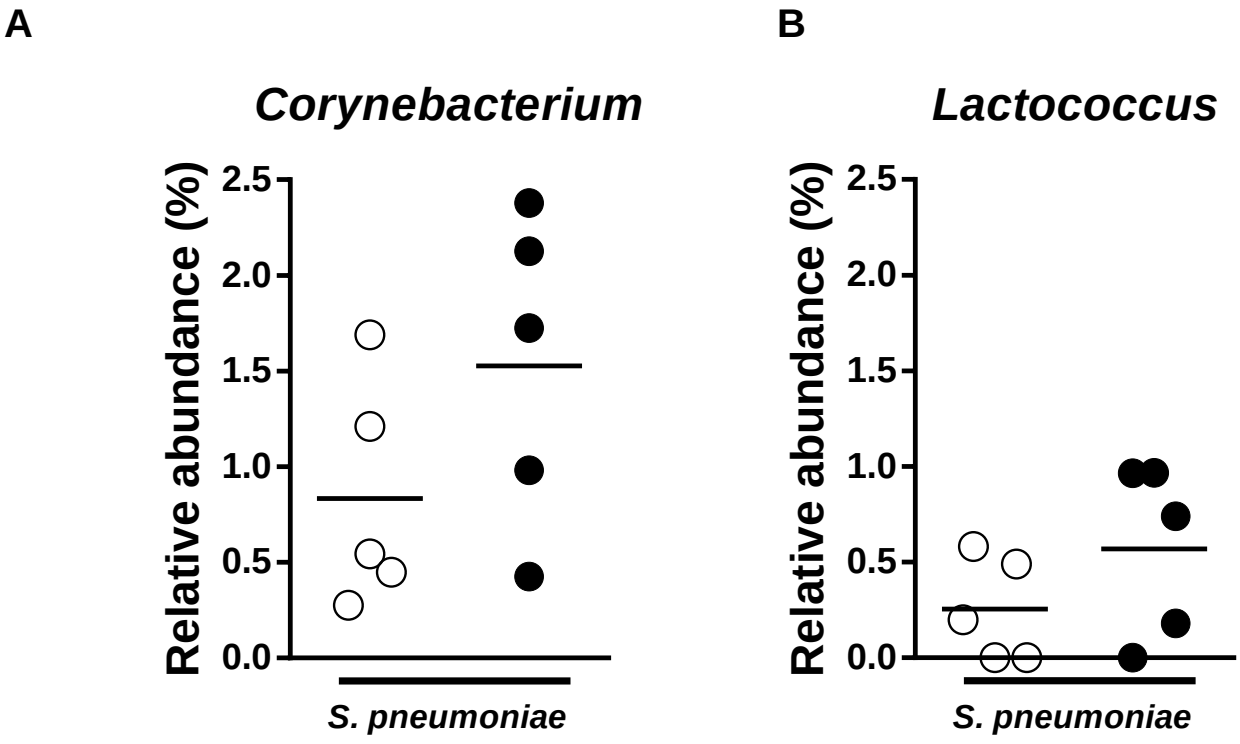
A
Corynebacterium
Relative abundance (%)
2.5
2.0
1.5
1.0
0.5
0.0
S. pneumoniae
B
Lactococcus
Relative abundance (%)
2.5
2.0
1.5
1.0
0.5
0.0
S. pneumoniae

Figure 26

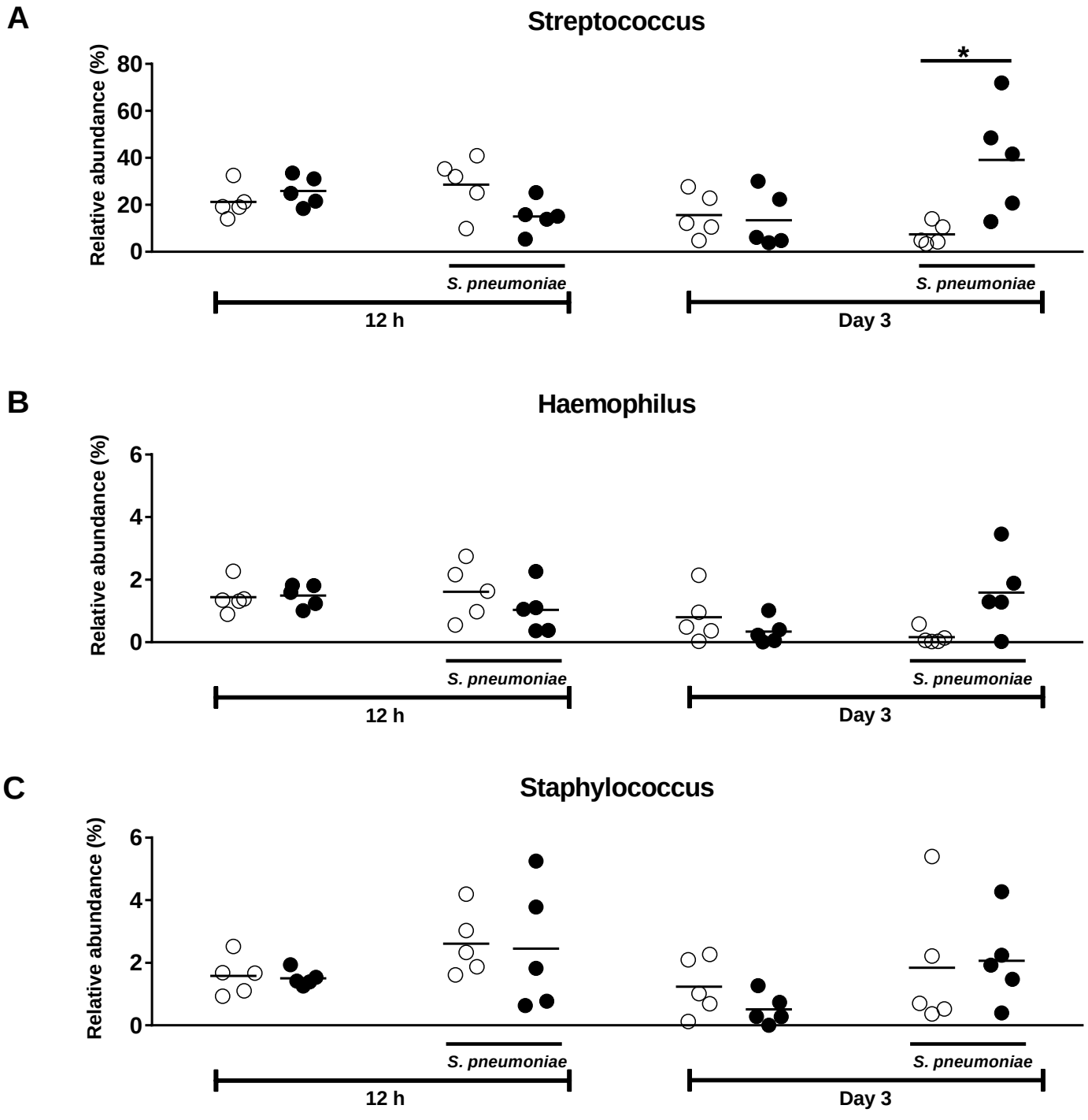
A
Streptococcus
Relative abundance (%)
80
60
40
20
0
*
S. pneumoniae
S. pneumoniae
12 h
Day 3
B
Haemophilus
Relative abundance (%)
6
4
2
0
S. pneumoniae
S. pneumoniae
12 h
Day 3
C
Staphylococcus
Relative abundance (%)
6
4
2
0
S. pneumoniae
S. pneumoniae
12 h
Day 3

Table 1: Bacterial genera significantly different in cigarette smoke-exposed mice as compared to room air-exposed mice at day 3 post-nasal pneumococcal colonization

Phylum	Family	*Genus	Log2 fold change
Firmicutes	Streptococcaceae	Streptococcus	4253
Fusobacteria	Fusobacteriaceae	Fusobacterium	470.7
Firmicutes	Gemellaceae	Gemella	93.77
Proteobacteria	Neisseriaceae	Neisseria	105.9
Firmicutes	Peptostreptococcaceae	Peptostreptococcus	67.69
Bacteroidetes	Porphyromonadaceae	Porphyromonas	53.27
Bacteroidetes	Porphyromonadaceae	Tannerella	40.58
Bacteroidetes	Chitinophagaceae	Sediminibacterium	6.18
Proteobacteria	Neisseriaceae	Simonsiella	13.10
Actinobacteria	Coriobacteriaceae	Atopobium	11.04
Proteobacteria	Pasteurellaceae	Aggregatibacter	11.95
Proteobacteria	Neisseriaceae	Kingella	8.07
Firmicutes	Veillonellaceae	Anaeroglobus	8.33
Spirochaetes	Spirochaetaceae	Treponema	8.87
Proteobacteria	Moraxellaceae	Acinetobacter	7.33

*Bacteria are listed in order of highest relative abundance